

**Modeling neutrino-nucleus interaction**  
R. Gonzalez-Jimenez (UGent)  
Wrocław, 8 Dec 2017



# Modeling neutrino-nucleus interaction for neutrino-oscillation experiments



**Raúl González Jiménez**

Department of Physics and Astronomy,  
Ghent University, Belgium



*Wrocław, 8 December, 2017*

# *In collaboration with...*

J. Enrique Amaro

Maria. B. Barbaro

Juan A. Caballero

T. William Donnelly

Martin V. Ivanov

Guillermo D. Megias

José M. Udías

Natalie Jachowicz

Kajetan Niewczas

Alexis Nikolakopoulos

Jannes Nys

Vishvas Pandey

Jan Ryckebusch

Tom Van Cuyck

Nils Van Dessel

# Outline

- I History***
- II Some Nobel Prize experiments***
- III New era***
- IV Nuclear physics in modern neutrino  
oscillation experiments***
- V Conclusions***



*Original - Photostatic copy of No. 1393*  
Abschrift/15.12.56 **FM**

Offener Brief an die Gruppe der Radioaktiven bei der  
Gesamvereins-Tagung zu Tübingen.

Abschrift

Physikalisches Institut  
der Eidg. Technischen Hochschule  
Zürich

Zürich, 4. Dez. 1930  
Oliverastrasse

Liebe Radioaktive Damen und Herren,

Wie der Überbringer dieser Zeilen, den ich baldmöglichst  
anzuhören bitte, Ihnen das Näherere auseinandersetzen wird, bin ich  
angesichts der "falschen" Statistik der  $N$ - und  $Li-6$  Kerne, sowie  
des kontinuierlichen beta-Spektrums auf einen verweifelten Ausweg  
verfallen um den "Wechselstich" (1) der Statistik und den Energiesatz  
zu retten. Nämlich die Möglichkeit, es könnten elektrisch neutrale  
Teilchen, die ich Neutronen nennen will, in den Kernen existieren,  
welche dem Spin  $1/2$  haben und das Ausschliessungsprinzip befolgen und  
~~sich~~ von Lichtquanten ausserdem noch dadurch unterscheiden, dass sie  
nicht mit Lichtgeschwindigkeit laufen. Die Masse der Neutronen  
müsste von derselben Grössenordnung wie die Elektronenmasse sein und  
jedenfalls nicht grösser als  $0,01$  Protonenmasse. Das kontinuierliche  
beta-Spektrum wäre dann verständlich unter der Annahme, dass beim  
beta-Zerfall mit dem Elektron jeweils noch ein Neutron emittiert  
wird, derart, dass die Summe der Energien von Neutron und Elektron  
konstant ist.

In that time (1930), the **nucleus was made of protons and electrons**: A nucleus of mass  $A$  was made of  $A$  protons and  $Z$  electrons.

Among others, there were two clear inconsistencies that needed to be solved:

### + Nuclear Spin

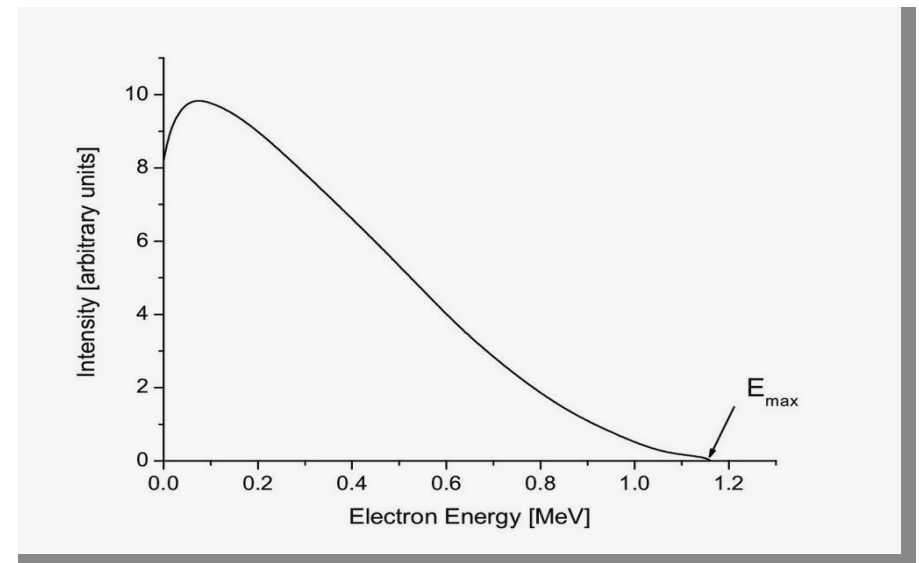
(1928) Nuclear Spin of Nitrogen 14 = 1 (hbar)

An integer spin cannot be explained by coupling an odd number of spin  $\frac{1}{2}$  particles (14 protons and 7 electrons)

### + Beta decay Spectrum



The spectrum cannot be continuous if only one particle is emitted.



## **Pauli's letter of the 4th of December 1930**

**Dear Radioactive Ladies and Gentlemen,**

As the bearer of these lines, to whom I graciously ask you to listen, will explain to you in more detail, how **because of the "wrong" statistics of the N and Li6 nuclei and the continuous beta spectrum, I have hit upon a desperate remedy to save the "exchange theorem" of statistics and the law of conservation of energy.** Namely, **the possibility that there could exist in the nuclei electrically neutral particles, that I wish to call neutrons,** which have spin  $1/2$  and obey the exclusion principle and which further differ from light quanta in that they do not travel with the velocity of light. The mass of **the neutrons should be of the same order of magnitude as the electron mass** and in any event not larger than  $0.01$  proton masses. **The continuous beta spectrum would then become understandable by the assumption that in beta decay a neutron is emitted in addition to the electron** such that the sum of the energies of the neutron and the electron is constant... I agree that **my remedy could seem incredible because one should have seen those neutrons much earlier if they really exist.** **But only the one who dare can win** and the difficult situation, due to the continuous structure of the beta spectrum, is lighted by a remark of my honoured predecessor, Mr Debye, who told me recently in Bruxelles: "Oh, it's well better not to think to this at all, like new taxes". From now on, every solution to the issue must be discussed. Thus, dear radioactive people, look and judge.

Unfortunately, I cannot appear in Tübingen personally since I am indispensable here in Zurich because of a ball on the night of 6/7 December. With my best regards to you, and also to Mr Back.

Your humble servant . **W. Pauli, December 1930**

# The Nobel Prize in Physics 1995



**Martin L. Perl**  
Prize share: 1/2



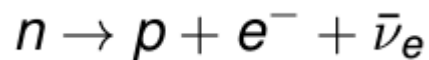
© University of California  
Regents  
**Frederick Reines**  
Prize share: 1/2

The Nobel Prize in Physics 1995 was awarded *"for pioneering experimental contributions to lepton physics"* jointly with one half to Martin L. Perl *"for the discovery of the tau lepton"* and with one half to Frederick Reines *"for the detection of the neutrino"*.

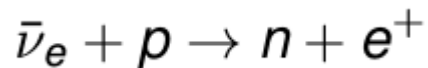
# The neutrino is detected for the first time

In the **mid 1950's**, **Frederick Reines and Clyde L. Cowan, Jr.** came up with an experiment to verify the existence of the neutrino. It made use of the fact that nuclear reactors were expected to produce neutrino fluxes on the order of  $10^{12}$ - $10^{13}$  neutrinos per second per  $\text{cm}^2$ , far higher than any attainable flux from radioactive sources.

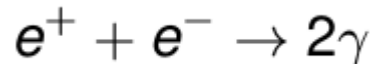
1. Nuclear reactor produces antineutrinos



2. The antineutrino interacts with a proton in the detector

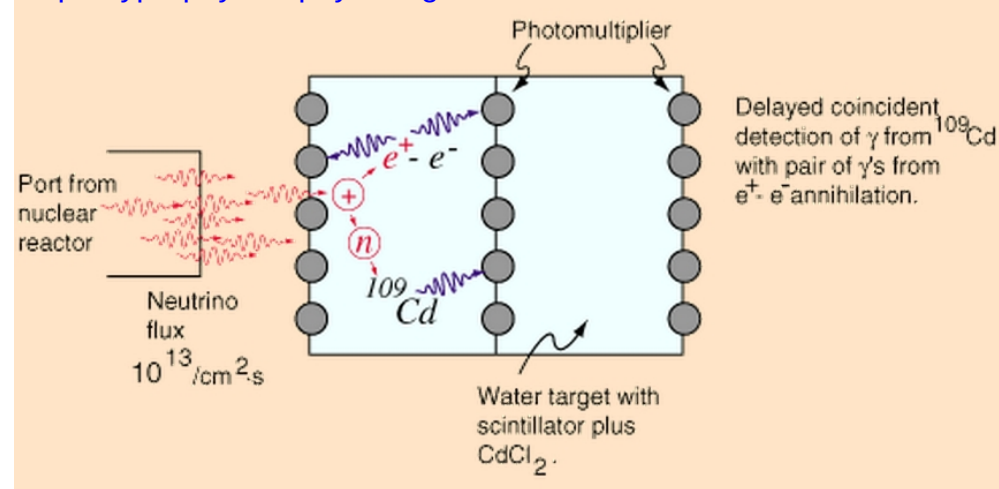


3. The positron annihilates immediately with an electron of the media



4. If the two gammas and the neutron are detected within a time windows → **antineutrino**

<http://hyperphysics.phy-astr.gsu.edu/hbase/Particles/cowan.html>



After months of data collection, they had accumulated data on about three neutrinos per hour in their detector.



**Raymond Davis Jr.**  
Prize share: 1/4



**Masatoshi Koshiba**  
Prize share: 1/4

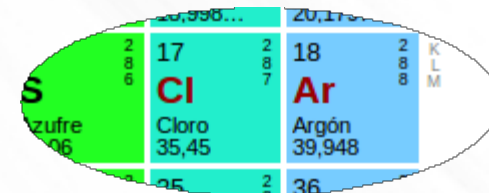
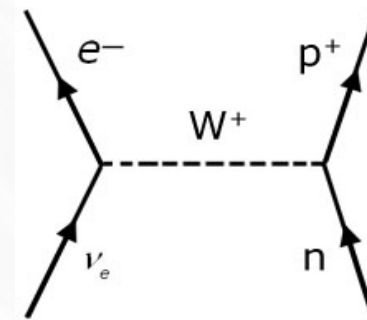
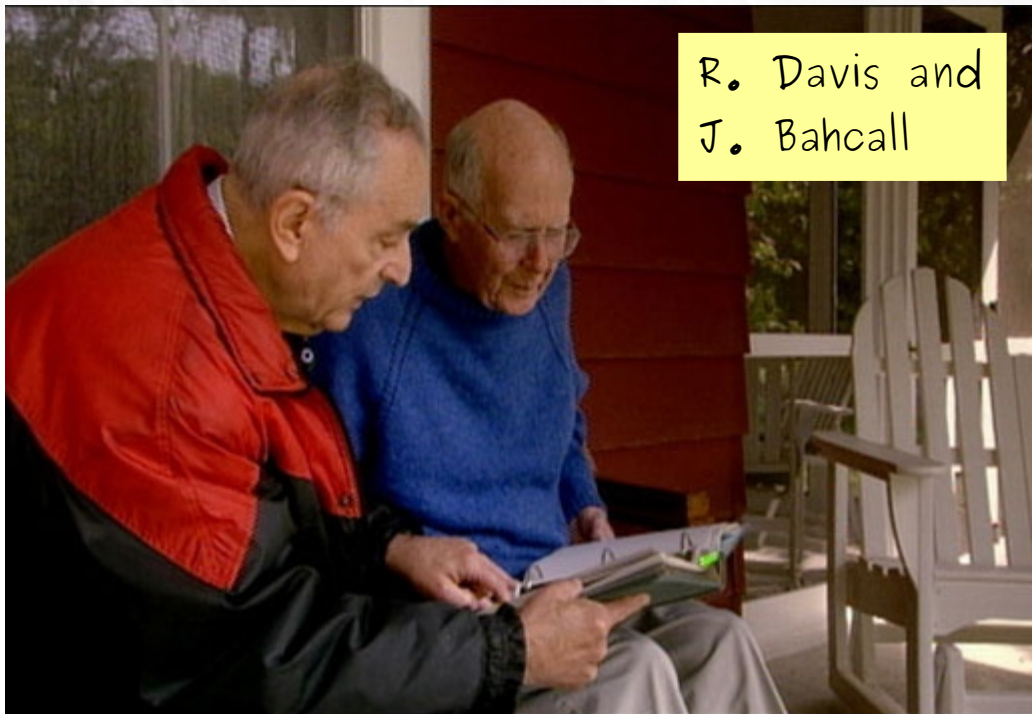


**Riccardo Giacconi**  
Prize share: 1/2

The Nobel Prize in Physics 2002 was divided, one half jointly to **Raymond Davis Jr. and Masatoshi Koshiba** *"for pioneering contributions to astrophysics, in particular for the detection of cosmic neutrinos"* and the other half to Riccardo Giacconi *"for pioneering contributions to astrophysics, which have led to the discovery of cosmic X-ray sources"*.

## 2 Homestake Solar Neutrino Detector

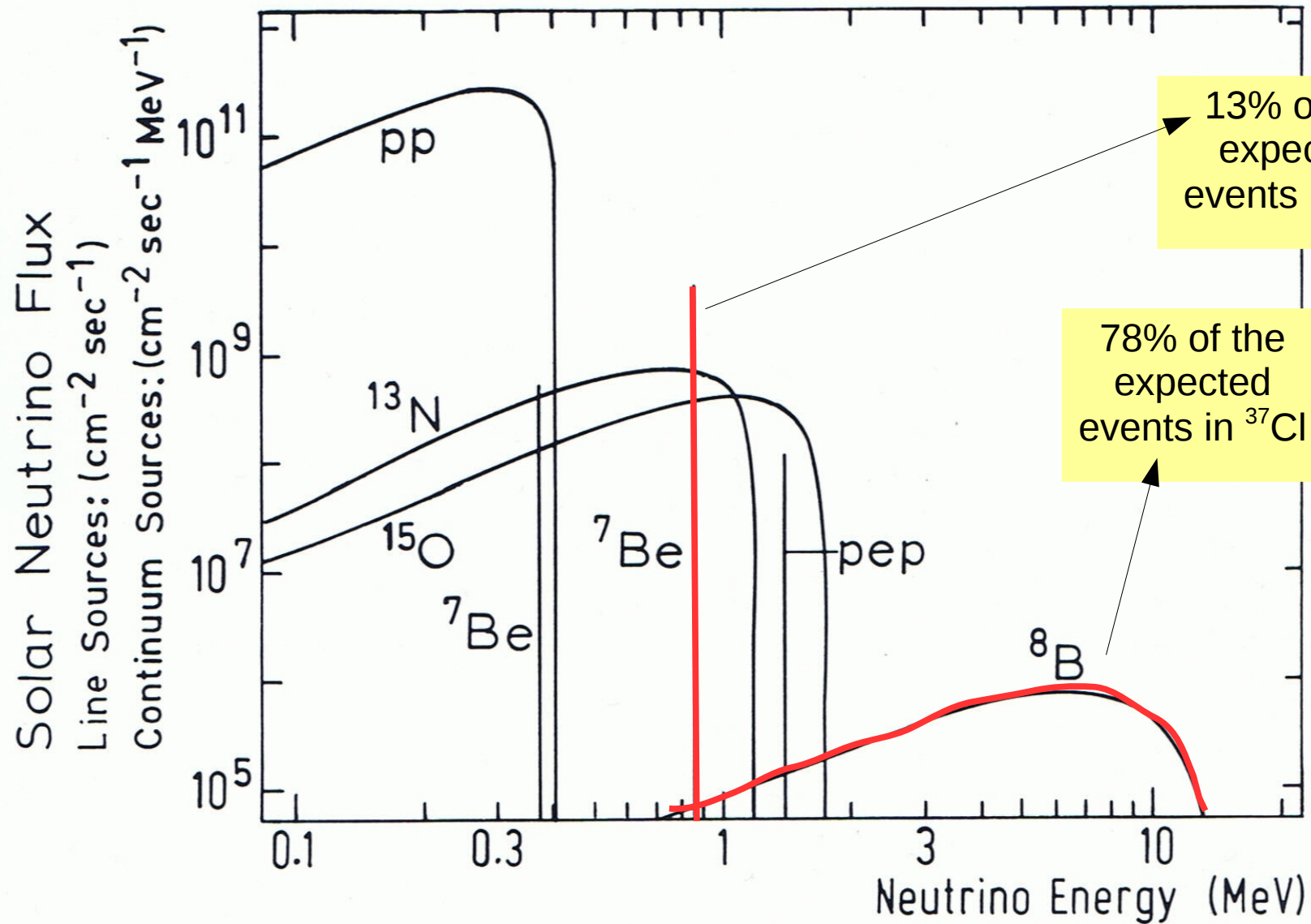
- It was built in the period 1965-1967.
- Originally, the goal was to measure the total flux of solar neutrinos with an energy above 0.814 MeV.
- The technique to count the neutrinos consists in an original idea by Pontecorvo (1946).



A snippet of the periodic table showing the elements Sulfur (S), Chlorine (Cl), and Argon (Ar). The elements are highlighted in a rounded rectangle.

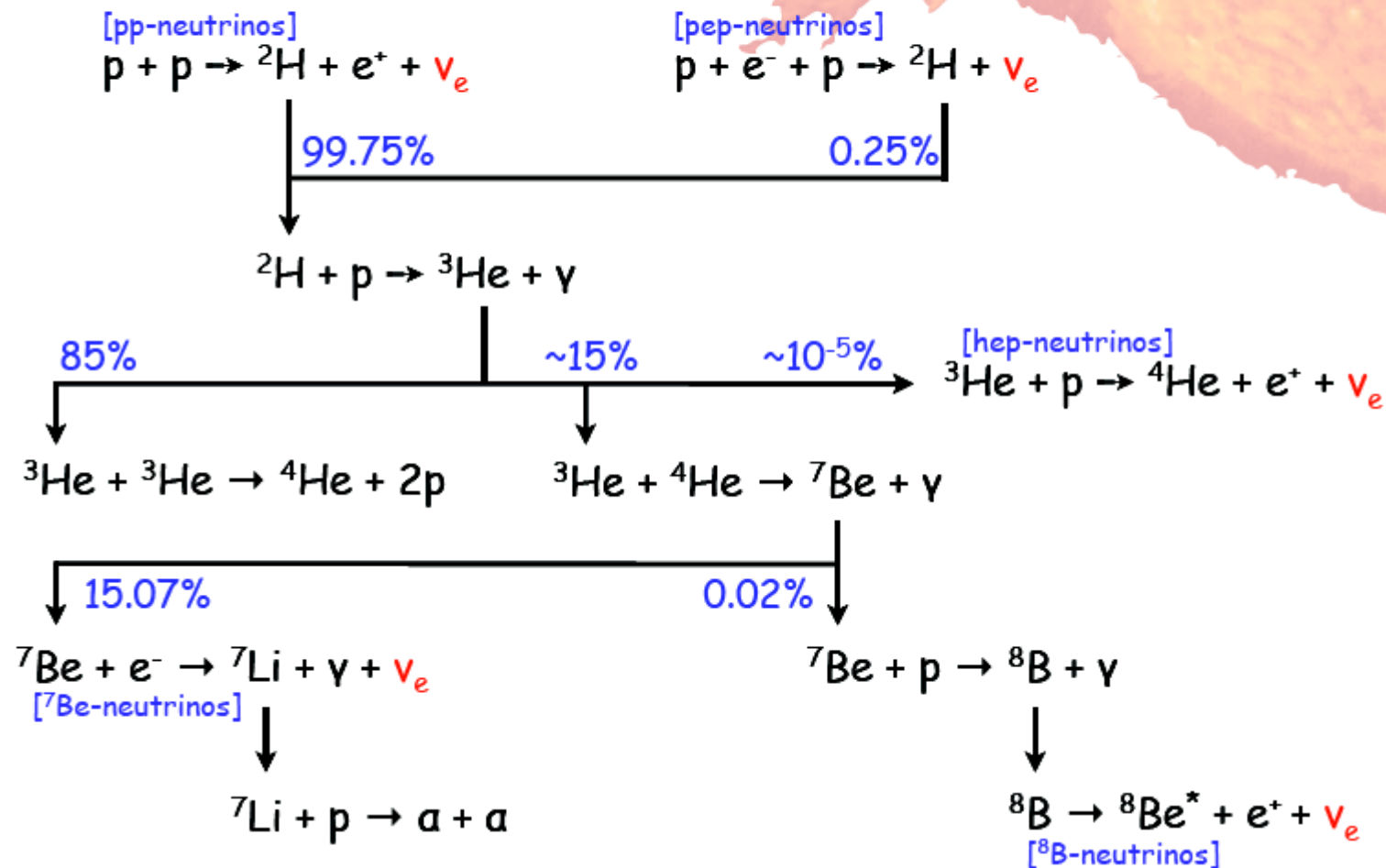
16	17	18
Sulfuro	Cloro	Argón
32,06	35,45	39,948

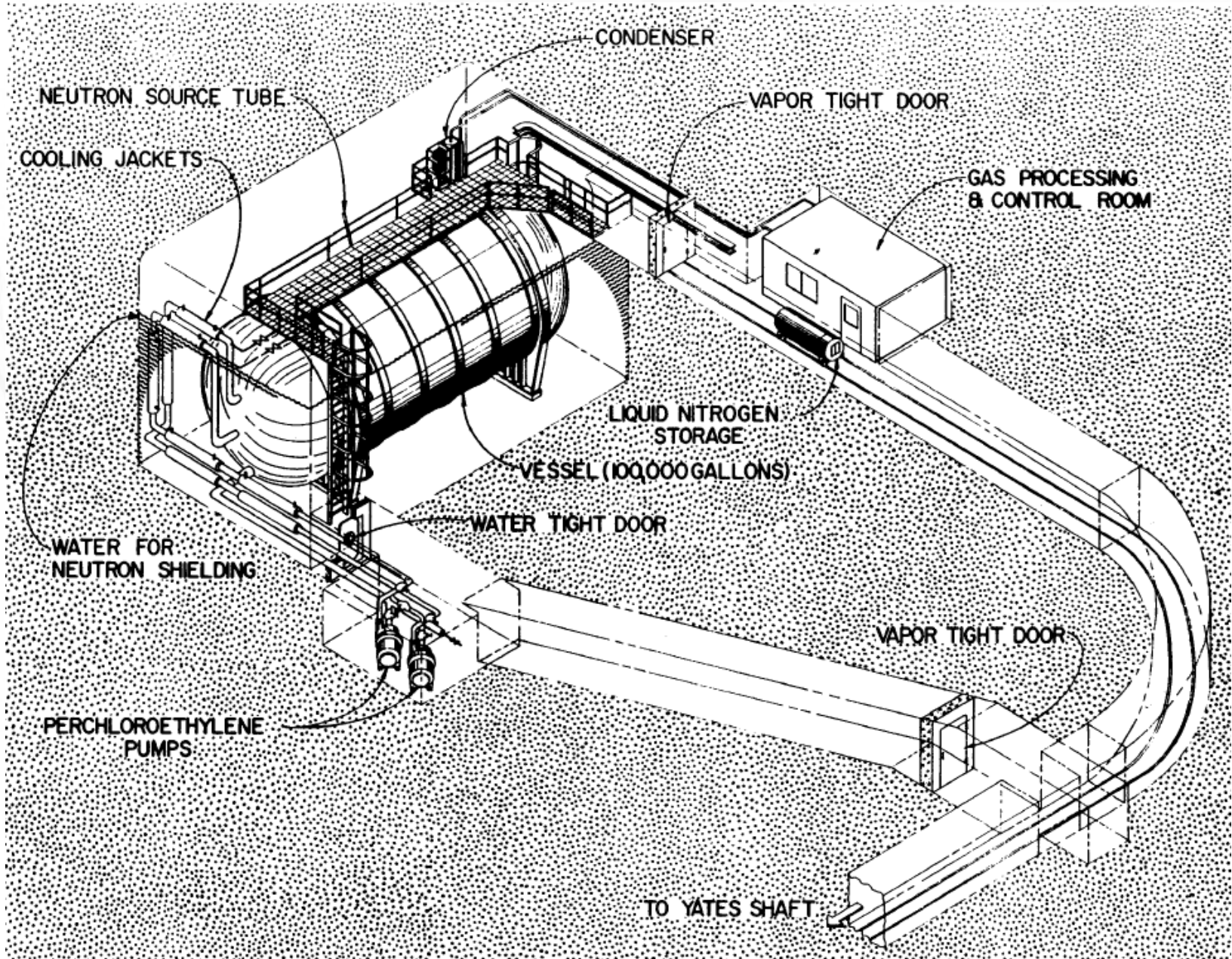
# Relevant solar neutrino fluxes



# Neutrinos from the Sun [pp chain]

[also: CNO cycle]



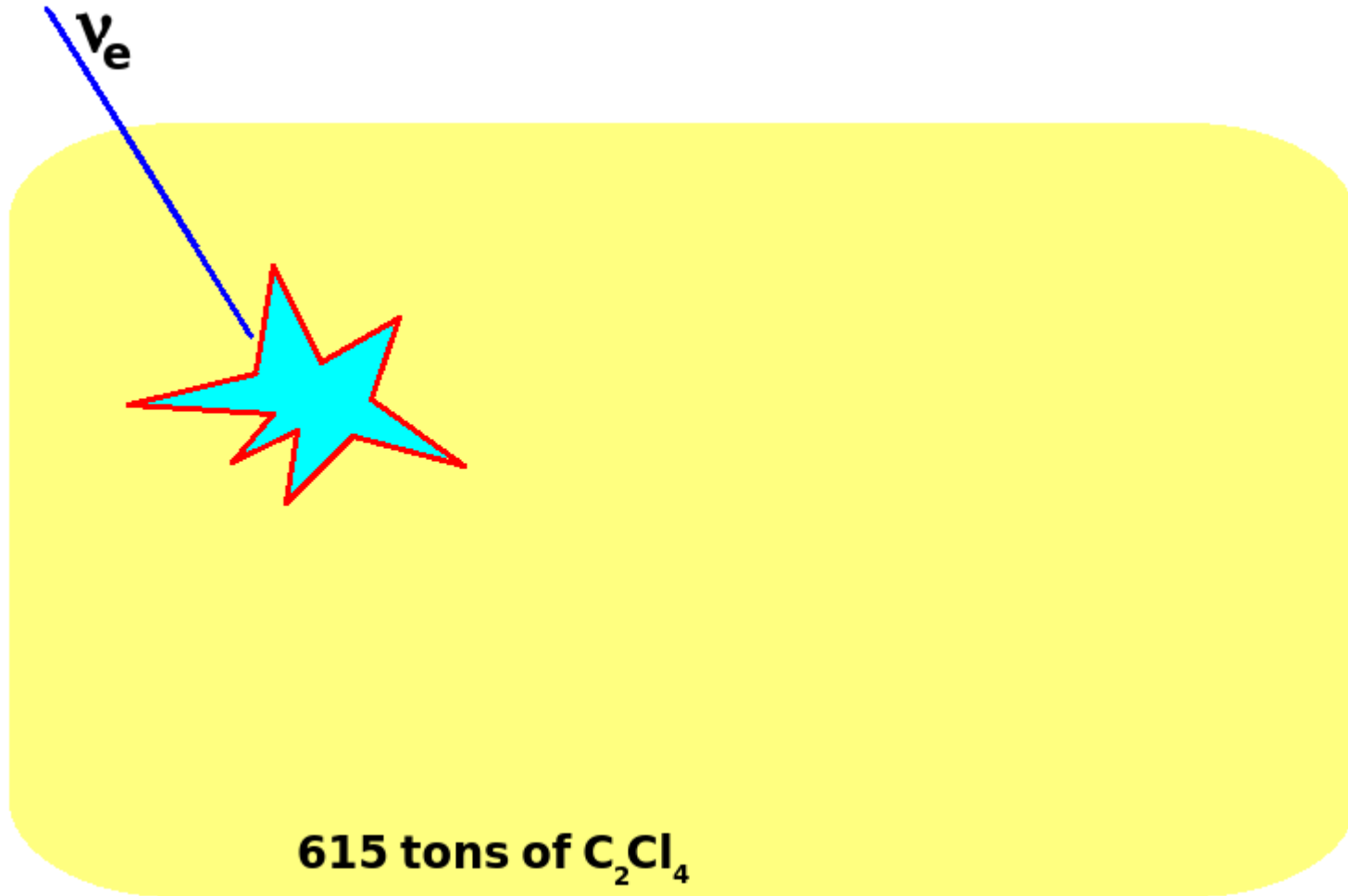


## *THE EXPERIMENT*

- 615 tons of tetrachloroethylene,  $C_2Cl_4$ ,  
(natural abundance of  $^{37}Cl$  is ~24%).

**615 tons of  $C_2Cl_4$**

# THE EXPERIMENT

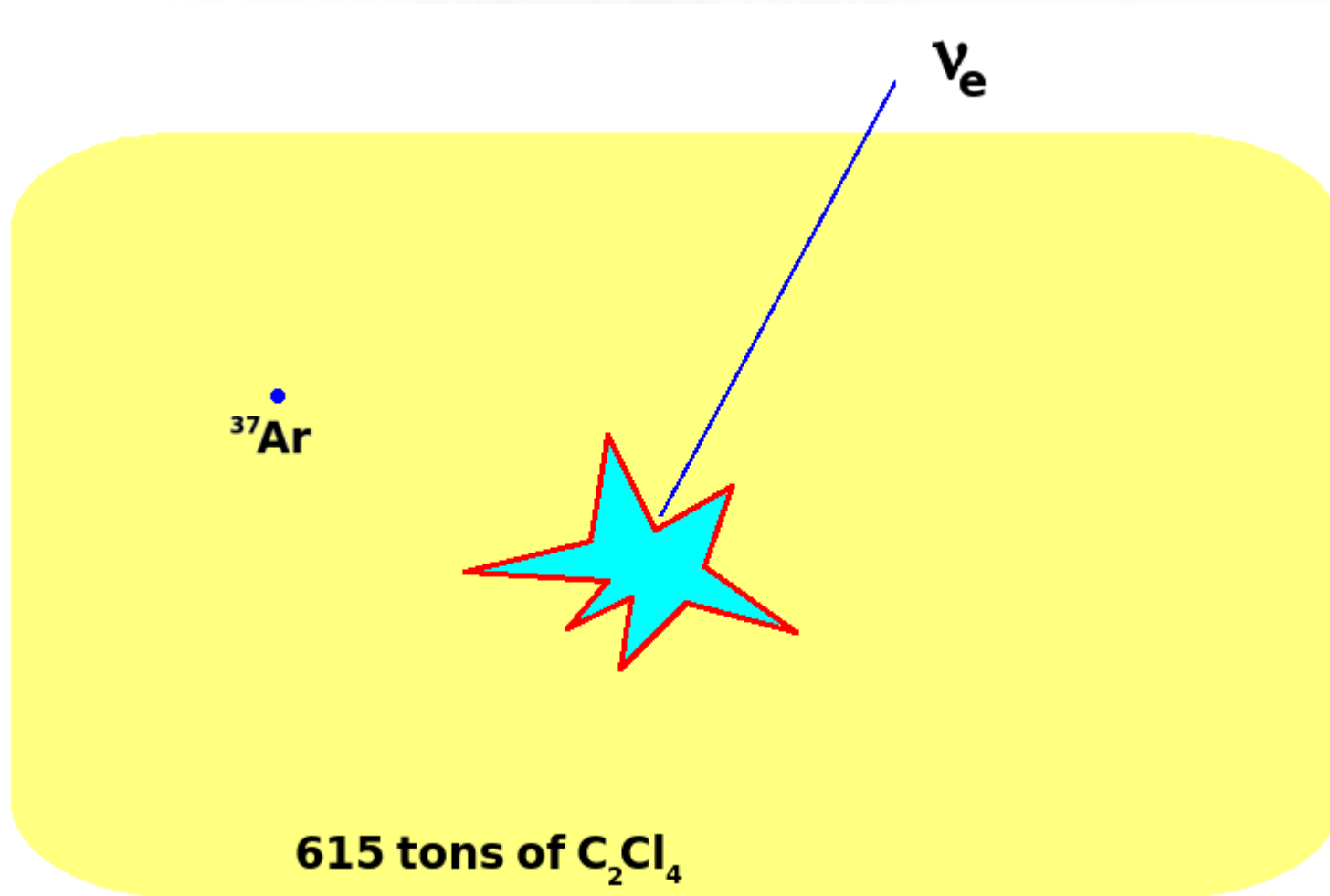


# THE EXPERIMENT



615 tons of  $\text{C}_2\text{Cl}_4$

# THE EXPERIMENT



# THE EXPERIMENT

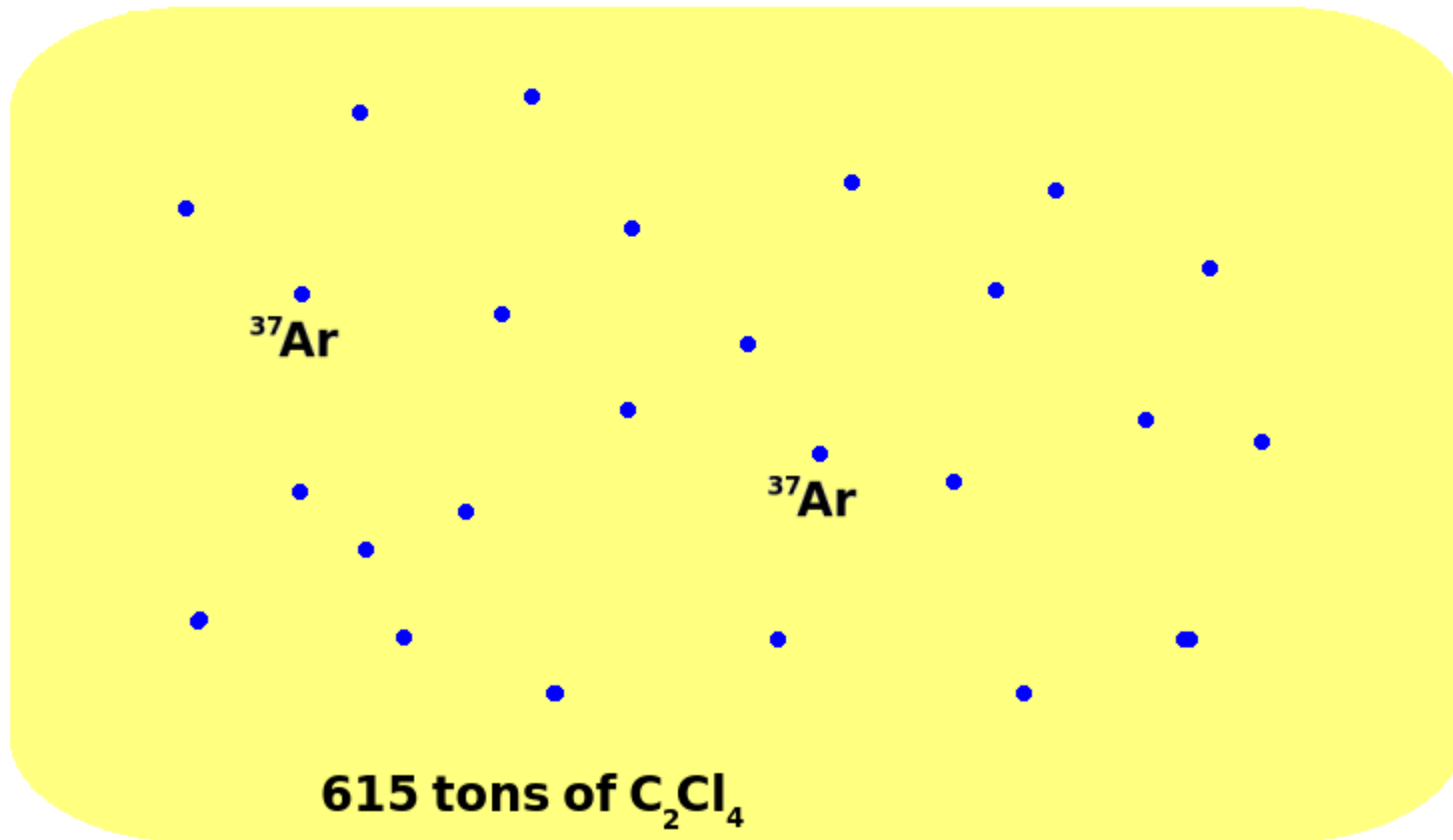
$^{37}\text{Ar}$

$^{37}\text{Ar}$

615 tons of  $\text{C}_2\text{Cl}_4$

# THE EXPERIMENT

***After 2 month...***



***... we have ~ 18 atoms of  $^{37}Ar$  !!!***

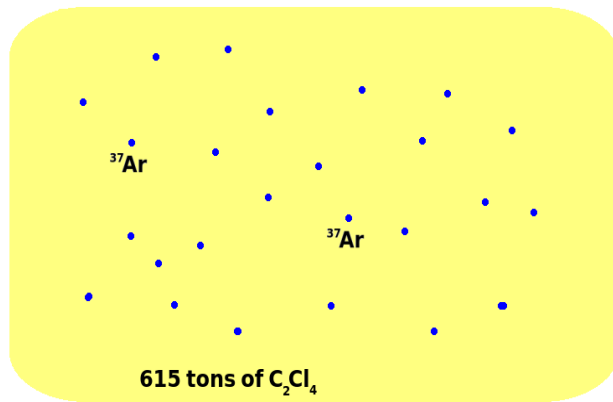
## THE EXPERIMENT

$^{37}\text{Ar}$  half-life ~ 35 days.

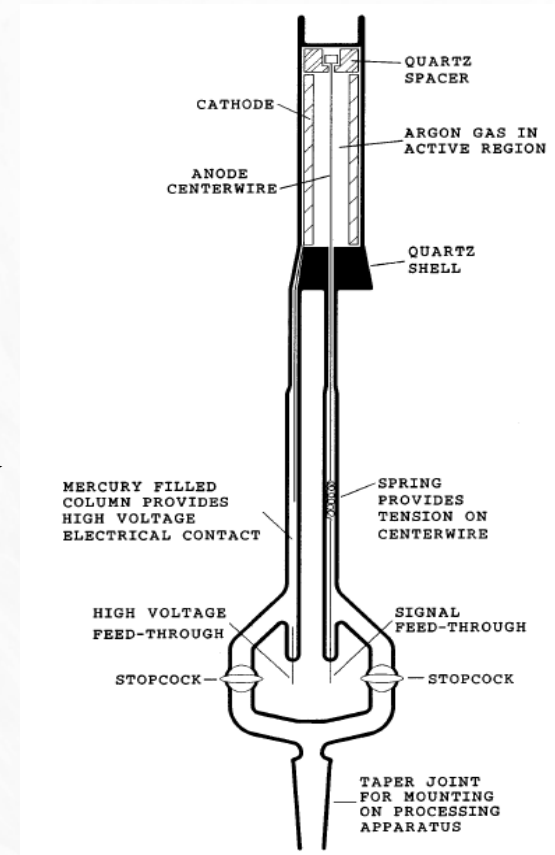
- The produced argon starts decaying immediately after the production so there exist a saturation level.
- **Saturation level in the tank is ~25  $^{37}\text{Ar}$  atoms.**
- A 60 days exposure results in 70% of saturation.
- Typical run is 2 month duration.

615 tons of  $\text{C}_2\text{Cl}_4$

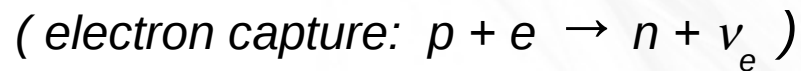
# THE EXPERIMENT

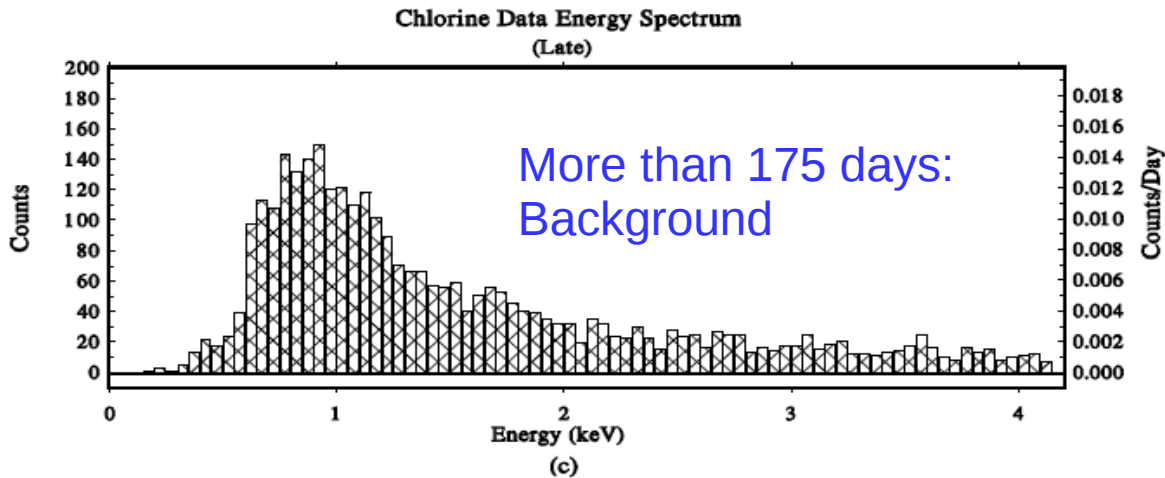
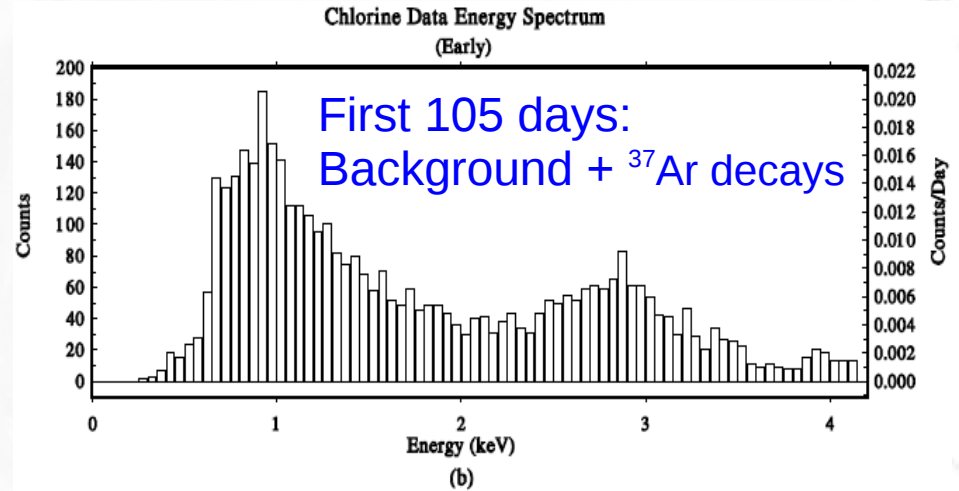
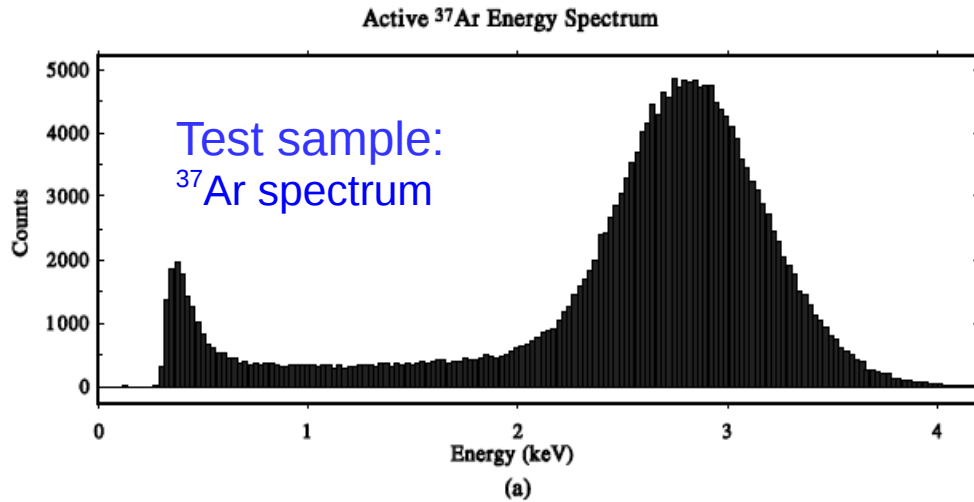


Extraction of Argon



$^{37}\text{Ar}$  decays in  $^{37}\text{Cl}$  by **electron capture** producing 3-5 **Auger electrons** which deposit an energy of 2.82 KeV in the counter.





- After ~ 2 months the argon is extracted and placed in a tiny proportional counter.
- $^{37}\text{Ar}$  half-life ~ 35 days.
  - Within 105 (3 half-lives) days 87.5% of the atoms have decayed.
  - After 175 days (5 half-lives) only ~3%  $^{37}\text{Ar}$  atoms remain in the counter.

FIG. 9.—(a) Energy spectrum from a counter filled with active  $^{37}\text{Ar}$ . (b) Cumulative energy spectrum from 93 solar neutrino observations (early counting data: 0–105 days following the end of an extraction). (c) Cumulative energy spectrum from 93 solar neutrino observations (late counting data: 175–350 days following the end of an extraction). Plots (b) and (c) are of events with normalized ADP between 0.85 and 1.02 (i.e., fast events).

## Results after 25 years

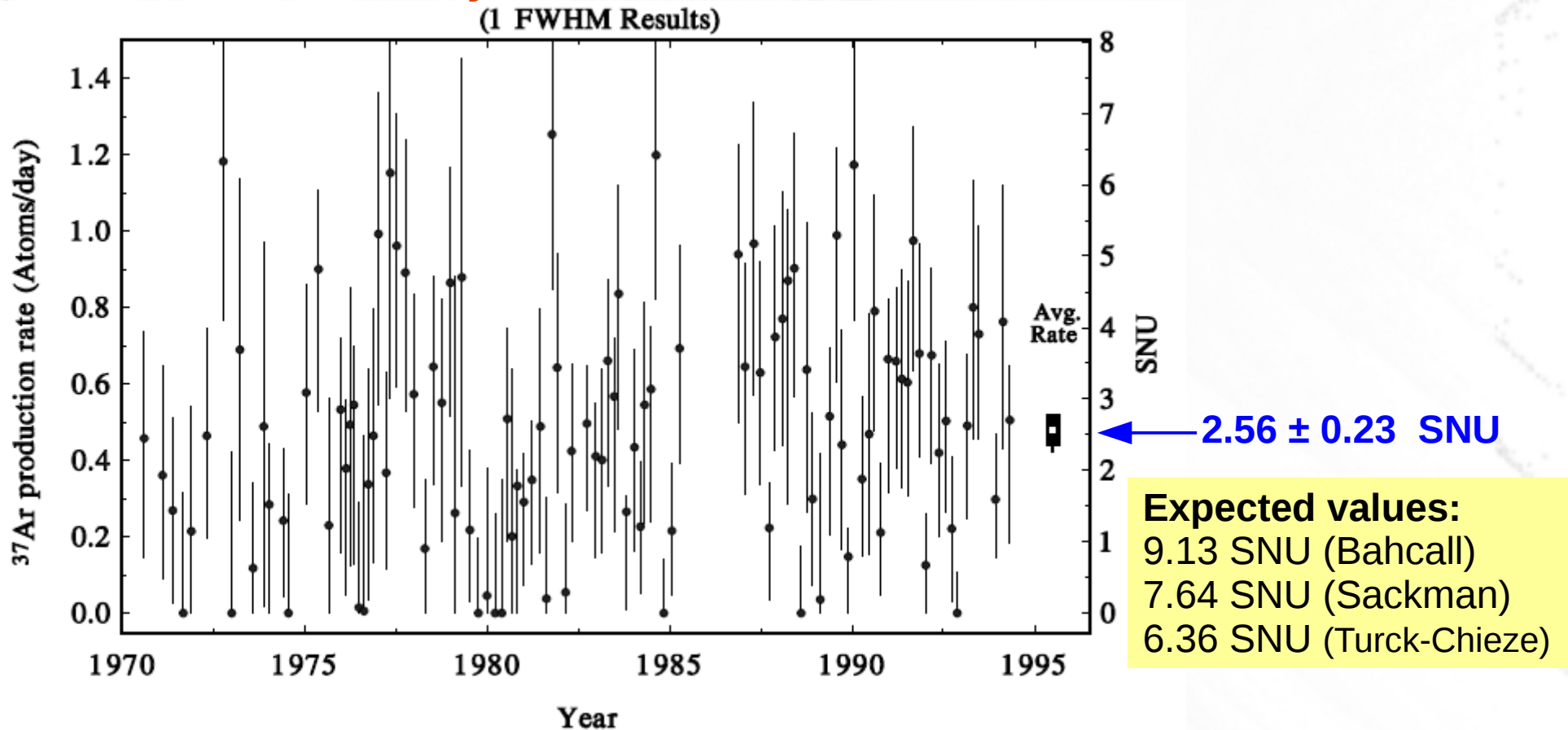
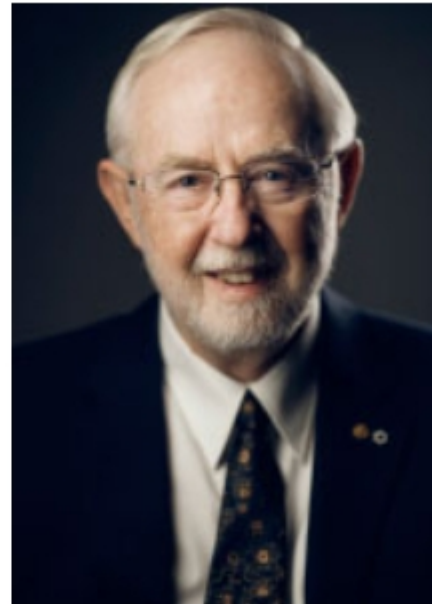


FIG. 13.—Homestake Experiment—one FWHM results. Results for 108 individual solar neutrino observations made with the Homestake chlorine detector. The production rate of  $^{37}\text{Ar}$  shown has already had all known sources of nonsolar  $^{37}\text{Ar}$  production subtracted from it. The errors shown for individual measurements are statistical errors only and are significantly non-Gaussian for results near zero. The error shown for the cumulative result is the combination of the statistical and systematic errors in quadrature.



**Takaaki Kajita**

Prize share: 1/2



**Arthur B. McDonald**

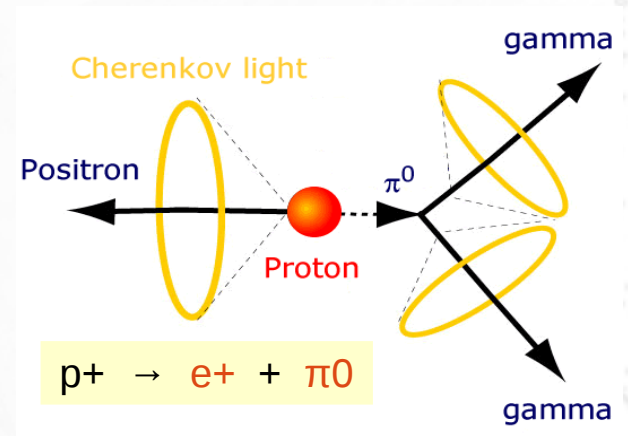
Prize share: 1/2

The Nobel Prize in Physics 2015 was awarded jointly to Takaaki Kajita and Arthur B. McDonald "for the discovery of neutrino oscillations, which shows that neutrinos have mass"

### 3 *KamiokaNDE*

KamiokaNDE experiment was designed to search for proton decay.

→ A proton decay detector must be extremely well isolated from backgrounds since the lower limit for proton half-life is  $\sim 10^{34}$  years.



#### Kamiokande detector:

1000 m underground (2700 m.w.e.).

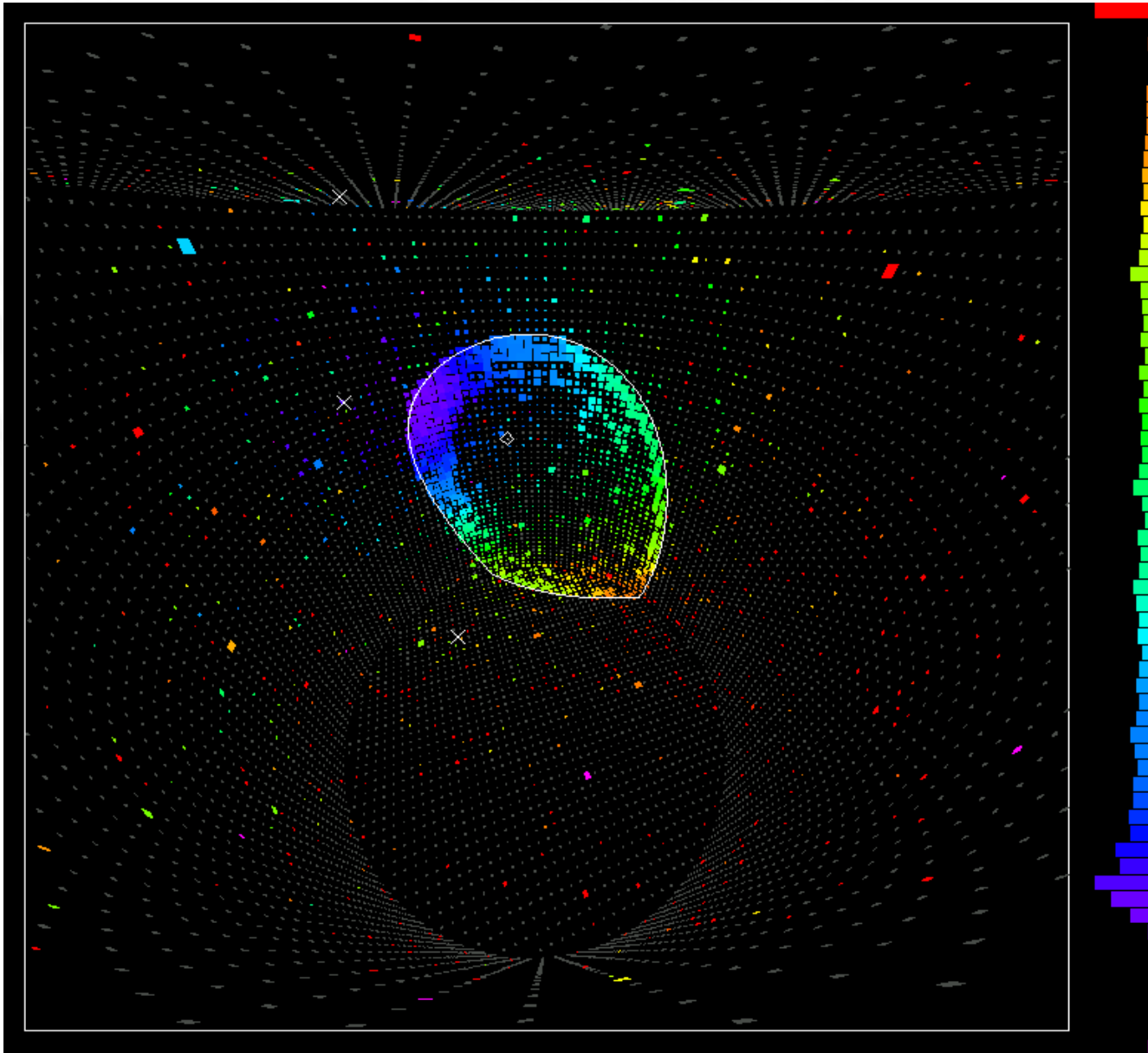
Start operating on July 1983.

Cylinder  $\sim$  15.6 m diameter x 16 m height.

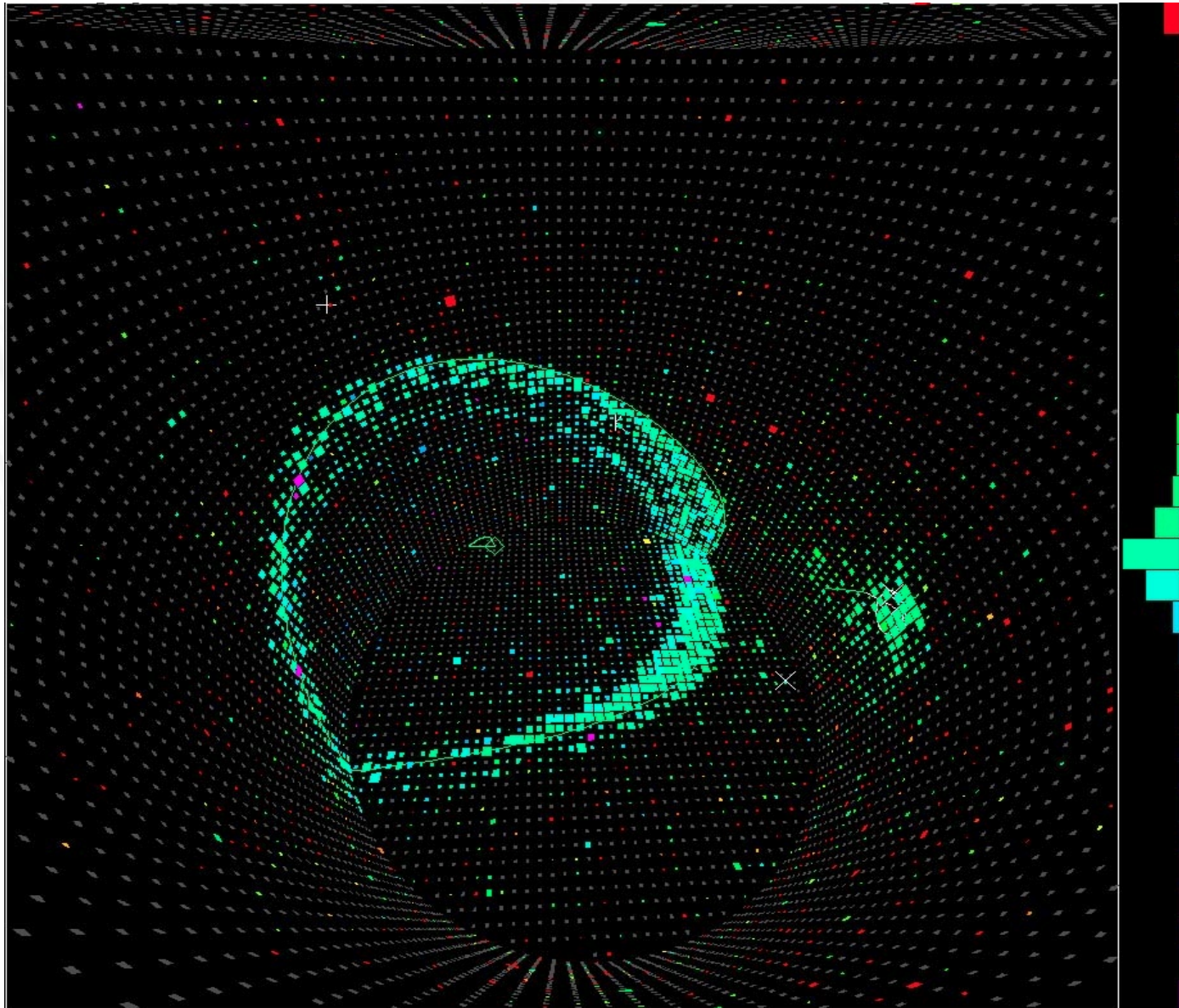
Thousands of photomultiplier tubes fill the inner surface of the cylinder.

Tons of water **Cerenkov detector.**

# Event in Super-Kamiokande Cerenkov detector

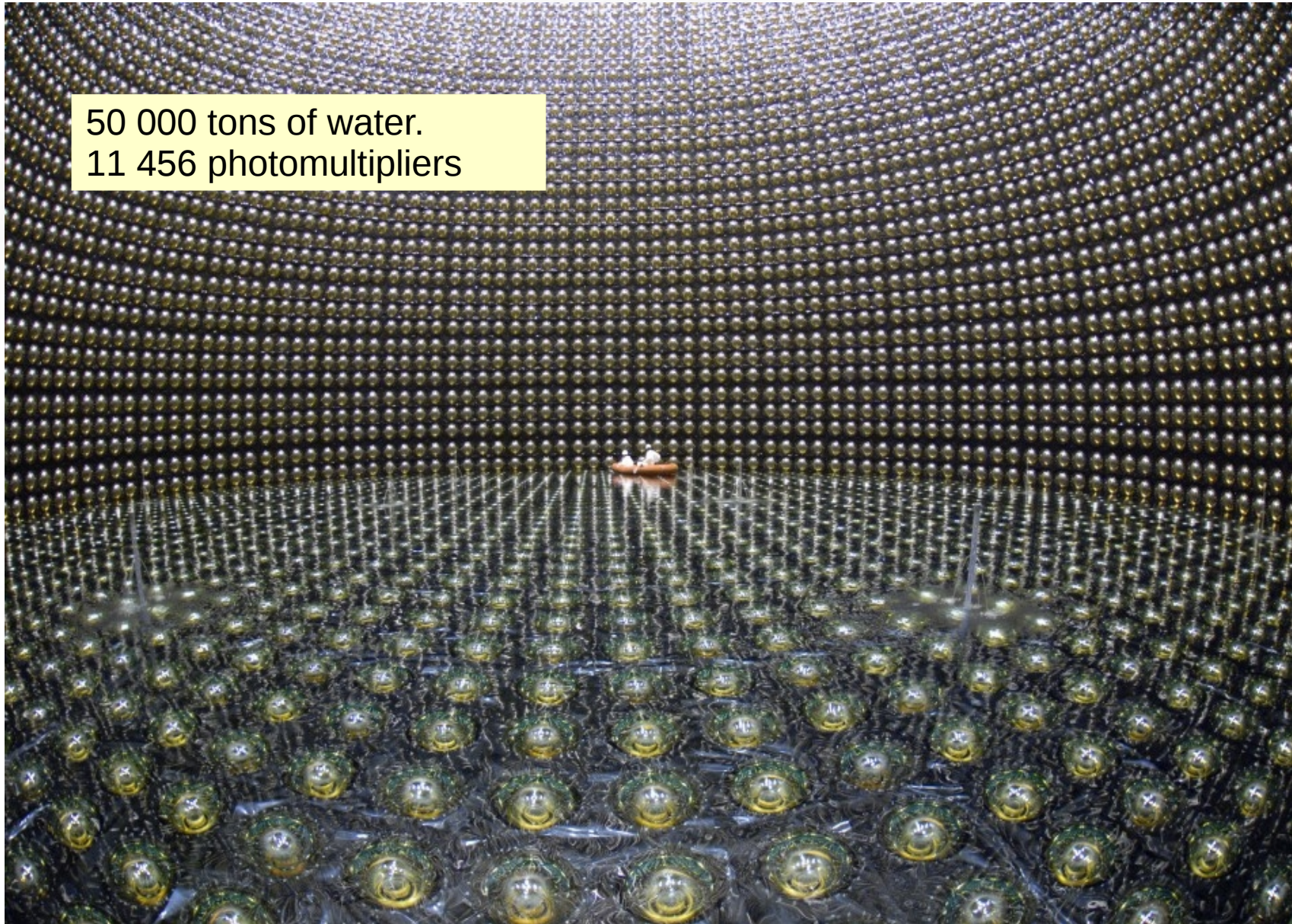


# *Event in Super-Kamiokande Cerenkov detector*



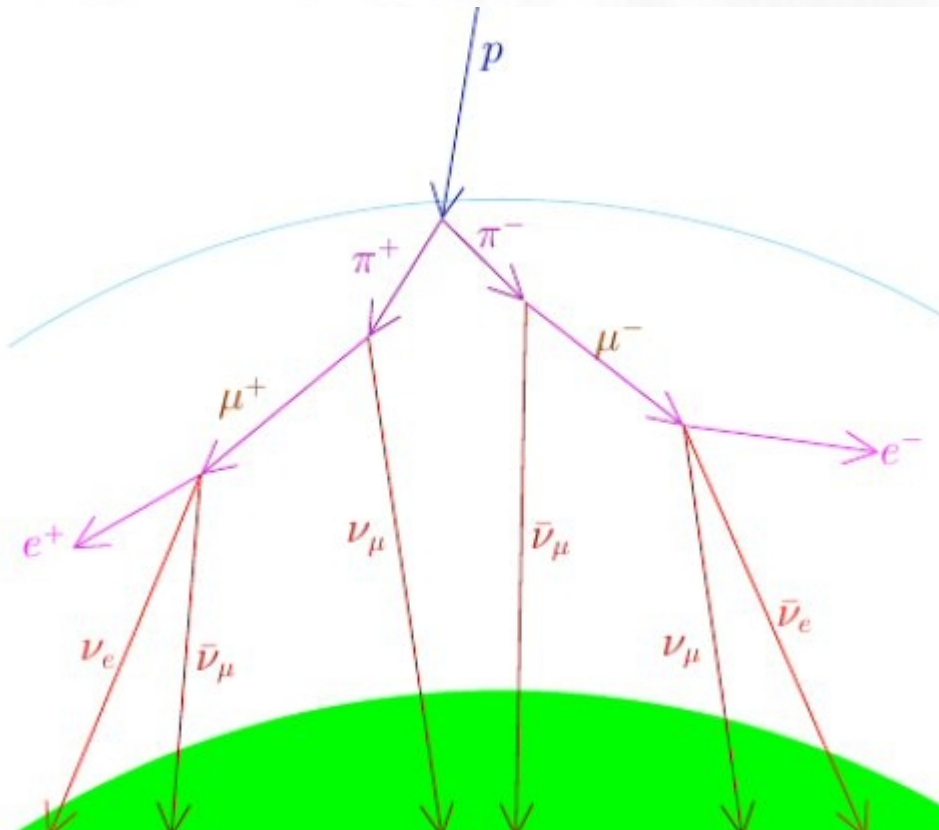
## *Super-Kamiokande*

50 000 tons of water.  
11 456 photomultipliers



### 3 KamiokaNDE

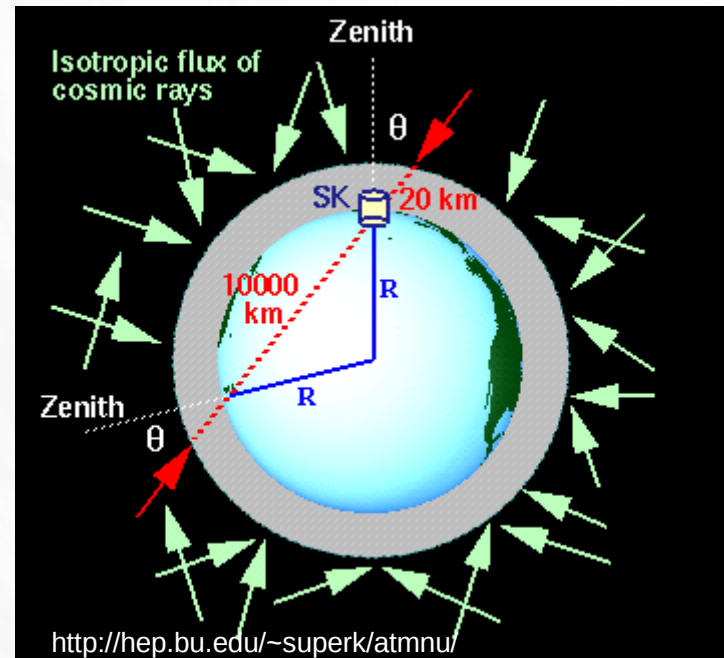
## Neutrino production in the atmosphere



<http://www.twinkletoesengineering.info/neutrinos.htm>

Prediction for the neutrino fluxes:

$$R_{\text{Theor}} = (\nu_{\mu} + \bar{\nu}_{\mu}) / (\nu_e + \bar{\nu}_e) \sim 2$$



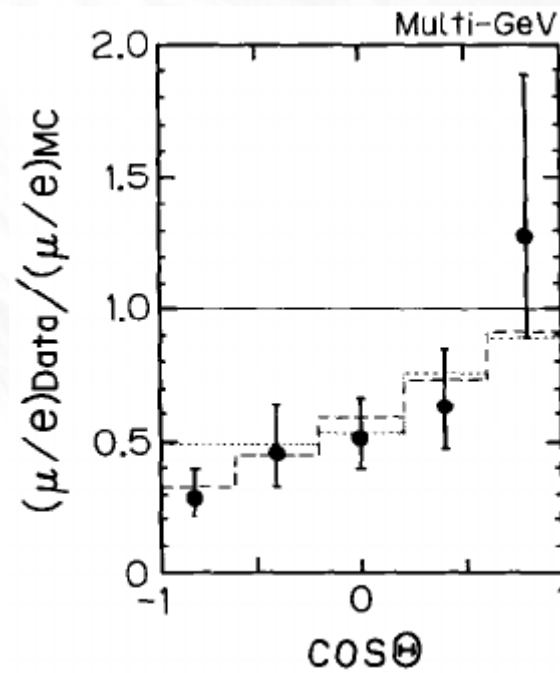
Atmospheric neutrinos enter the detector from every direction.

Experiment (1992, Kam-I and Kam-II):

$$R_{\text{data}} / R_{\text{Theor}} = 0.60 \pm 0.09$$

**Far from 1 !!!**

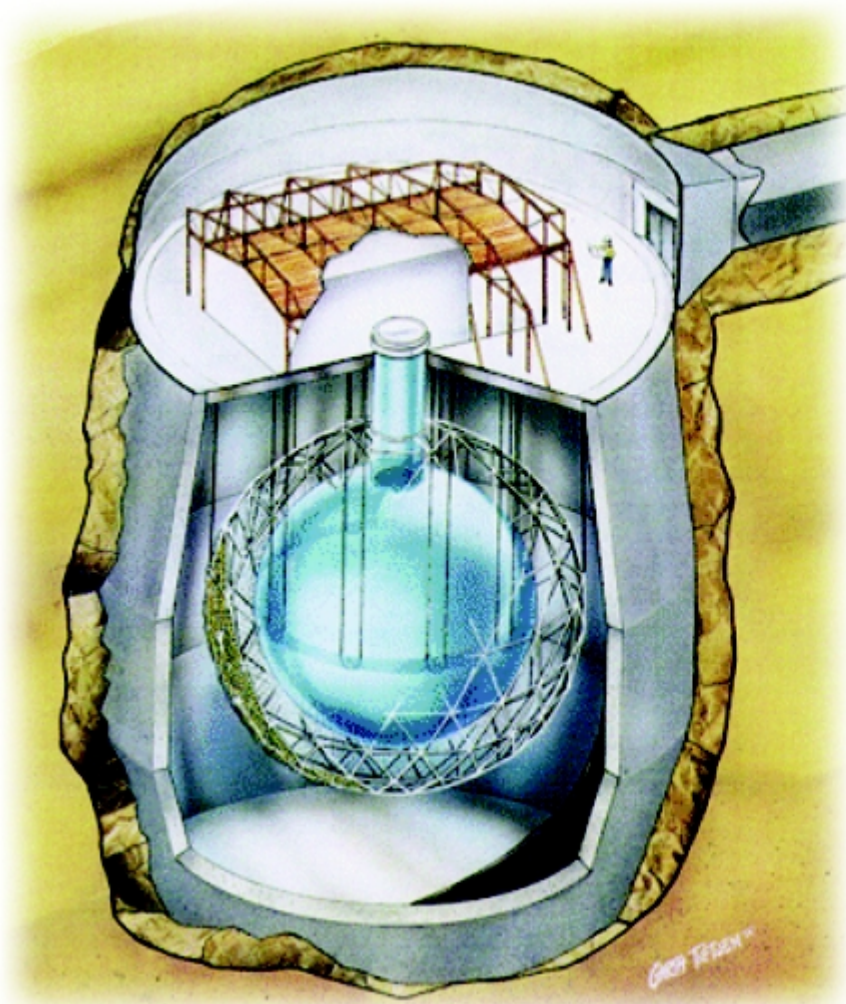
### Atmospheric $\nu_\mu/\nu_e$ ratio in the multi-GeV energy range



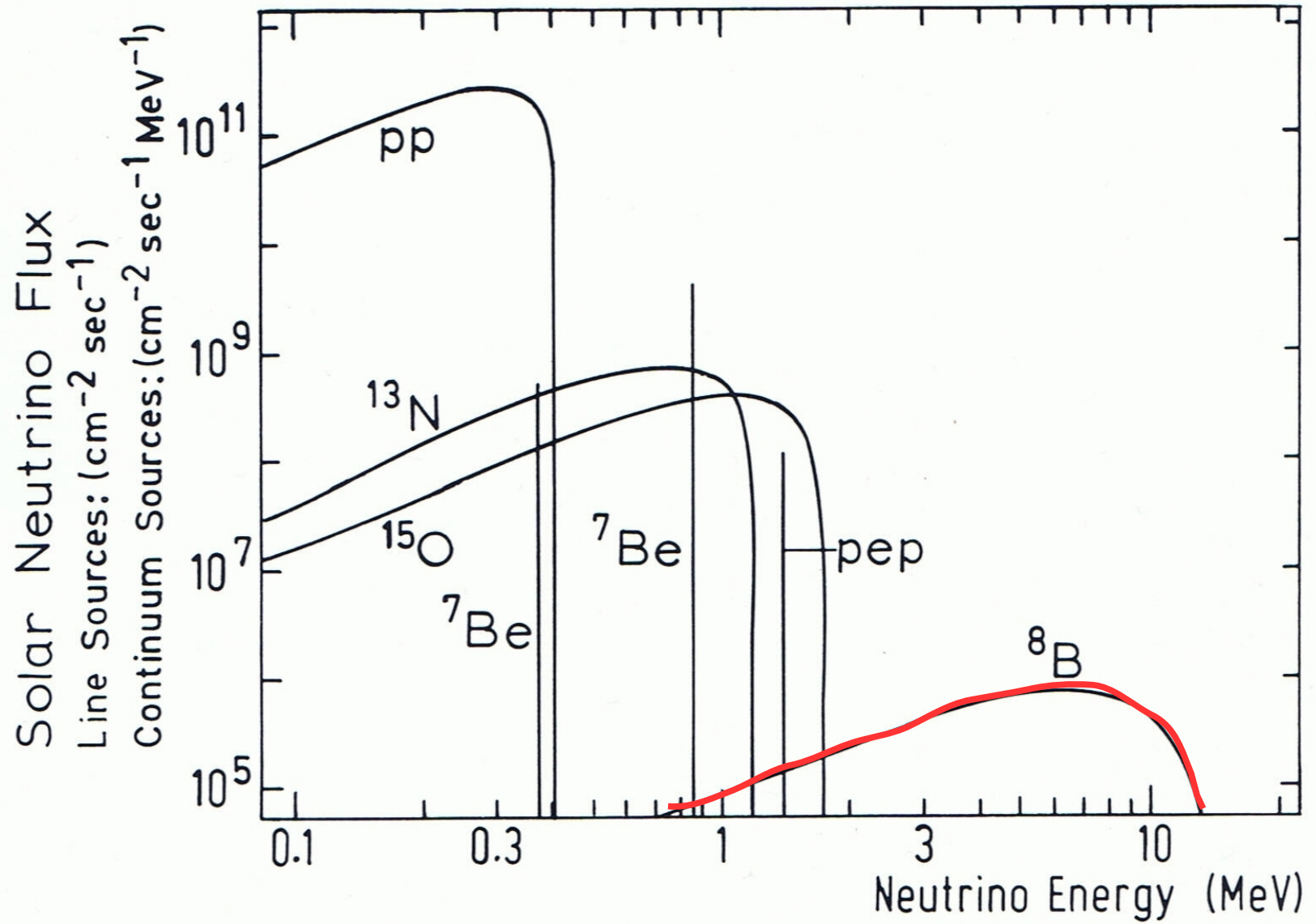
**Strong dependence on the zenith angle**

Results in the multi-GeV region ( $E_{\text{lepton}} > 1.3 \text{ GeV}$ )

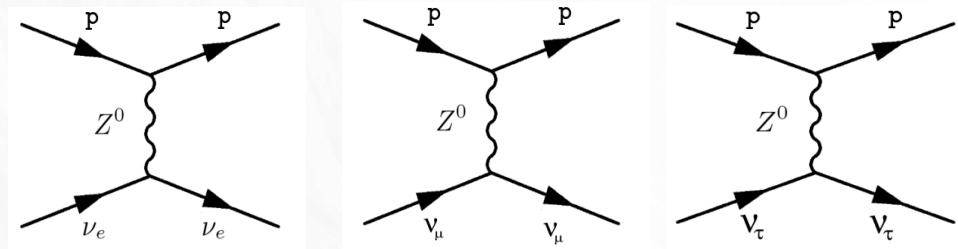
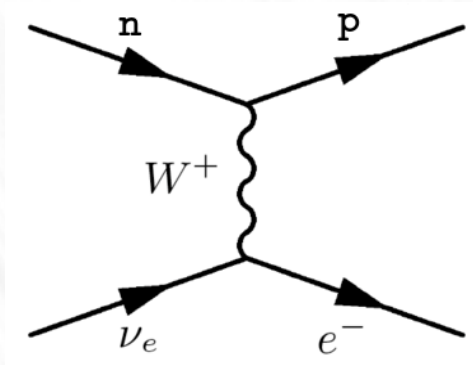
## 4 Solar Neutrinos at the Sudbury Neutrino Observatory (SNO)



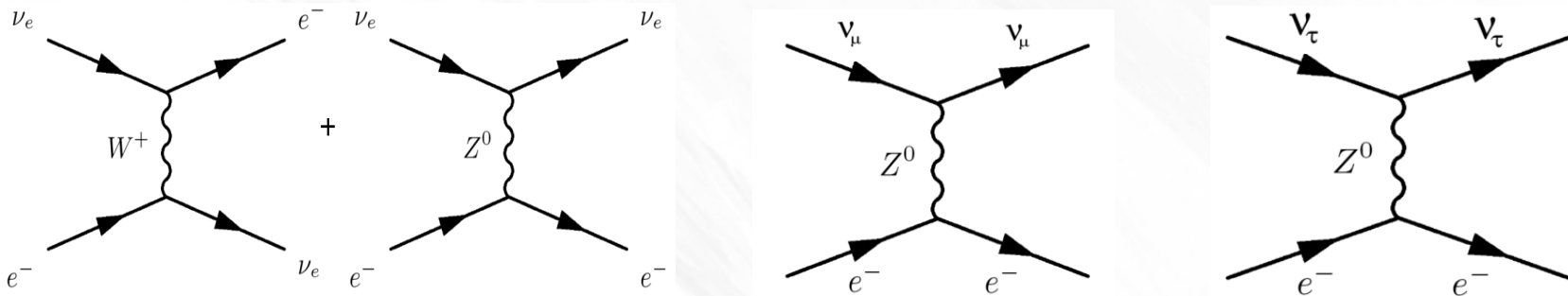
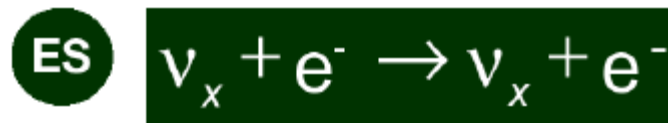
Remember: Solar neutrino fluxes



# Reaction channels, detection and identification



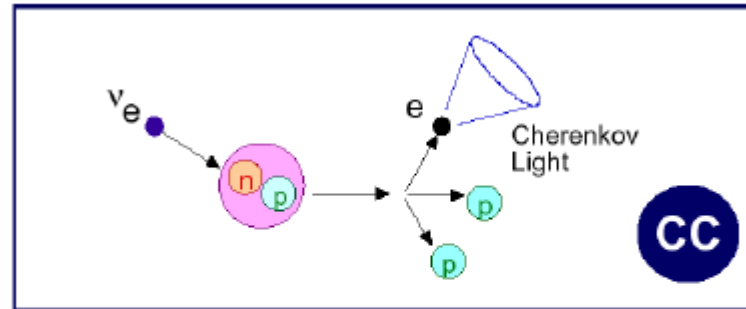
+ interactions with the neutron from deuterium



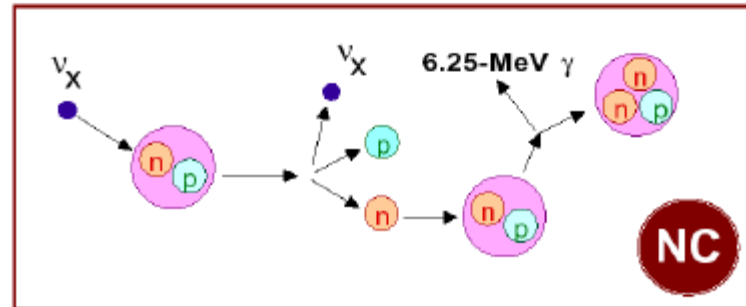
# Reaction channels, detection and identification



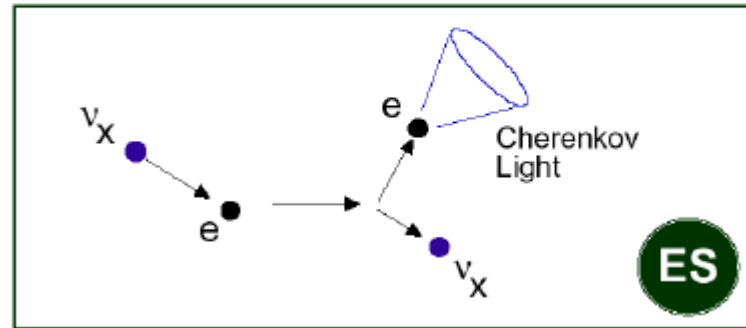
- Measurement of  $\nu_e$  energy spectrum
- Weak directionality:  $1 - 0.340 \cos\theta$



- Measure total  $^8\text{B}$   $\nu$  flux from the sun
- $\sigma(\nu_e) = \sigma(\nu_\mu) = \sigma(\nu_\tau)$



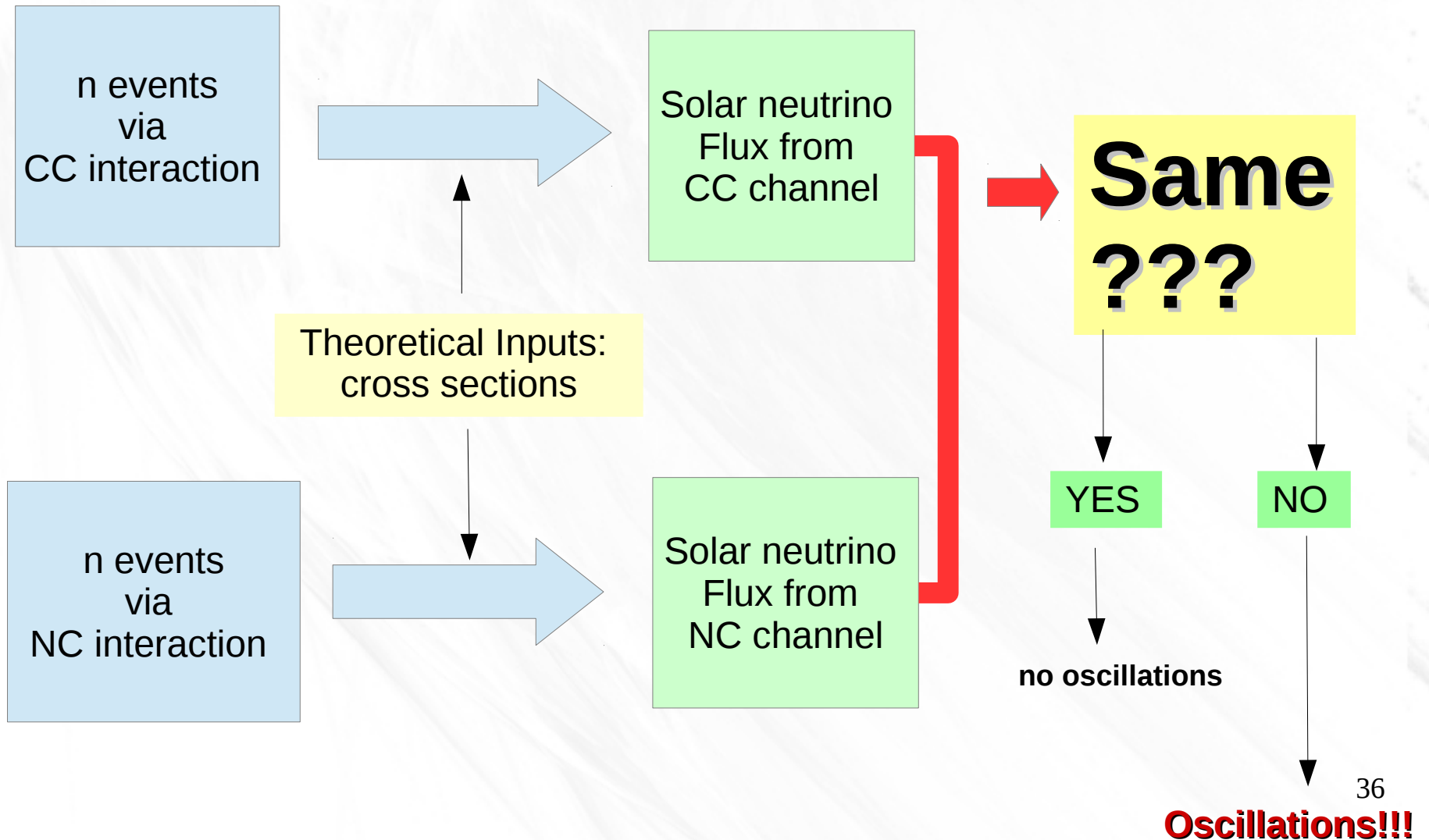
- Low Statistics
- $\Sigma\phi = \phi(\nu_e) + 0.154 \phi(\nu_\mu + \nu_\tau)$
- Strong directionality:  
 $\theta_e \leq 18^\circ$  ( $T_e = 10 \text{ MeV}$ )



- CC and ES channel. Total amount of Cerenkov light is correlated with the energy of the incoming neutrino.
- NC channel. Detection of neutrons: 6.25 MeV gamma rays due to neutron capture on  $^3\text{H}$  deuterium. The gamma rays produce Compton electrons or  $e^+e^-$  pairs. The Cerenkov light from these is detected.

Image from [http://www.kip.uni-heidelberg.de/~coulon/Lectures/SM/Free\\_PDFs/Lecture\\_HC\\_13.pdf](http://www.kip.uni-heidelberg.de/~coulon/Lectures/SM/Free_PDFs/Lecture_HC_13.pdf)

# Oscillations??



# RESULTS

Data recorded between 2 November 1999 and 28 May 2001.

After analyses:

$1967.7^{+61.9}_{-60.9}$  CC events,

$263.6^{+26.4}_{-25.6}$  ES events,

$576.5^{+49.5}_{-48.9}$  NC events

These events correspond to the following fluxes

if no-oscillations are considered

$$\phi_{\text{CC}}^{\text{SNO}} = 1.76^{+0.06}_{-0.05}(\text{stat})^{+0.09}_{-0.09}(\text{syst}),$$

$$\phi_{\text{ES}}^{\text{SNO}} = 2.39^{+0.24}_{-0.23}(\text{stat})^{+0.12}_{-0.12}(\text{syst}),$$

$$\phi_{\text{NC}}^{\text{SNO}} = 5.09^{+0.44}_{-0.43}(\text{stat})^{+0.46}_{-0.43}(\text{syst}).$$

All fluxes in units:  
 $10^6 \text{ cm}^{-2} \text{ s}^{-1}$

**The excess of the NC flux over the CC and ES fluxes implies neutrino flavor transformations**

Note that the NC is in excellent agreement with the prediction for the 8B flux by the Standard Solar Model (SSM).

$$\phi_{\text{SSM}} = 5.05^{+1.01}_{-0.81}$$

# RESULTS

Data recorded between 2 November 1999 and 28 May 2001.

After analyses:

$1967.7^{+61.9}_{-60.9}$  CC events,

$263.6^{+26.4}_{-25.6}$  ES events,

$576.5^{+49.5}_{-48.9}$  NC events

These events correspond to the following fluxes

if no-oscillations are considered

$$\phi_{\text{CC}}^{\text{SNO}} = 1.76^{+0.06}_{-0.05}(\text{stat})^{+0.09}_{-0.09}(\text{syst}),$$

$$\phi_{\text{ES}}^{\text{SNO}} = 2.39^{+0.24}_{-0.23}(\text{stat})^{+0.12}_{-0.12}(\text{syst}),$$

$$\phi_{\text{NC}}^{\text{SNO}} = 5.09^{+0.44}_{-0.43}(\text{stat})^{+0.46}_{-0.43}(\text{syst}).$$

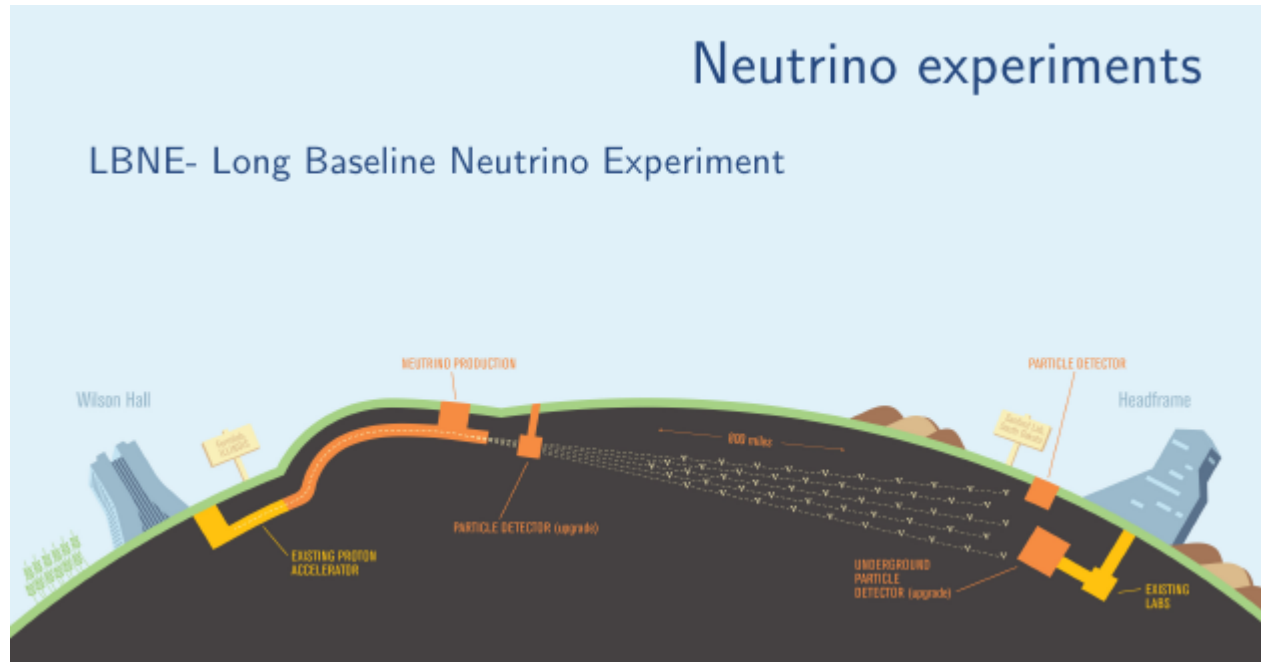
All fluxes in units:  
 $10^6 \text{ cm}^{-2} \text{ s}^{-1}$

**The excess of the NC flux over the CC and ES fluxes implies neutrino flavor transformations**

Note that the NC is in excellent agreement with the prediction for the 8B flux by the Standard Solar Model (SSM).

$$\phi_{\text{SSM}} = 5.05^{+1.01}_{-0.81}$$

# Accelerator-based neutrino oscillation experiments



$$P(\nu_x \rightarrow \nu_y) = \sin^2 2\theta \sin^2 \left( 1.27 \frac{\Delta m^2 (eV^2) L (km)}{E (GeV)} \right)$$

## Some accelerator-based neutrino experiments

Experiment	Physics studied	Status
MiniBooNE	Neutrino oscillations	Finnished
T2K	$\theta_{13}, \theta_{23}, \Delta m_{13}^2, \Delta m_{23}^2$	Running
ArgoNeuT	Neutrino interactions, LArTPC	Analysis
Minerva	Neutrino interactions	Running
MINOS	$\theta_{13}, \theta_{23}, \Delta m_{13}^2, \Delta m_{23}^2$	Running
No $\nu$ a	$\theta_{13}, \theta_{23}, \Delta m_{13}^2, \Delta m_{23}^2, \delta_{CP}$	Under construction
LBNE	$\theta_{13}, \theta_{23}, \Delta m_{13}^2, \Delta m_{23}^2, \delta_{CP}$	In development
Hyper-K	$\theta_{13}, \theta_{23}, \Delta m_{13}^2, \Delta m_{23}^2, \delta_{CP}$	Proposed

(2015)

# Goals of the Neutrino Oscillation Programme

## NuSTEC<sup>a</sup> White Paper: Status and Challenges of Neutrino-Nucleus Scattering

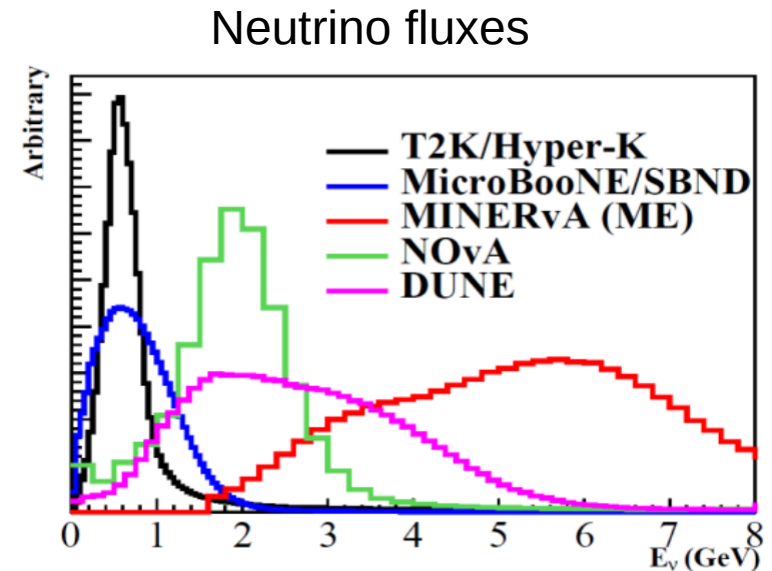
L. Alvarez-Ruso,<sup>1</sup> M. Sajjad Athar,<sup>2</sup> M. B. Barbaro,<sup>3</sup> D. Cherdack,<sup>4</sup> M. E. Christy,<sup>5</sup> P. Coloma,<sup>6</sup> T. W. Donnelly,<sup>7</sup> S. Dytman,<sup>8</sup> A. de Gouvêa,<sup>9</sup> R. J. Hill,<sup>10,6</sup> P. Huber,<sup>11</sup> N. Jachowicz,<sup>12</sup> T. Katori,<sup>13</sup> A. S. Kronfeld,<sup>6</sup> K. Mahn,<sup>14</sup> M. Martini,<sup>15</sup> J. G. Morfín,<sup>6</sup> J. Nieves,<sup>1</sup> G. Perdue,<sup>6</sup> R. Petti,<sup>16</sup> D. G. Richards,<sup>17</sup> F. Sánchez,<sup>18</sup> T. Sato,<sup>19,20</sup> J. T. Sobczyk,<sup>21</sup> and G. P. Zeller<sup>6</sup>

1. establish whether nature violates CP in the lepton sector and, if so, measure  $\delta_{CP}$ ;
2. improve the accuracy on  $\theta_{23}$  and, if not maximal, a determination of the octant it belongs to:  $\theta_{23} < \pi/4$  vs.  $\theta_{23} > \pi/4$ ;
3. determine the neutrino mass ordering at high confidence level:  $m_1 < m_2 < m_3$  vs.  $m_3 < m_1 < m_2$ .

	$\theta_{12}$	$\theta_{13}$	$\theta_{23}$	$\Delta m_{21}^2/10^{-5}$	$\Delta m_{3j}^2/10^{-3}$	$\delta_{CP}$
Normal Ordering	$33.56^{+0.77}_{-0.75}$	$8.46^{+0.15}_{-0.15}$	$41.6^{+1.5}_{-1.2}$	$7.50^{+0.19}_{-0.17}$	$2.524^{+0.039}_{-0.040}$	$261^{+51}_{-59}$
Inverted Ordering	$33.56^{+0.77}_{-0.75}$	$8.49^{+0.15}_{-0.15}$	$50.0^{+1.1}_{-1.4}$	$7.50^{+0.19}_{-0.17}$	$-2.514^{+0.038}_{-0.041}$	$277^{+40}_{-46}$

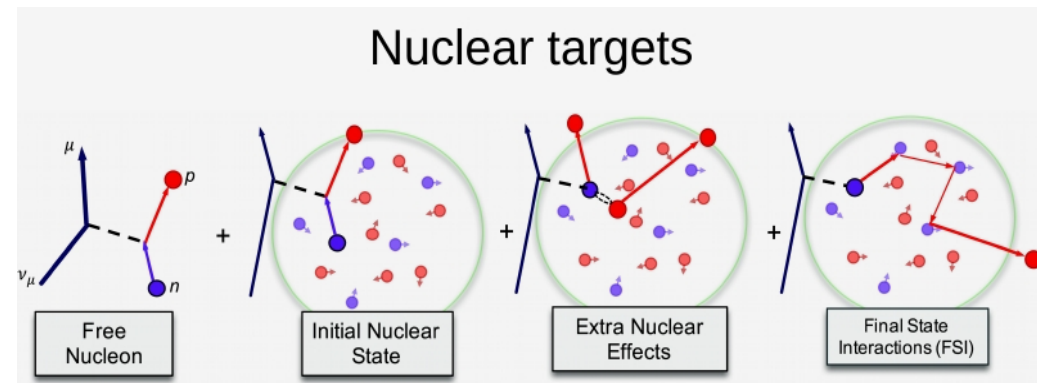
## Two major problems slow down this programme:

**1. Neutrino beams**, contrary to electron beams, are **not mono-energetic**. One needs to model all reactions channels in the broad energy band covered by the neutrino beam.



## 2. “Complex” nuclear targets (compared to the 'easy-to-model' $H_2$ target).

The necessity to accumulate huge amounts of detector material makes it impossible to use the (explosive!) hydrogen target. The use of other molecules, made of more complex nuclei, such as mineral oils ( $CH_x$ ), **water**, or liquid **argon**, allows for the accumulation of tons of detector material, thereby notably increasing the number of events in the detectors.



plot by C. Wilkinson (NUISANCE)

# Determining the oscillation probability

Number of events

$$N_{\beta}(E_{\nu}?) \sim \underbrace{\Phi_{\nu_{\alpha}}(E_{\nu})}_{\nu \text{ flux}} \underbrace{\sigma_{\nu_{\beta}}(E_{\nu})}_{\nu \text{ cross section}} \underbrace{\varepsilon_{det.}}_{\text{Detector efficiency}} \underbrace{P_{\nu_{\alpha} \rightarrow \nu_{\beta}}(\{\Theta\}, E_{\nu})}_{\nu \text{ Energy in the oscillation probability}}$$

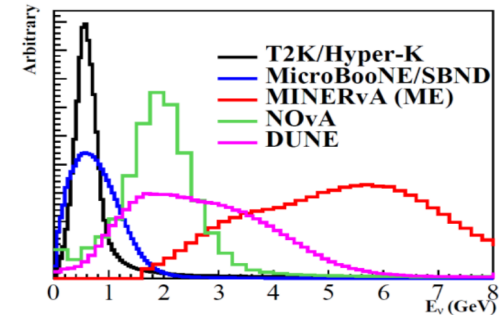
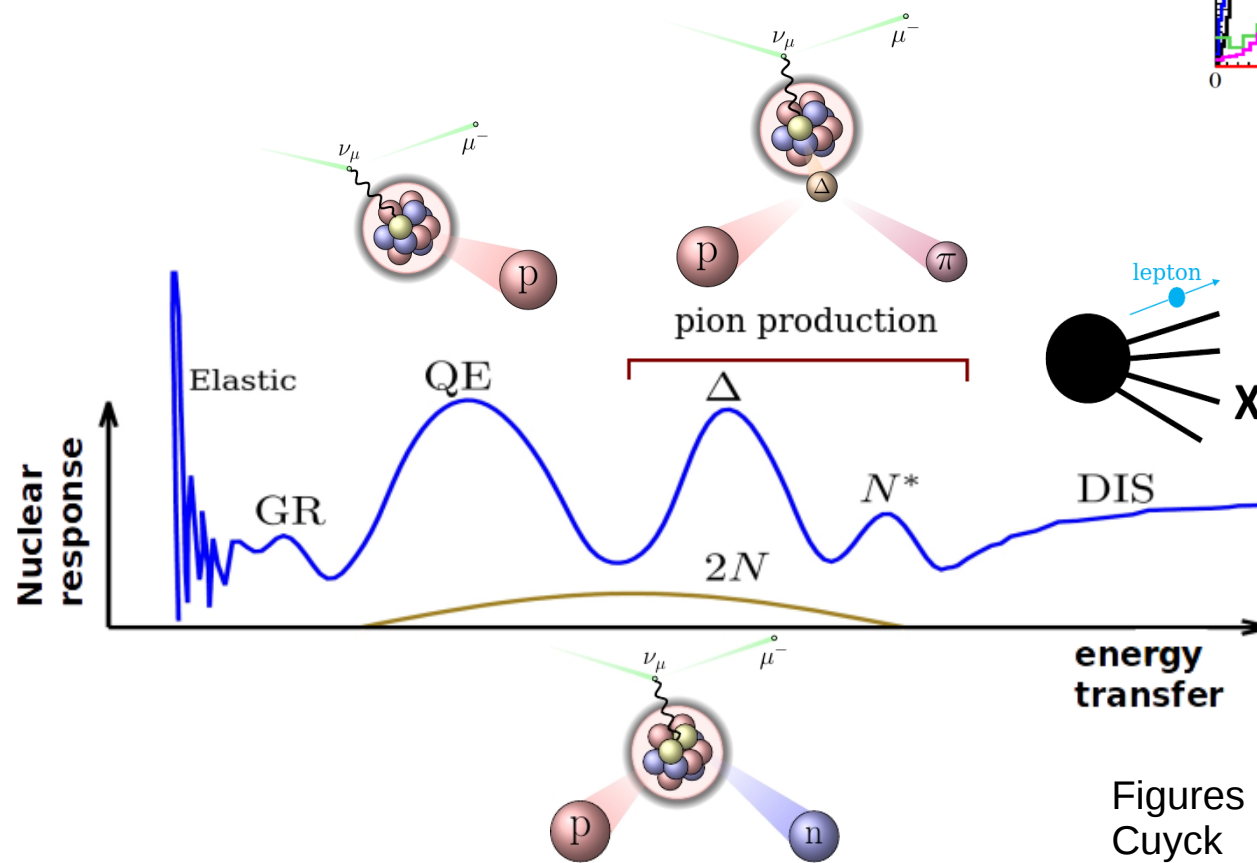
$\nu_{\alpha} \rightarrow \nu_{\beta}$

Adapted from M.Martini (NuFact17)

- 1) 'Number of event' corresponding to a given topology are measured in the detector (event distribution).
- 2) The energy of the incident neutrino that caused that event is unknown.
- 3) **This neutrino energy is reconstructed** combining theoretical information (cross sections) and experimental data.  
The reconstruction procedure introduce important uncertainties in the oscillation analyses.
- 4) The probability  $P_{\alpha \rightarrow \beta}$  is determined for each neutrino energy.

# What we know from (e,e')

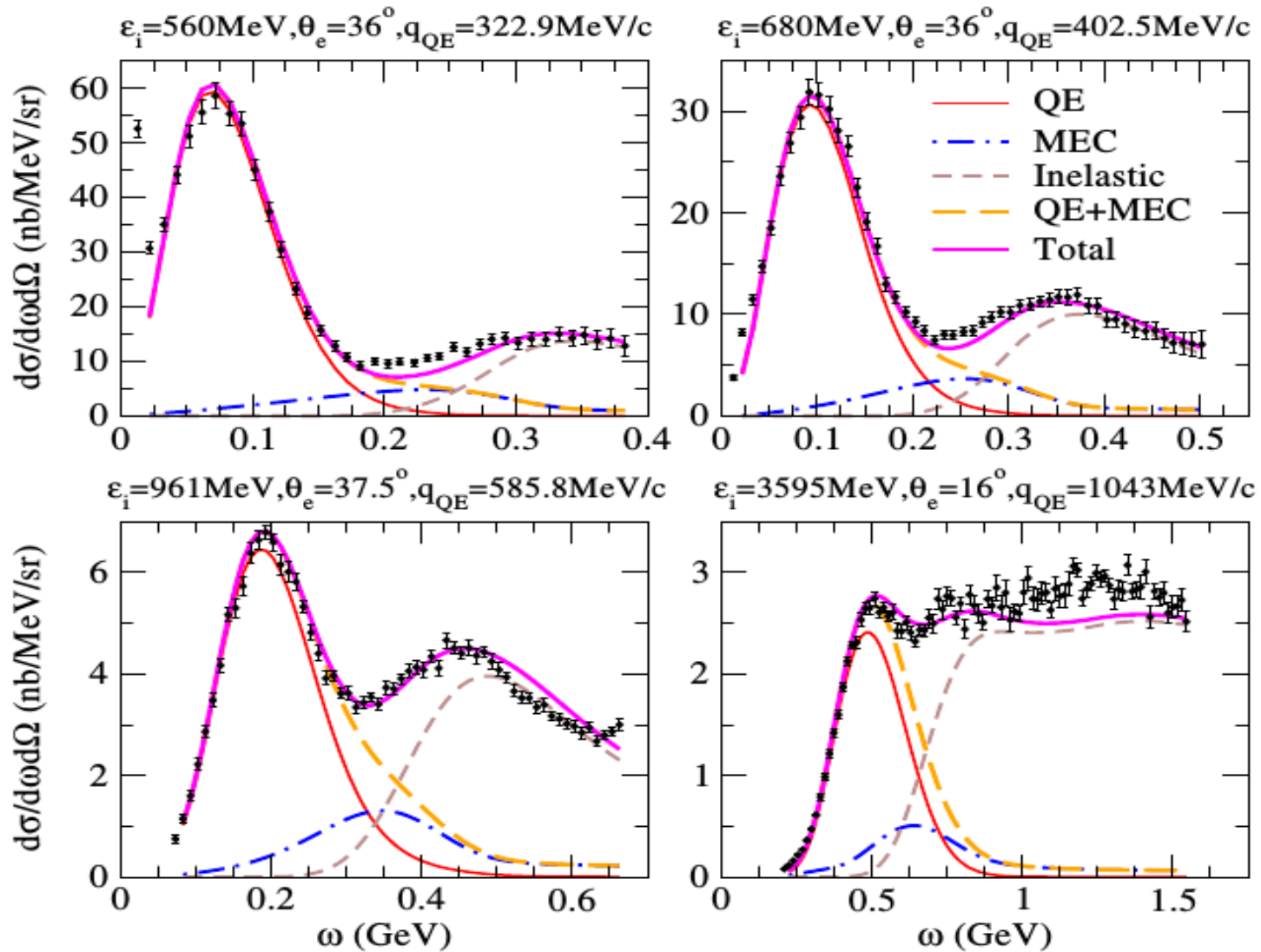
One needs to model all neutrino-nucleus reaction channels covered by the neutrino beam



Figures by T. Van Cuyck

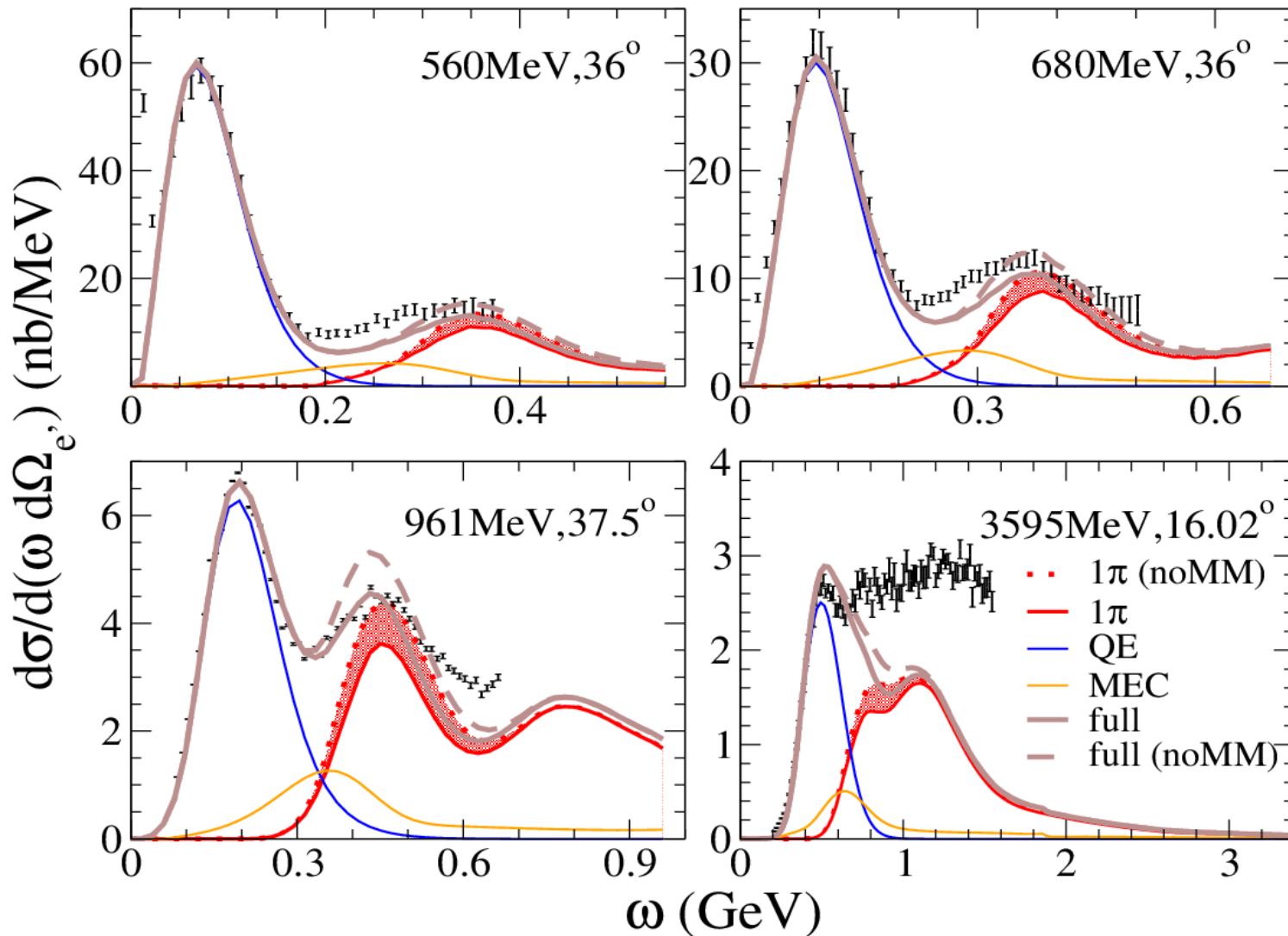
# What we know from (e,e')

Superscaling approach (Megias et al., Phys. Rev. D 91, 073004 (2015) )



$^{12}\text{C}(e,e')$

# What we know from (e,e')



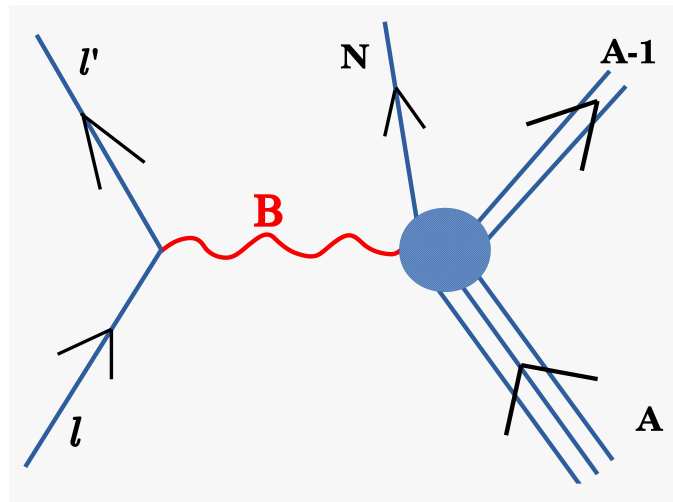
$^{12}\text{C}(e,e')$

**QE (SuSAv2):**  
RGJ et al., PRC 90,  
035501 (2014)

**MEC:** Megias et al.,  
PRD 91, 073004  
(2015)

**1pion:** RGJ et al.,  
PRD 95, 113007  
(2017);  
arXiv:1710.08374

# Quasielastic scattering



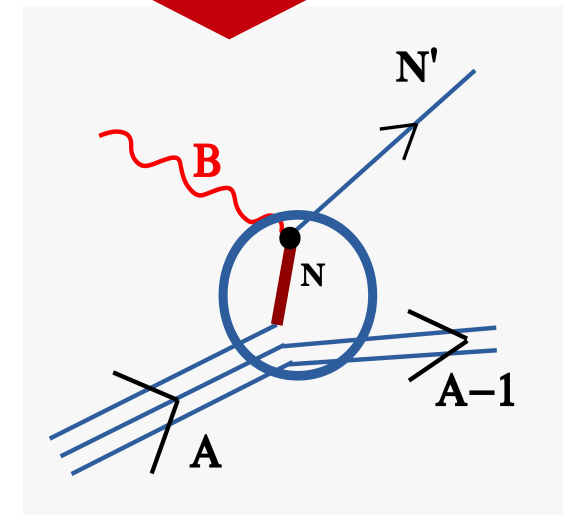
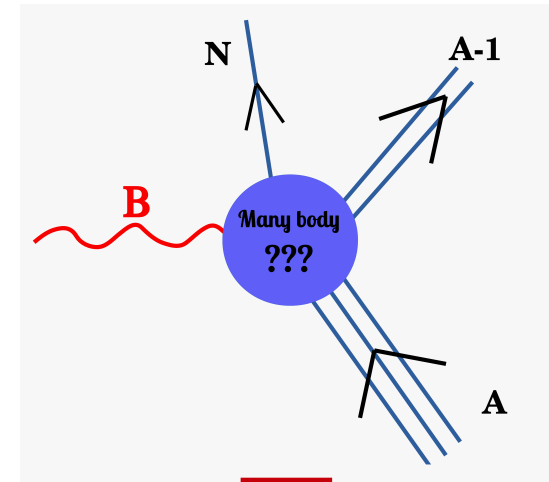
# Impulse approximation

$$J_{had}^{\mu} = \langle N, A - 1 | \hat{O}_{many-body}^{\mu} | A \rangle$$

**Impulse  
Approximation**

$$J_{had}^{\mu} = \sum_i^A \int d\mathbf{r} \bar{\Psi}_F(\mathbf{r}) \hat{O}_{one-body}^{\mu} \Psi_B(\mathbf{r}) e^{i\mathbf{q}\cdot\mathbf{r}}$$

where 
$$\hat{O}_{one-body}^{\mu} = F_1 \gamma^{\mu} + i \frac{F_2}{2M_N} \sigma^{\mu\alpha} Q_{\alpha}$$



# Impulse approximation

$$J_{had}^{\mu} = \langle N, A - 1 | \hat{O}_{many-body}^{\mu} | A \rangle$$

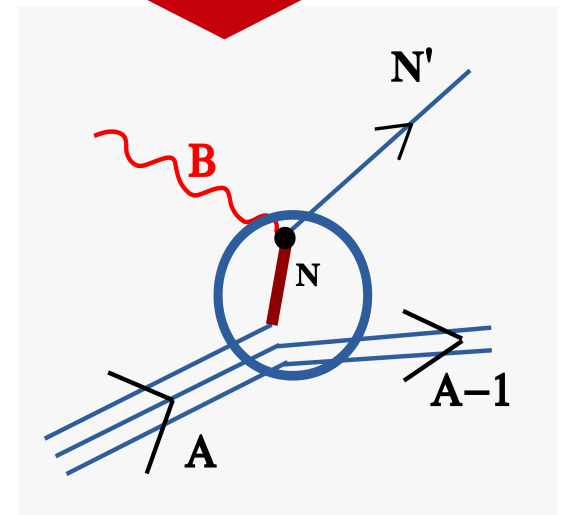
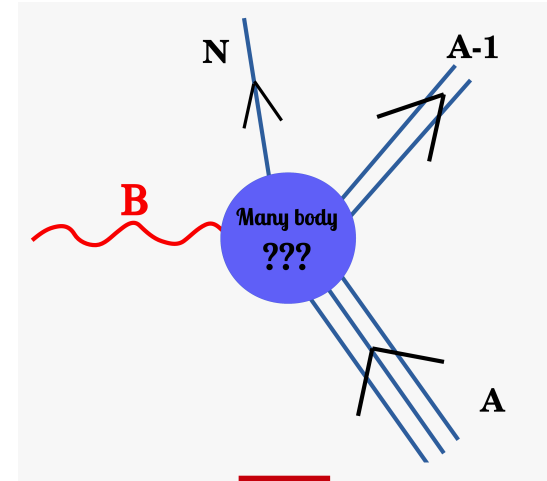
**Impulse  
Approximation**

**Relativistic mean-  
field wave functions**

$$J_{had}^{\mu} = \sum_i^A \int dr \bar{\Psi}_F(\mathbf{r}) \hat{O}_{one-body}^{\mu} \Psi_B(\mathbf{r}) e^{i\mathbf{q}\cdot\mathbf{r}}$$

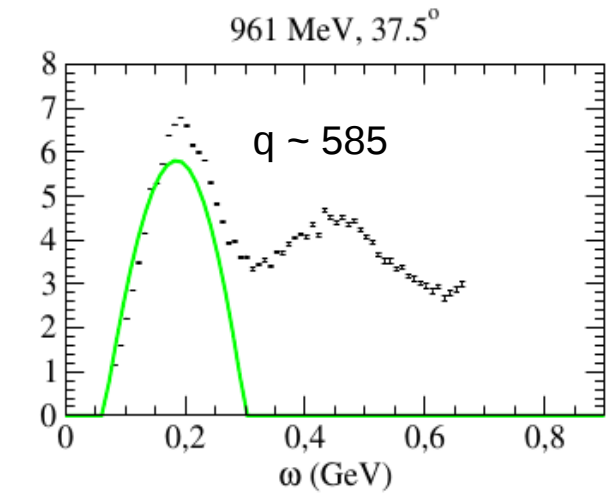
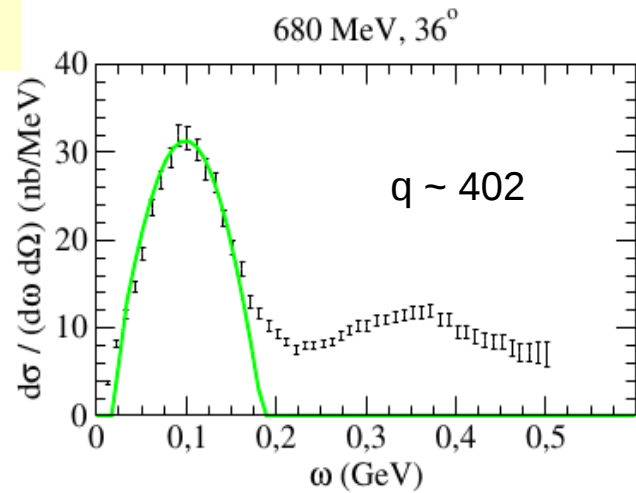
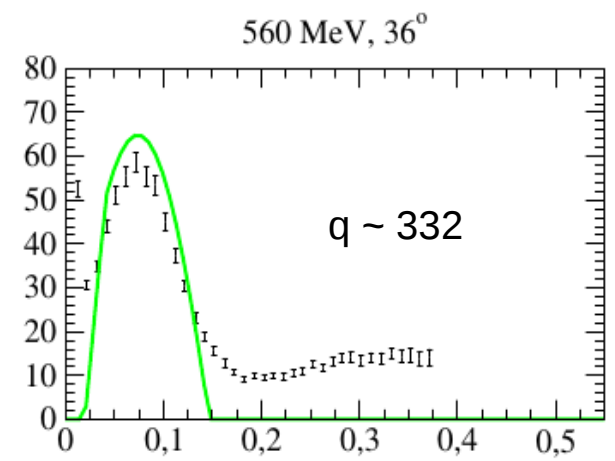
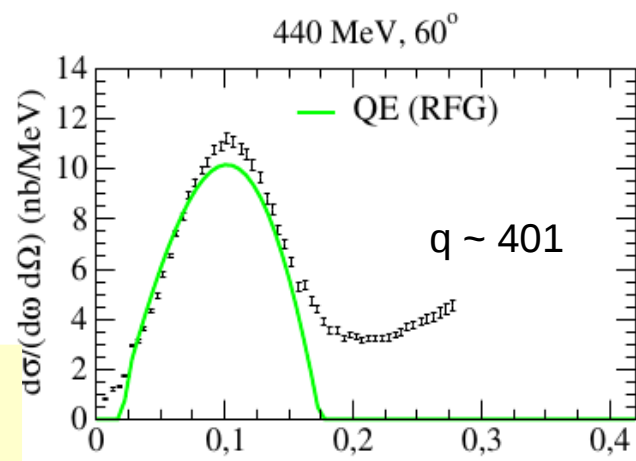
where

$$\hat{O}_{one-body}^{\mu} = F_1 \gamma^{\mu} + i \frac{F_2}{2M_N} \sigma^{\mu\alpha} Q_{\alpha}$$

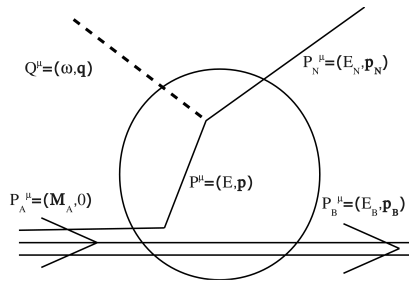


# Mean-field vs plane waves

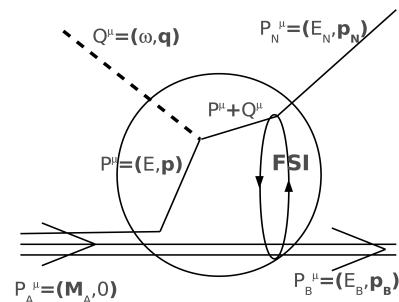
Intermediate energies (typical QE regime)



# Mean-field vs plane waves



**RPWIA:** Scattered nucleon wf is described as a Dirac plane wave.

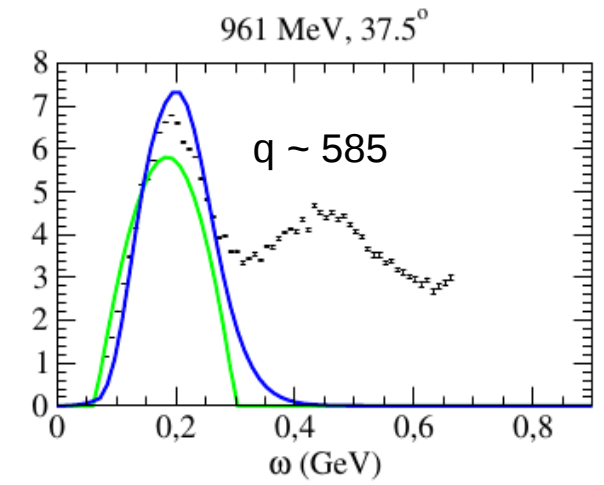
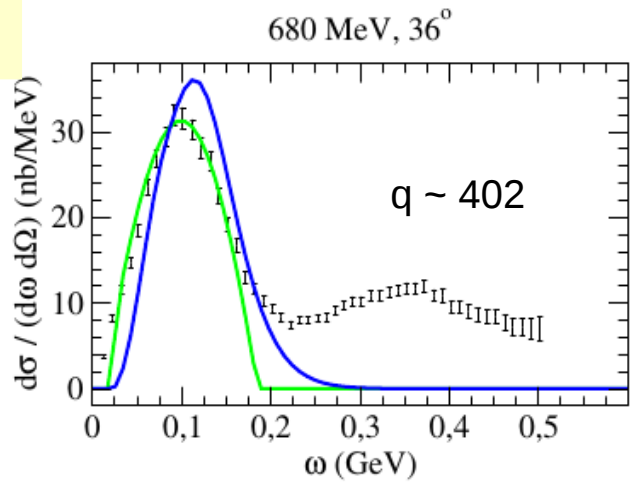
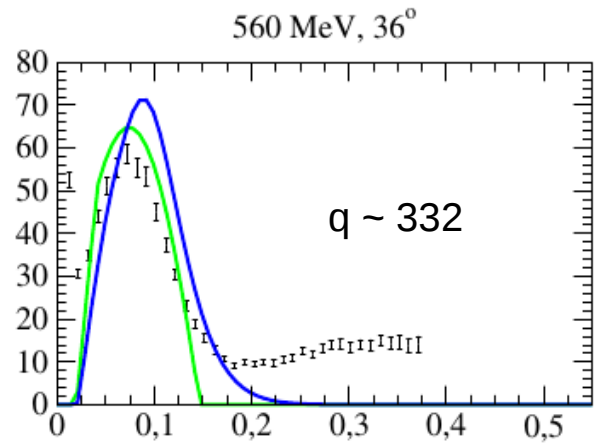
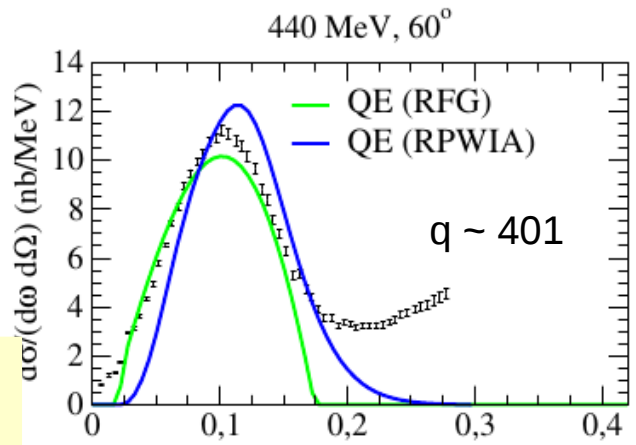


**RMF-FSI:** Scattered nucleon wf is solution of Dirac eq. in presence of the same potentials used to describe the bound nucleon wf.

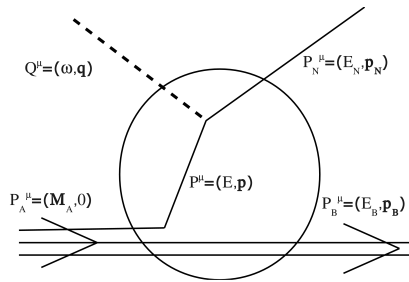
$$[-i\alpha \cdot \nabla + V(r) + \beta(M + S(r))]\Psi_i(\mathbf{r}) = E_i\Psi_i(\mathbf{r})$$

$$J_{had}^\mu = \sum_i^A \int d\mathbf{r} \bar{\Psi}_F(\mathbf{r}) \hat{O}_{one-body}^\mu \Psi_B(\mathbf{r}) e^{i\mathbf{q}\cdot\mathbf{r}}$$

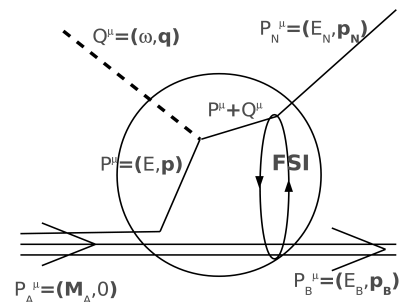
Intermediate energies (typical QE regime)



# Mean-field vs plane waves



**RPWIA:** Scattered nucleon wf is described as a Dirac plane wave.

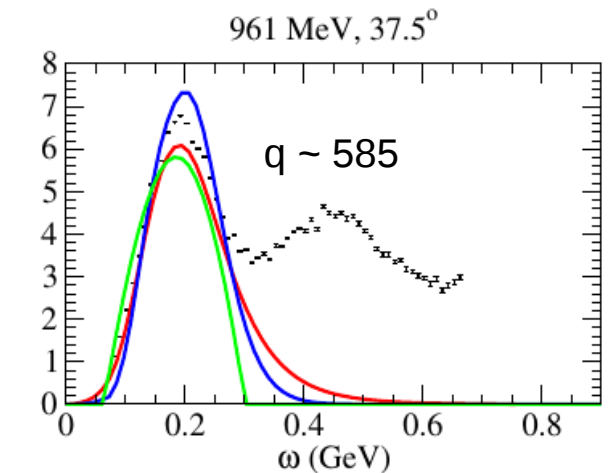
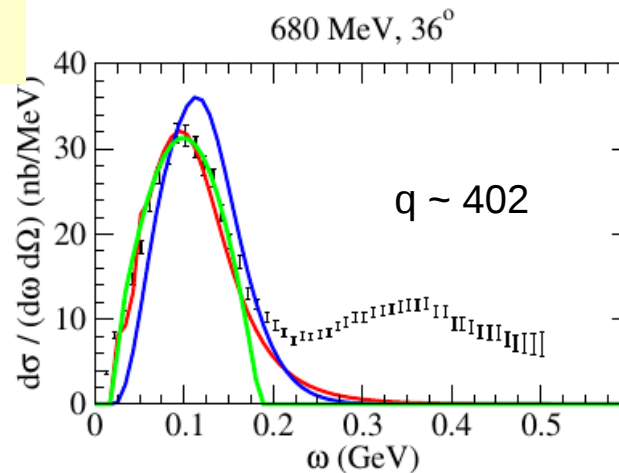
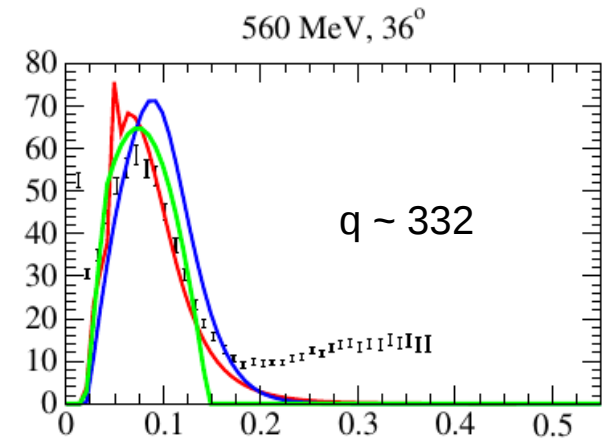
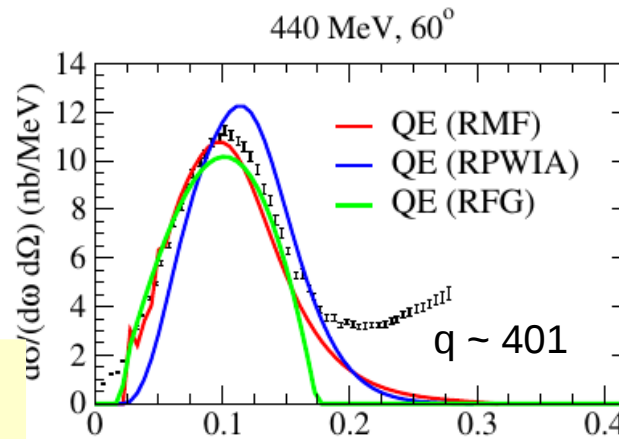


**RMF-FSI:** Scattered nucleon wf is solution of Dirac eq. in presence of the same potentials used to describe the bound nucleon wf.

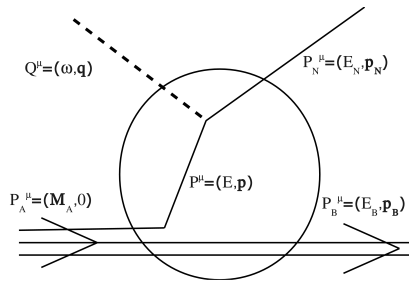
$$[-i\alpha \cdot \nabla + V(r) + \beta(M + S(r))]\Psi_i(\mathbf{r}) = E_i\Psi_i(\mathbf{r})$$

$$J_{had}^\mu = \sum_i^A \int d\mathbf{r} \bar{\Psi}_F(\mathbf{r}) \hat{O}_{one-body}^\mu \Psi_B(\mathbf{r}) e^{i\mathbf{q}\cdot\mathbf{r}}$$

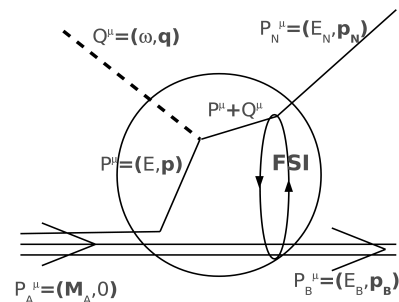
Intermediate energies (typical QE regime)



# Mean-field vs plane waves



**RPWIA:** Scattered nucleon wf is described as a Dirac plane wave.

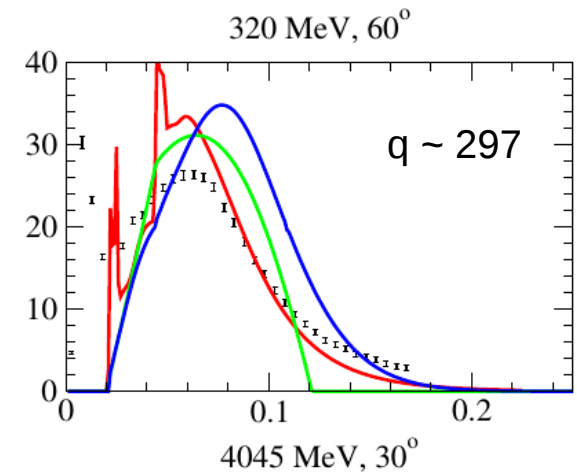
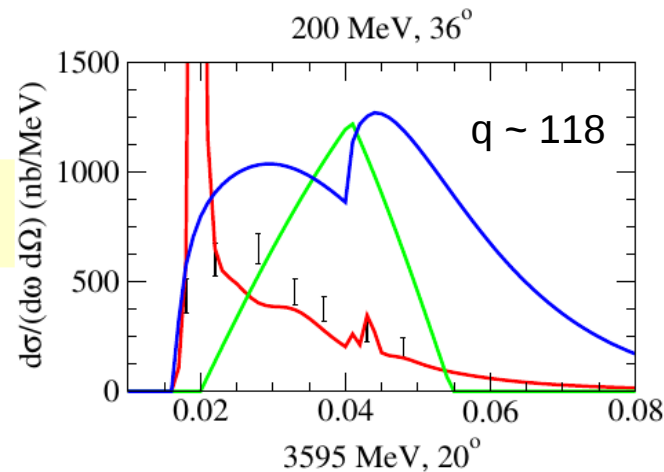


**RMF-FSI:** Scattered nucleon wf is solution of Dirac eq. in presence of the same potentials used to describe the bound nucleon wf.

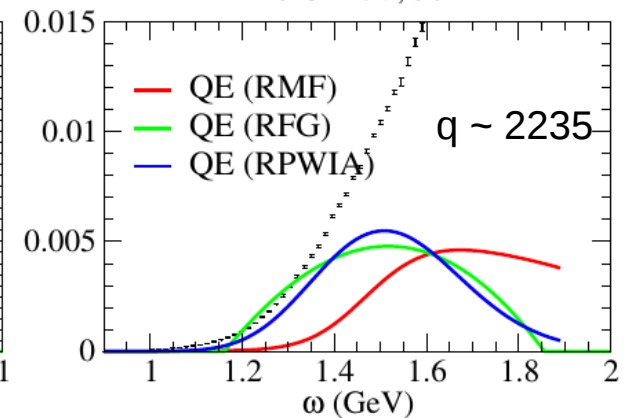
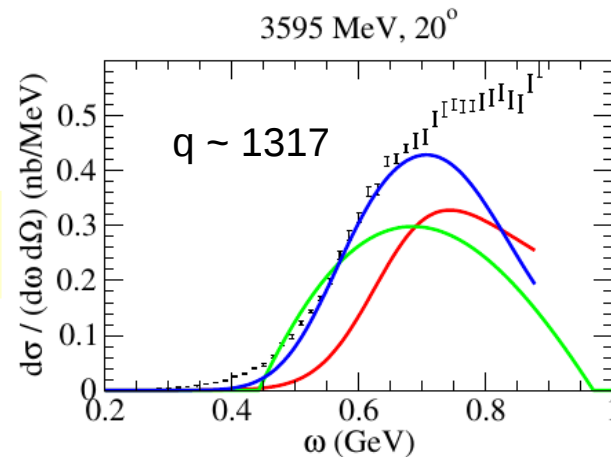
$$[-i\alpha \cdot \nabla + V(r) + \beta(M + S(r))]\Psi_i(\mathbf{r}) = E_i\Psi_i(\mathbf{r})$$

$$J_{had}^\mu = \sum_i^A \int d\mathbf{r} \bar{\Psi}_F(\mathbf{r}) \hat{O}_{one-body}^\mu \Psi_B(\mathbf{r}) e^{i\mathbf{q}\cdot\mathbf{r}}$$

Low energies



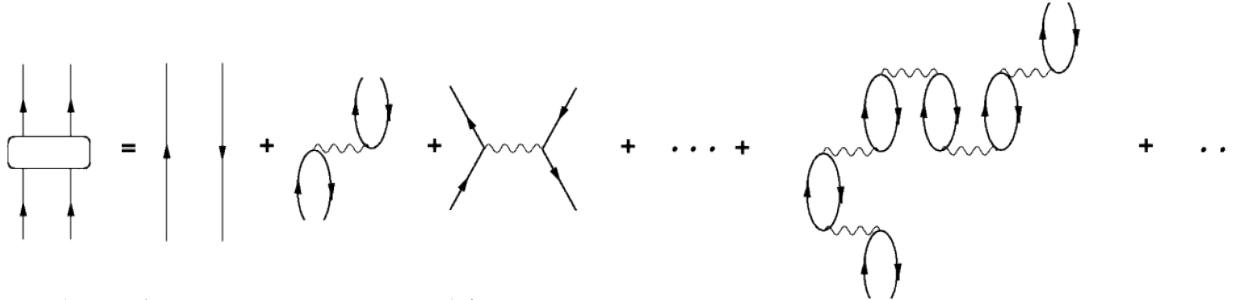
High energies



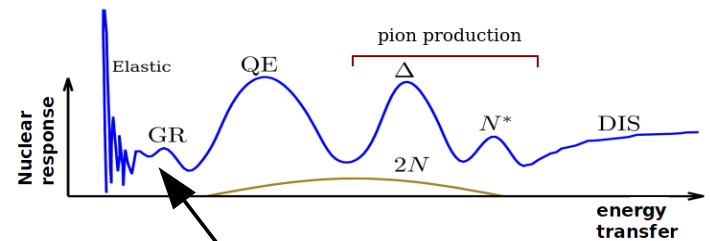
# Long-range correlations: CRPA model

+ Long-range correlations between the nucleons are introduced through a **continuum Random Phase Approximation (CRPA)**.

+ RPA equations are solved using a Green's function approach.



$$\begin{aligned} \Pi^{(RPA)}(x_1, x_2; \omega) &= \Pi^{(0)}(x_1, x_2; \omega) \\ &+ \frac{1}{\hbar} \int dx \int dx' \Pi^{(0)}(x_1, x; \omega) \tilde{V}(x, x') \Pi^{(RPA)}(x', x_2; \omega) \end{aligned}$$



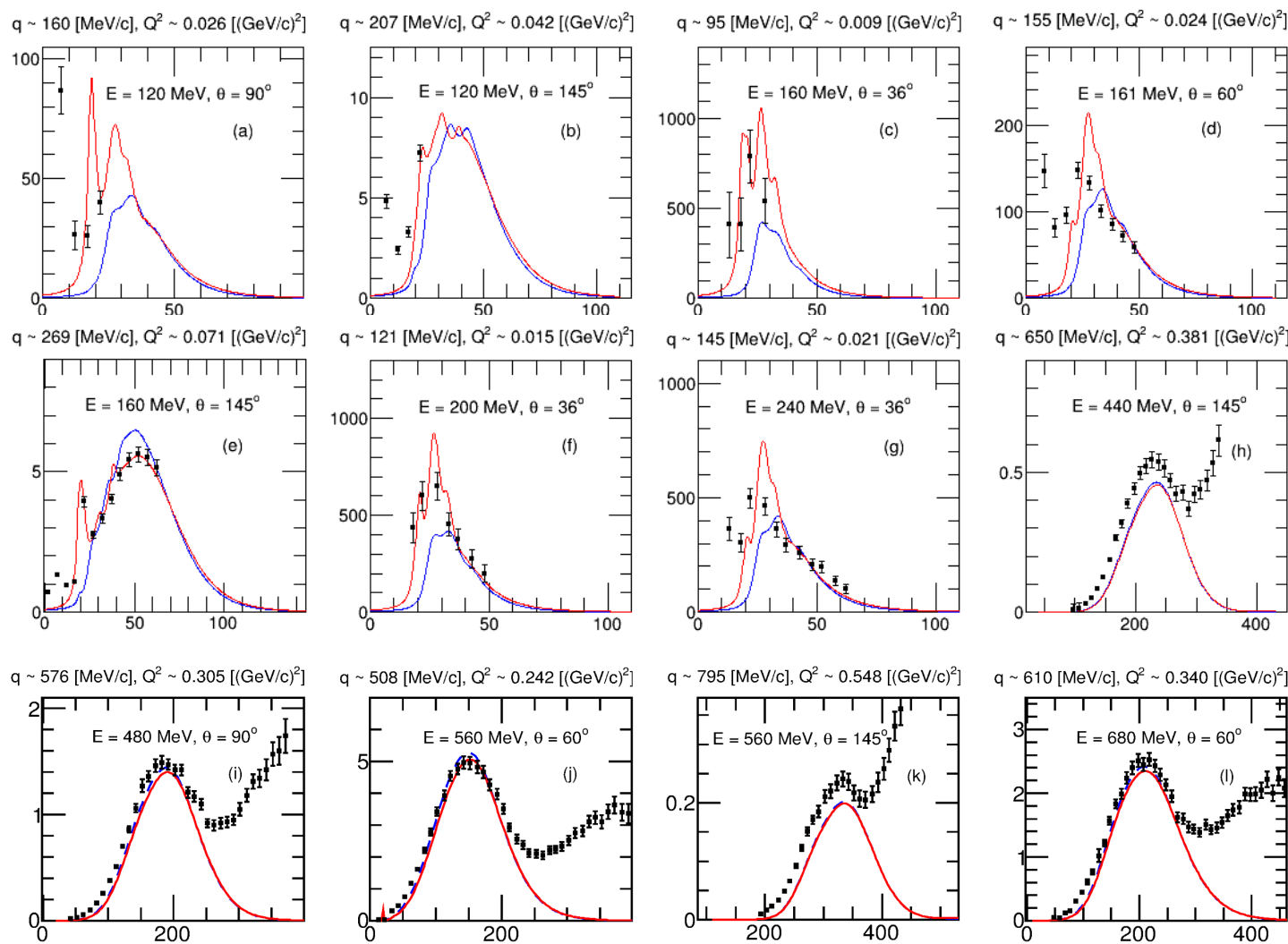
**Giant Resonance (GR) region: collective nuclear effects**

Excitations are obtained as linear combinations of different particle-hole configurations.

$$|\Psi_{RPA}\rangle = \sum_c \left\{ X_{(\Psi, C)} |ph^{-1}\rangle - Y_{(\Psi, C)} |hp^{-1}\rangle \right\}$$

# Long-range correlations: CRPA model

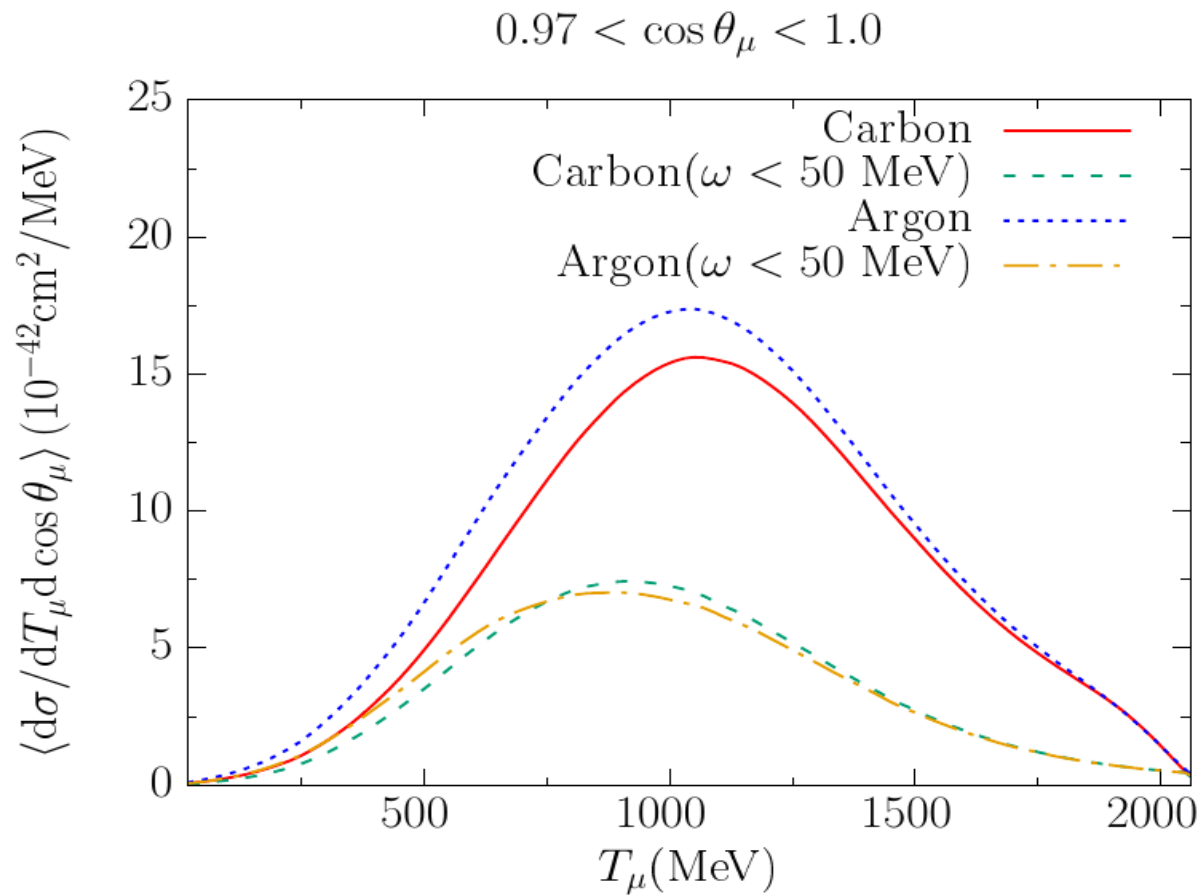
## $^{12}\text{C}(e, e')$



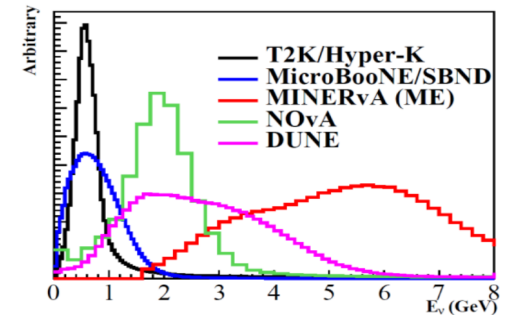
**HF (blue) vs  
CRPA (red)**

[V. Pandey PhD  
Thesis; PRC 92,  
024606 (2015)]

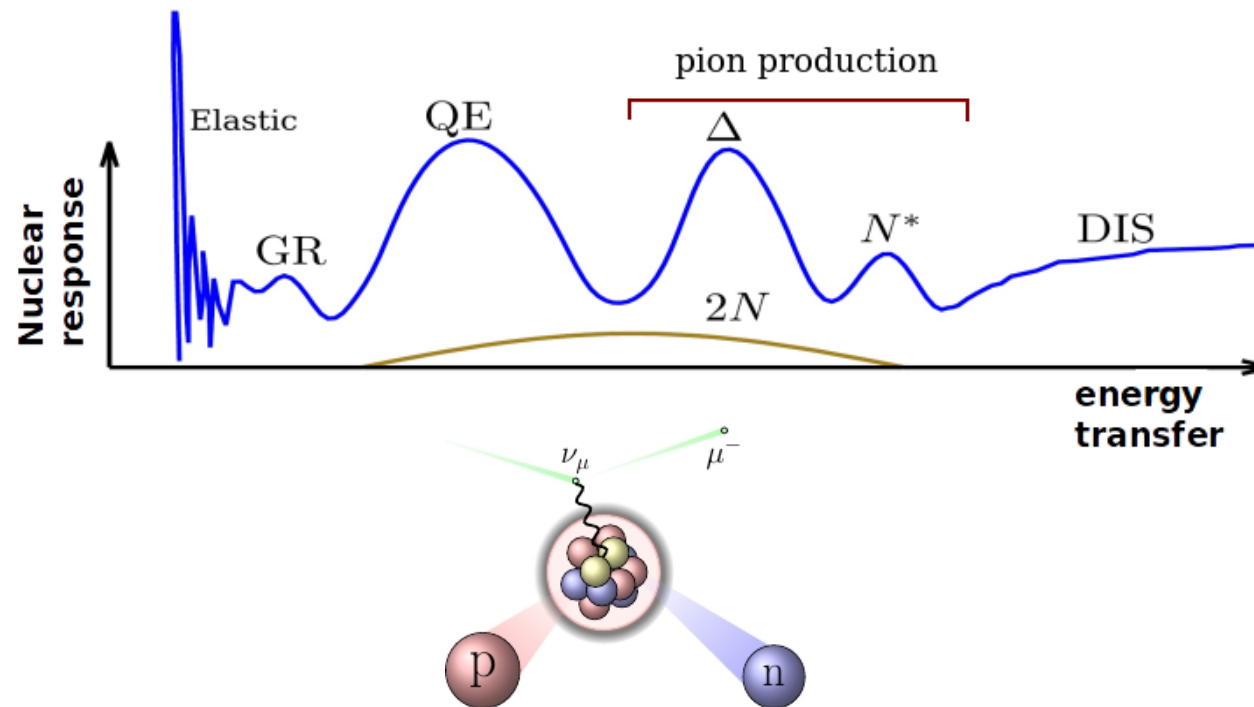
# Low-energy contributions in flux-folded XS



MicroBooNE flux-folded cross section.



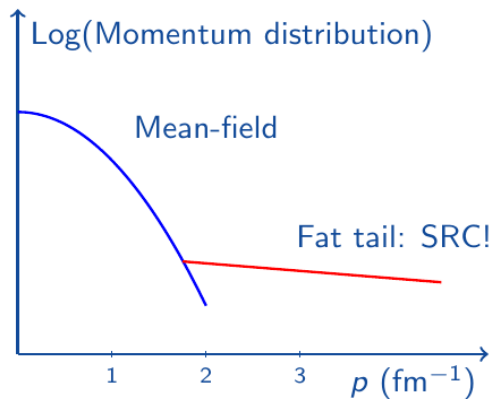
# Two-nucleon knockout processes



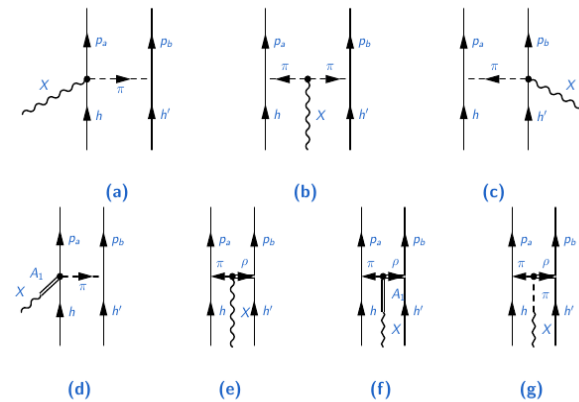
# Two-nucleon knockout processes

In our approach, two mechanisms give rise to the emission of two nucleons:

## Short-range correlations

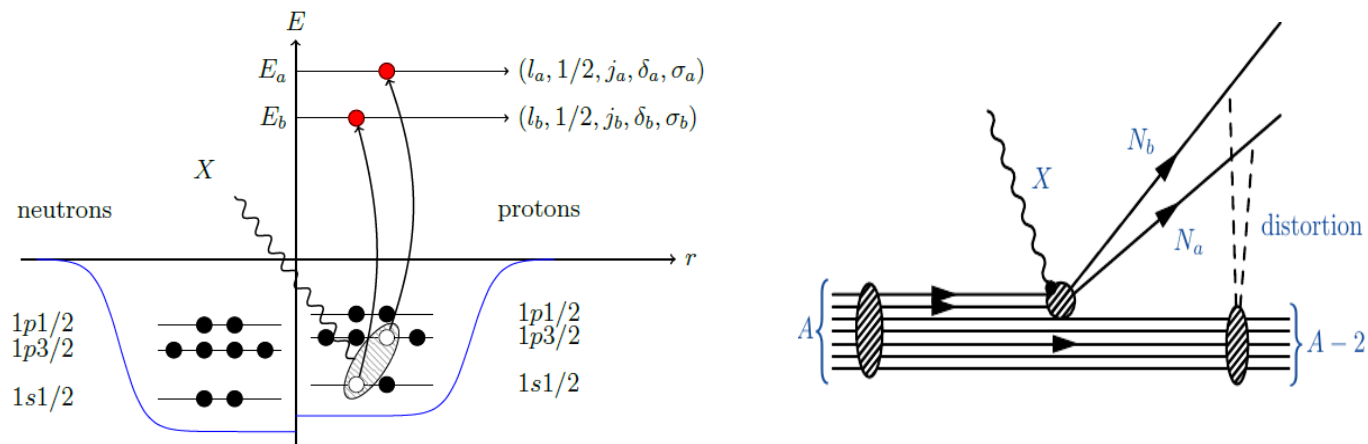


## Meson-exchange currents

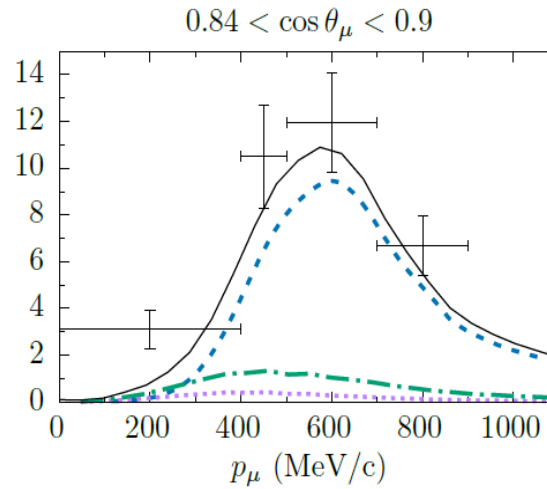
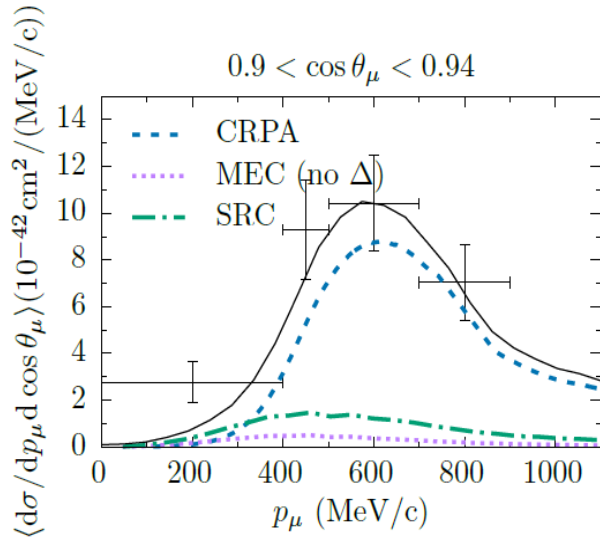


T. Van Cuyck's  
PhD Thesis

The same **mean-field** model is used to describe the **bound and scattered nucleons**:



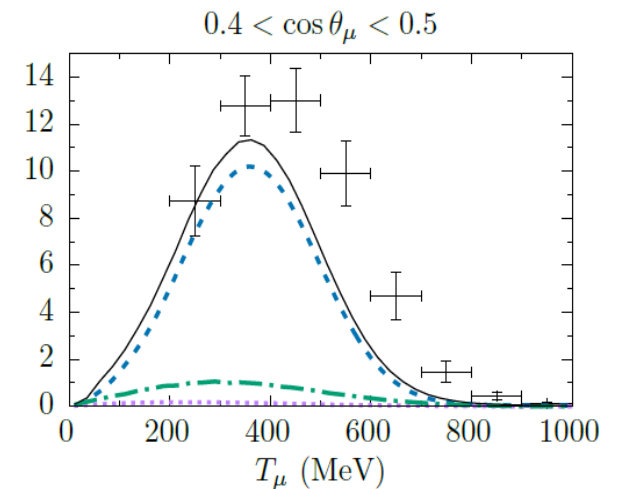
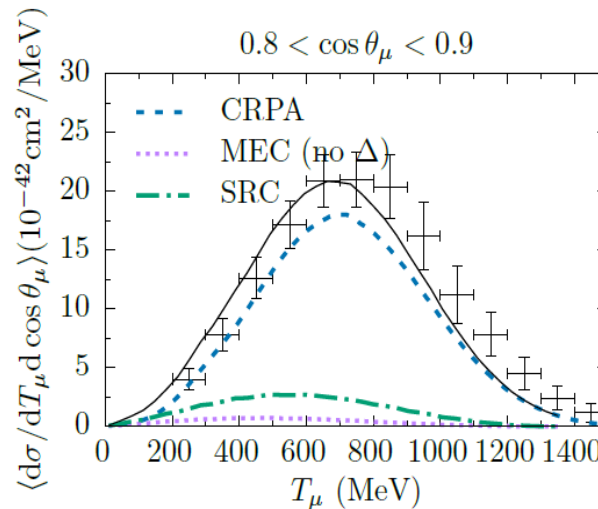
# Flux folded xs: MiniBooNE & T2K



**T2K**  
(inclusive data:  
QE, 2p2h, pions, DIS)

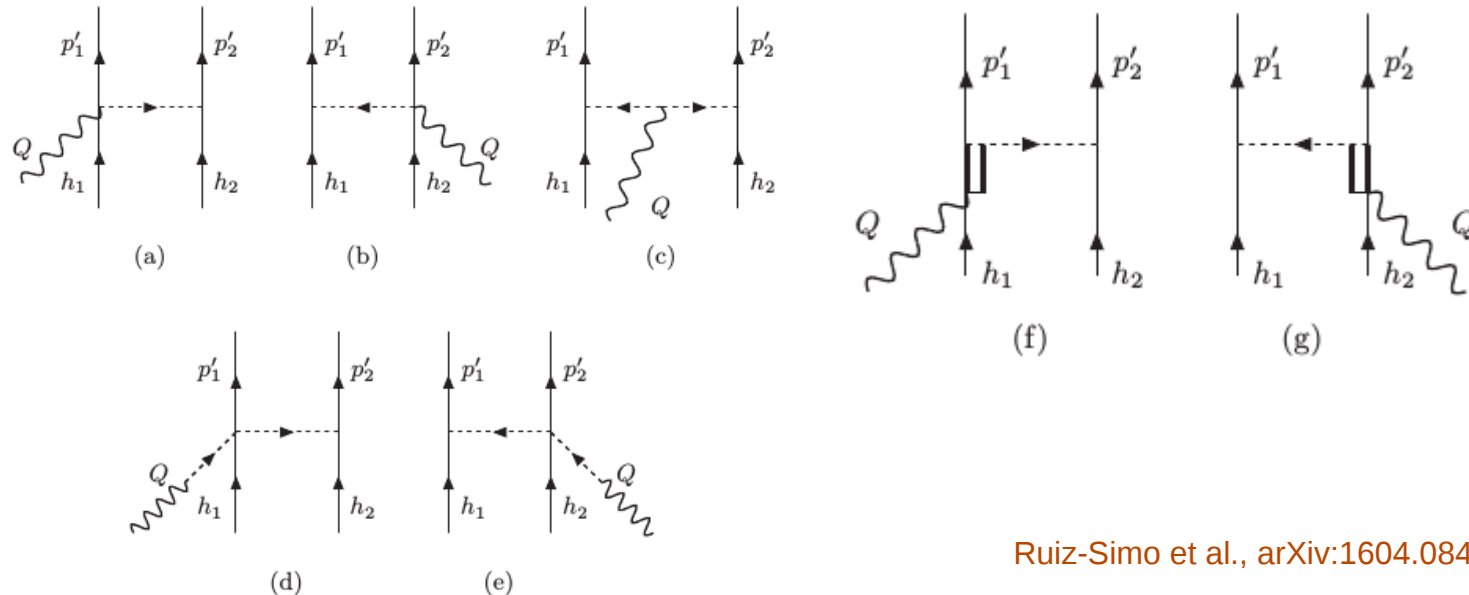
Van Cuyck et al., arXiv:1708.03723

MiniBooNE  
(QE-like: QE+2p2h)



# Meson-exchanged currents

Other approaches (Superscaling coll.) consider MEC as the only contribution to the 2N-nucleon knockout responses. Fully relativistic calculation that includes both vector and axial current contributions.



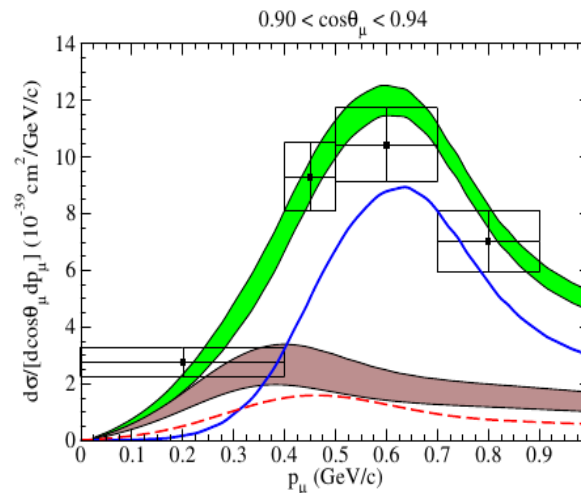
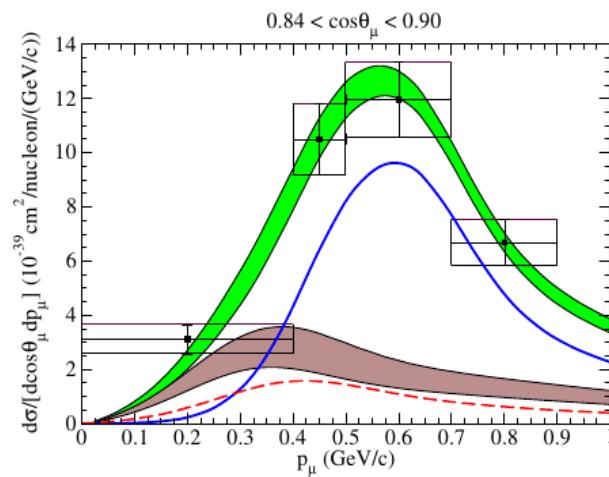
Ruiz-Simo et al., arXiv:1604.08423

# Meson-exchanged currents

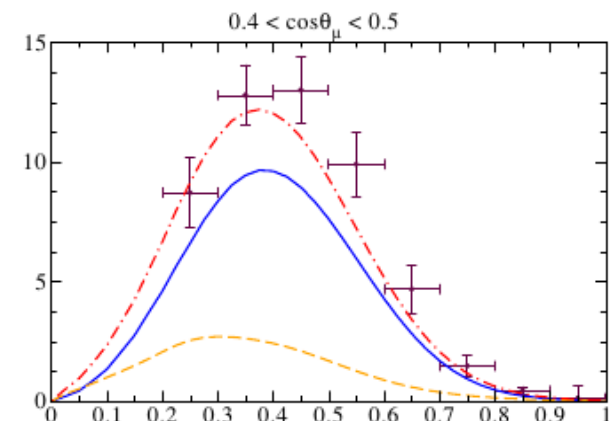
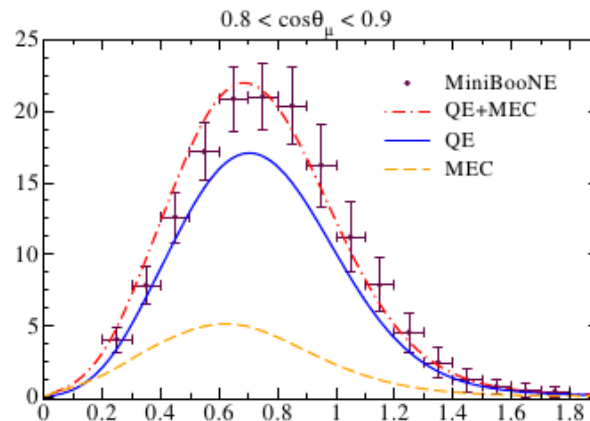
Other calculations (Superscaling coll.) consider MEC as the only contribution to the 2N-nucleon knockout responses. Fully relativistic calculation that includes both vector and axial current contributions.

Megias et al.,  
arXiv:1607.08565v2

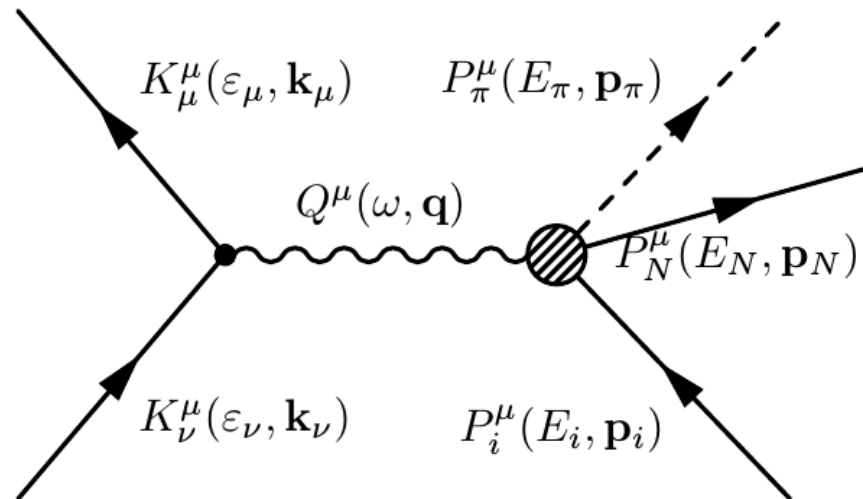
**T2K**  
(inclusive data:  
QE, 2p2h, pions, DIS)



**MiniBooNE**  
(QE-like: QE+2p2h)

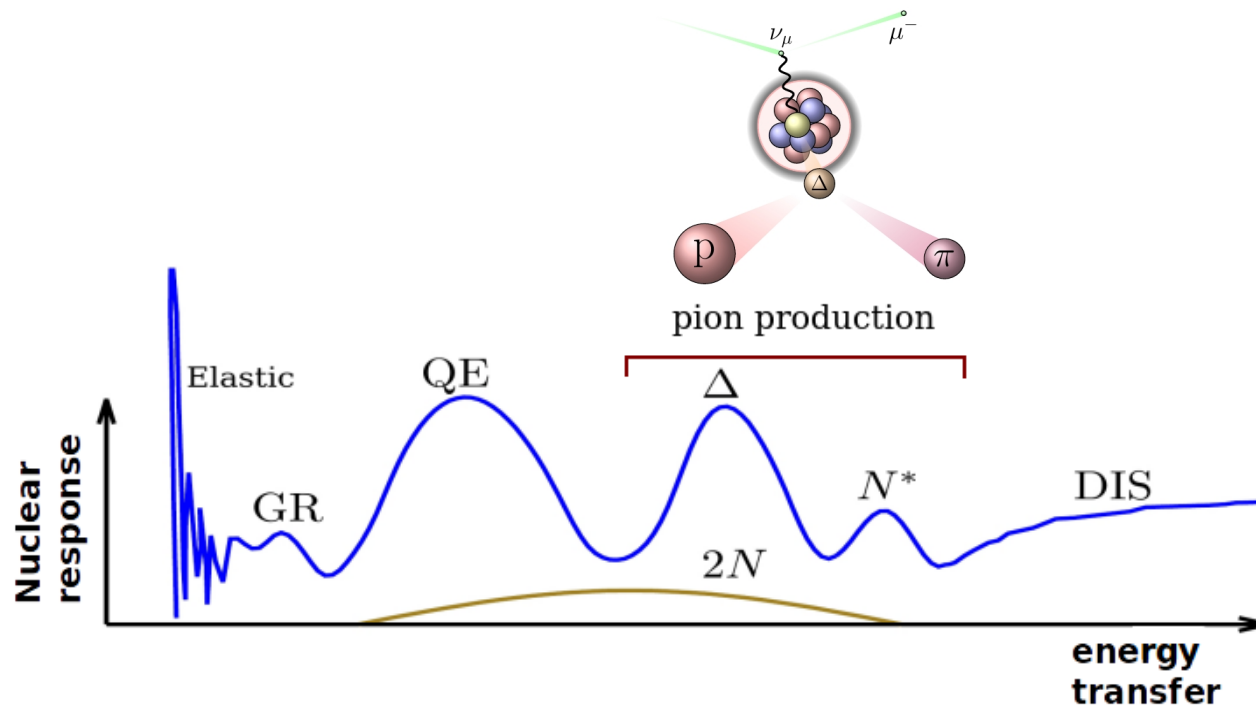


# Single-Pion Production on the nucleon

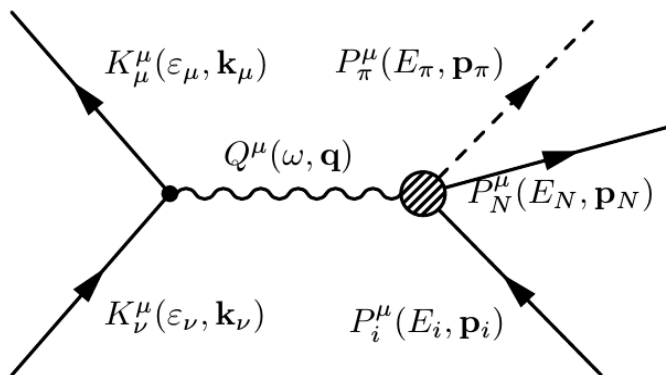


González-Jiménez et al., PRD 95, 113007 (2017)

# Single-Pion Production on the nucleon



# Low-energy model



Low-energy model for pion-production on the nucleon:

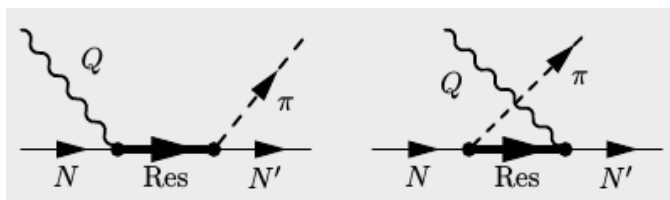
ChPT background + resonances

Valencia model

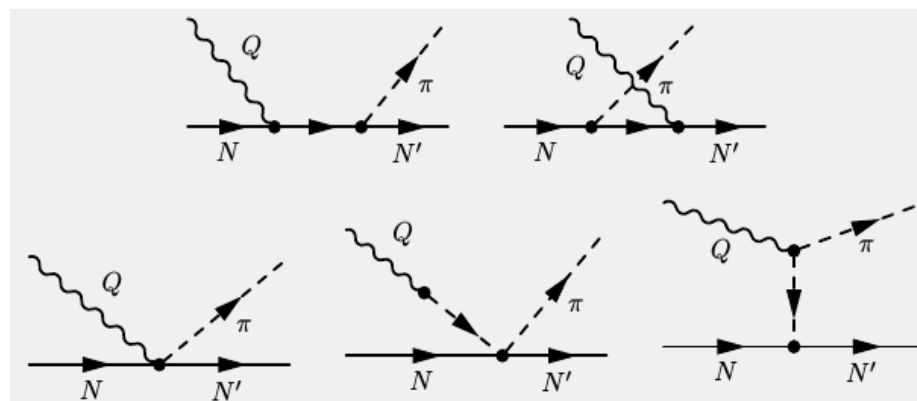
(PRD 76 (2007) 033005; PRD 87 (2013) 113009)

## Resonances:

P33(1232), D13(1520),  
S11(1535), P11(1440)

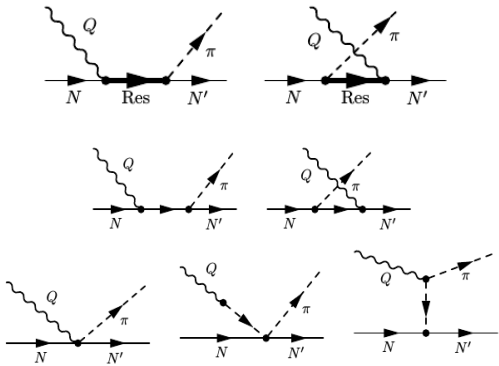


## ChPT background:



# The Problem

Low-energy model  
(resonances + ChPT bg)



Unphysical predictions at large invariant masses.

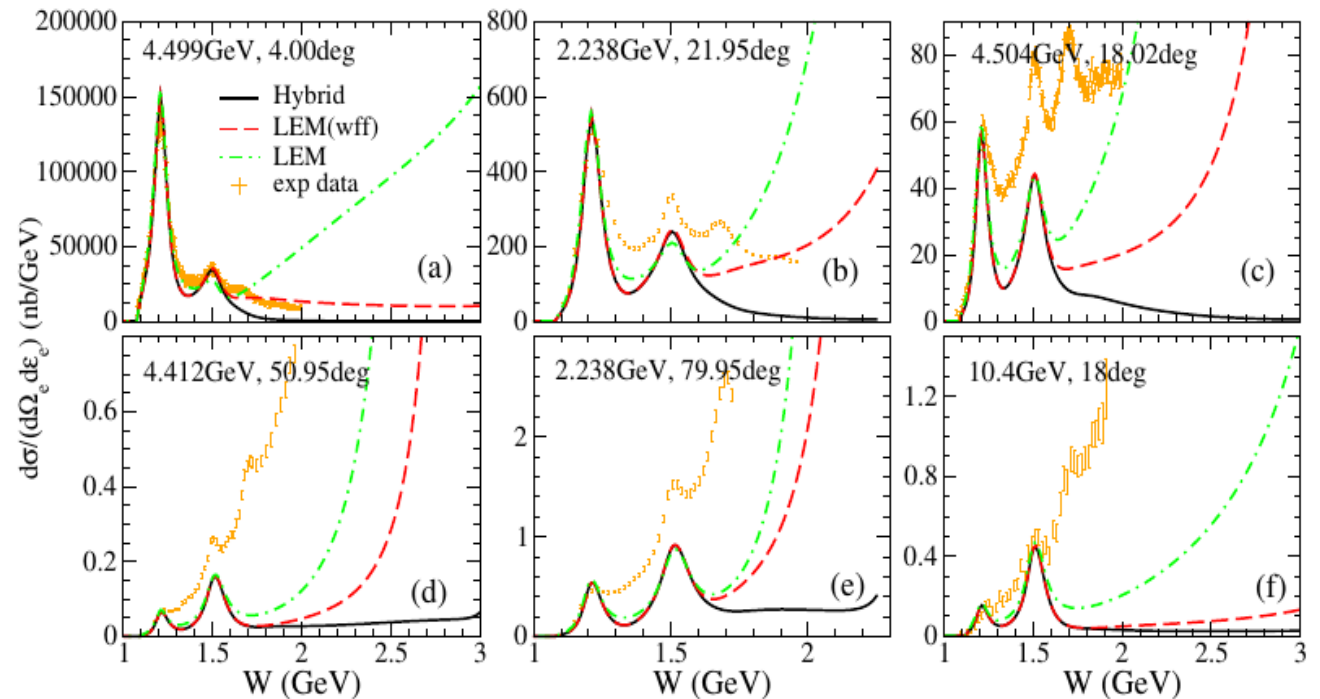
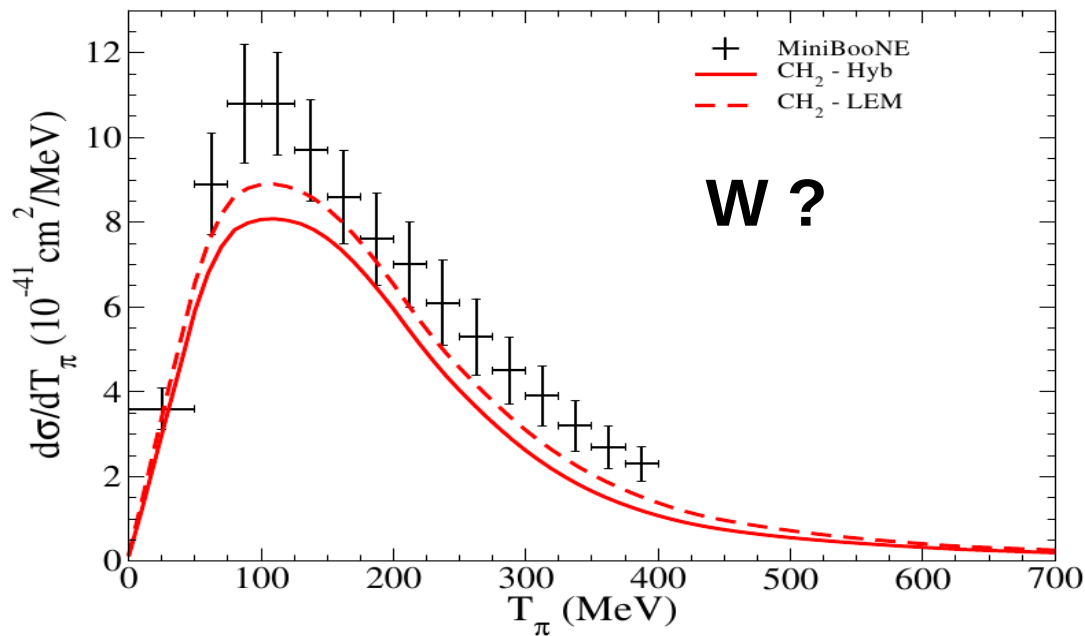


**Figure:** The model overshoots inclusive electron-proton scattering data.

# The Problem



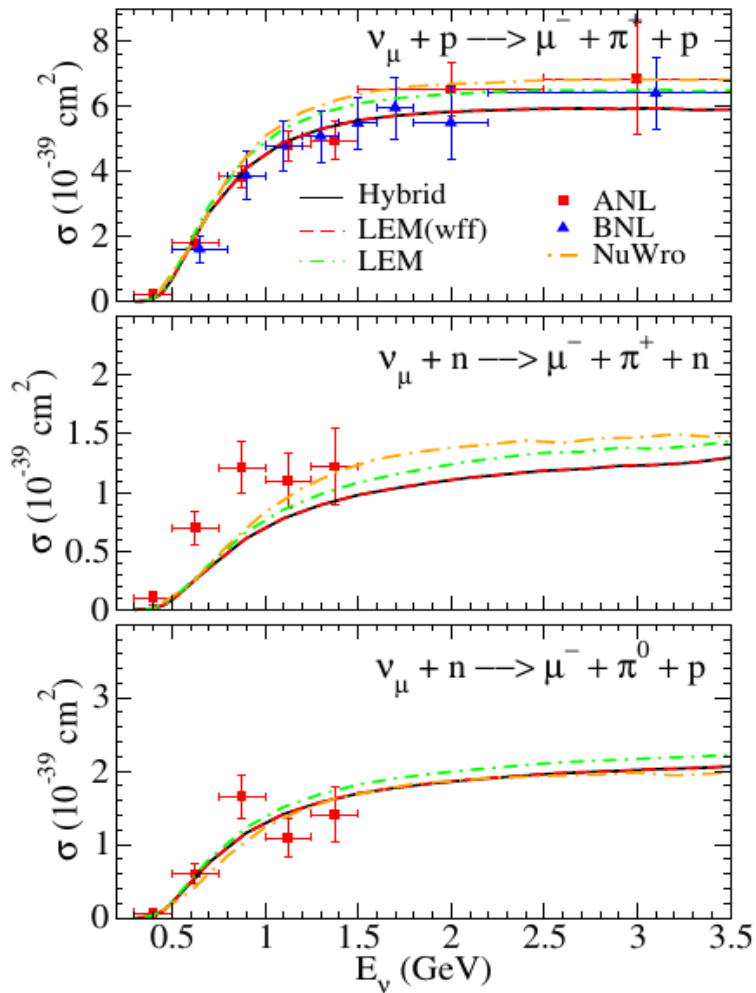
**W values?** We don't know...  
+ Fermi motion  
+ Flux-folding

Therefore, we need reliable predictions in:

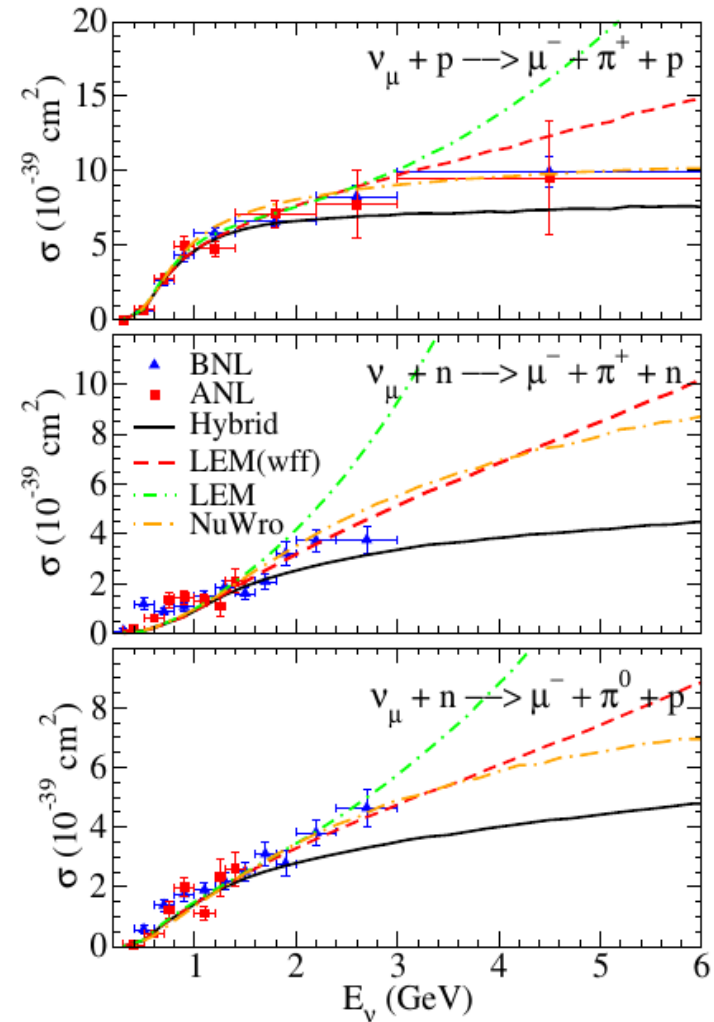
+ the **resonance region**  
 $W < 2 \text{ GeV}$ ,  
+ the **high-energy** energy  
region  $W > 2 \text{ GeV}$

# Hybrid model: results

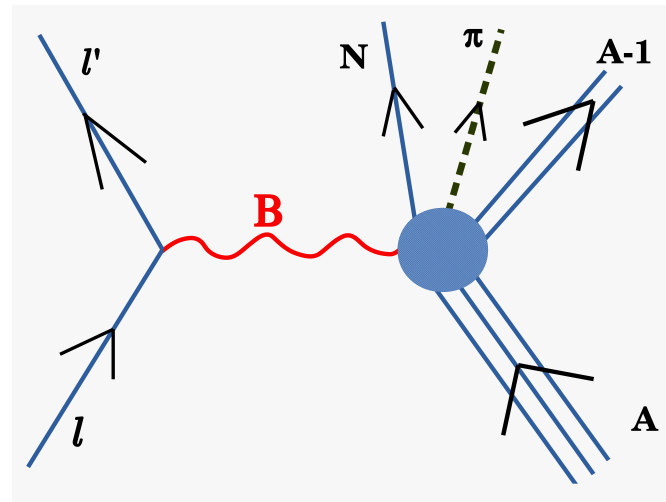
W < 1.4 GeV



No cut in W



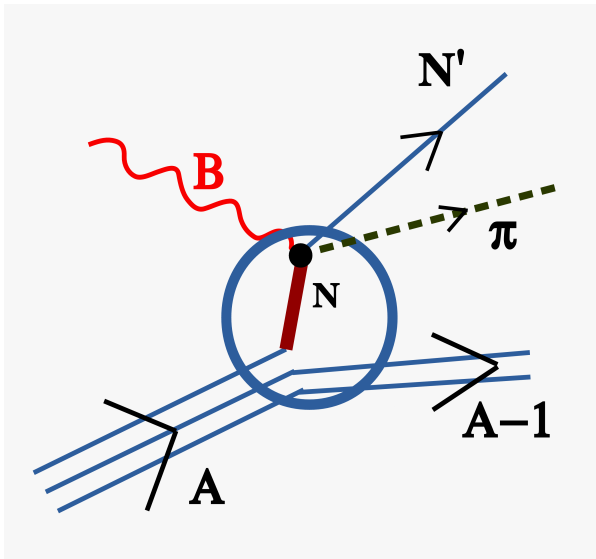
# *Electroweak one-pion production on nuclei*



RGJ et al., arXiv:1710.08374 [nucl-th]

# Relativistic mean field model

## Relativistic Impulse Approximation

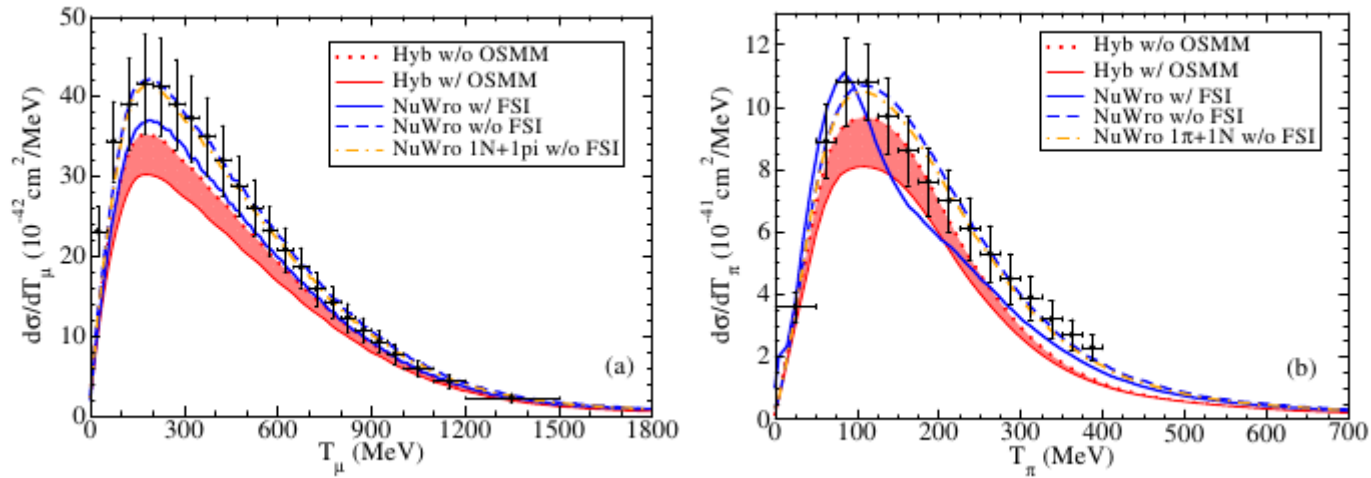


$$J_{had}^{\mu} = \sum_i^A \int d\mathbf{r} \bar{\Psi}_F(\mathbf{r}) \phi^*(\mathbf{r}) \hat{O}_{one-body}^{\mu}(\mathbf{r}) \Psi_B(\mathbf{r}) e^{i\mathbf{q}\cdot\mathbf{r}}$$

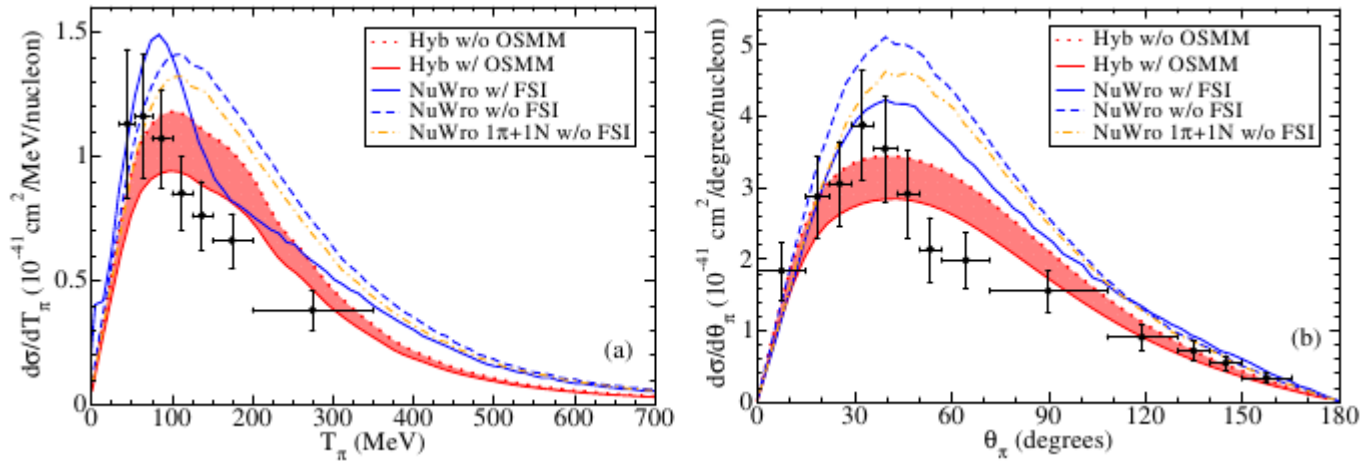
$$\frac{d^8\sigma}{d\varepsilon_f d\Omega_f dE_{\pi} d\Omega_{\pi} d\Omega_N} = \frac{m_i m_f}{(2\pi)^8} \frac{M_N p_N k_{\pi}}{E_N f_{rec}} \frac{k_f}{\varepsilon_i} \sum_{fi} |\mathcal{M}_{fi}|^2$$

8-fold differential cross section:  
Computationally very demanding

## MiniBooNE neutrino CC 1pion+.

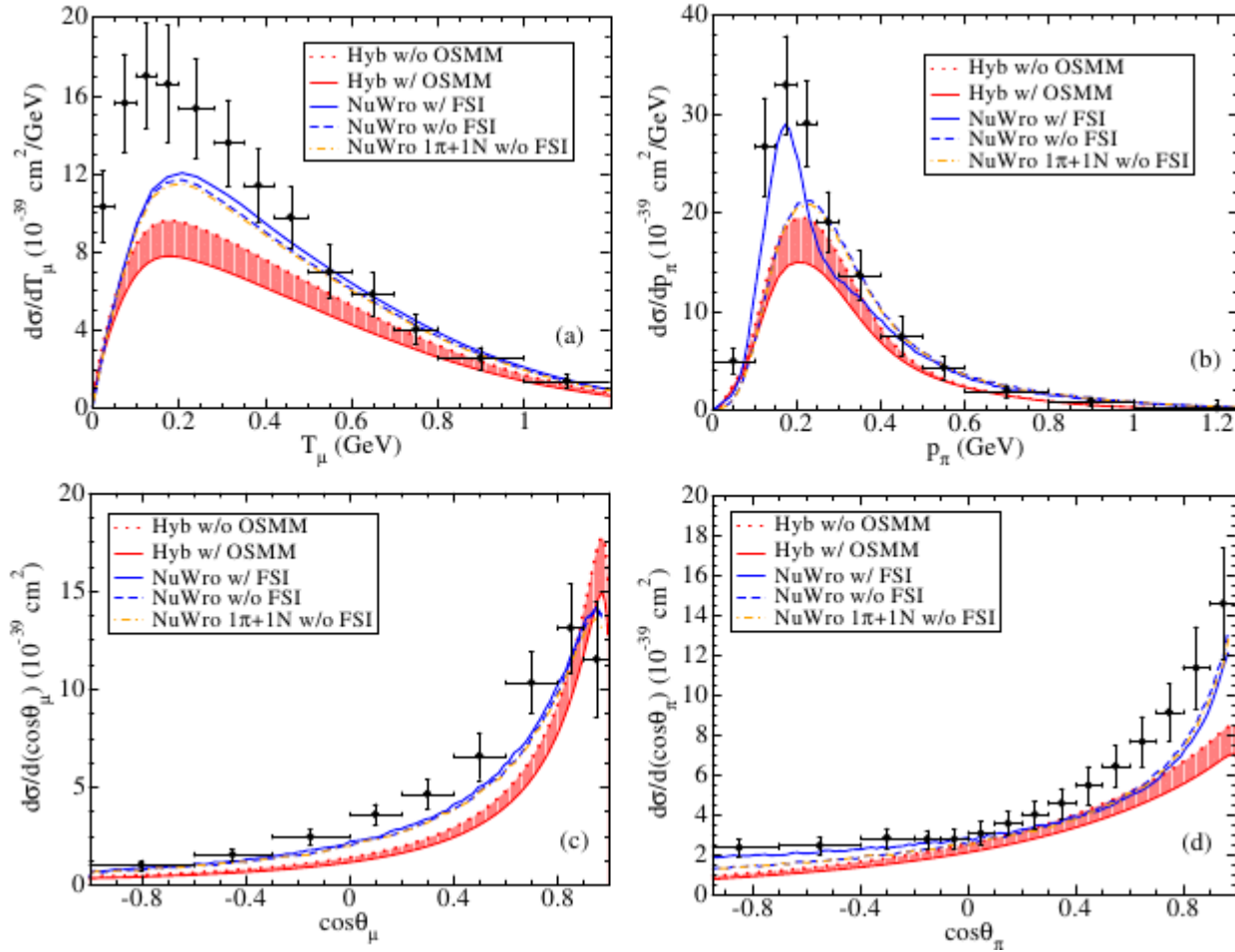


## MINERvA antineutrino CC 1pion0.



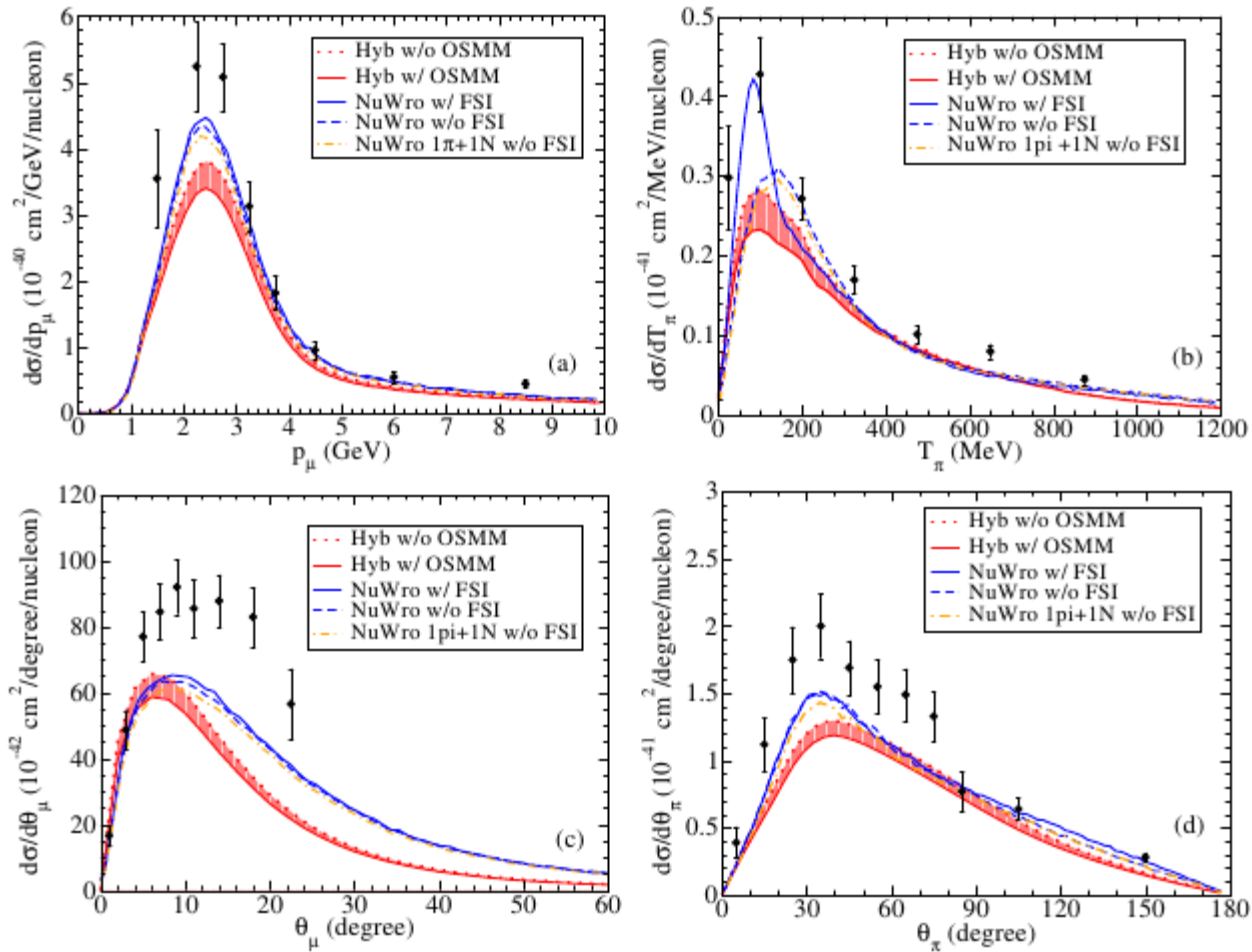
RGJ et al., arXiv:1710.08374 [nucl-th]

## MiniBooNE neutrino CC 1pion0.



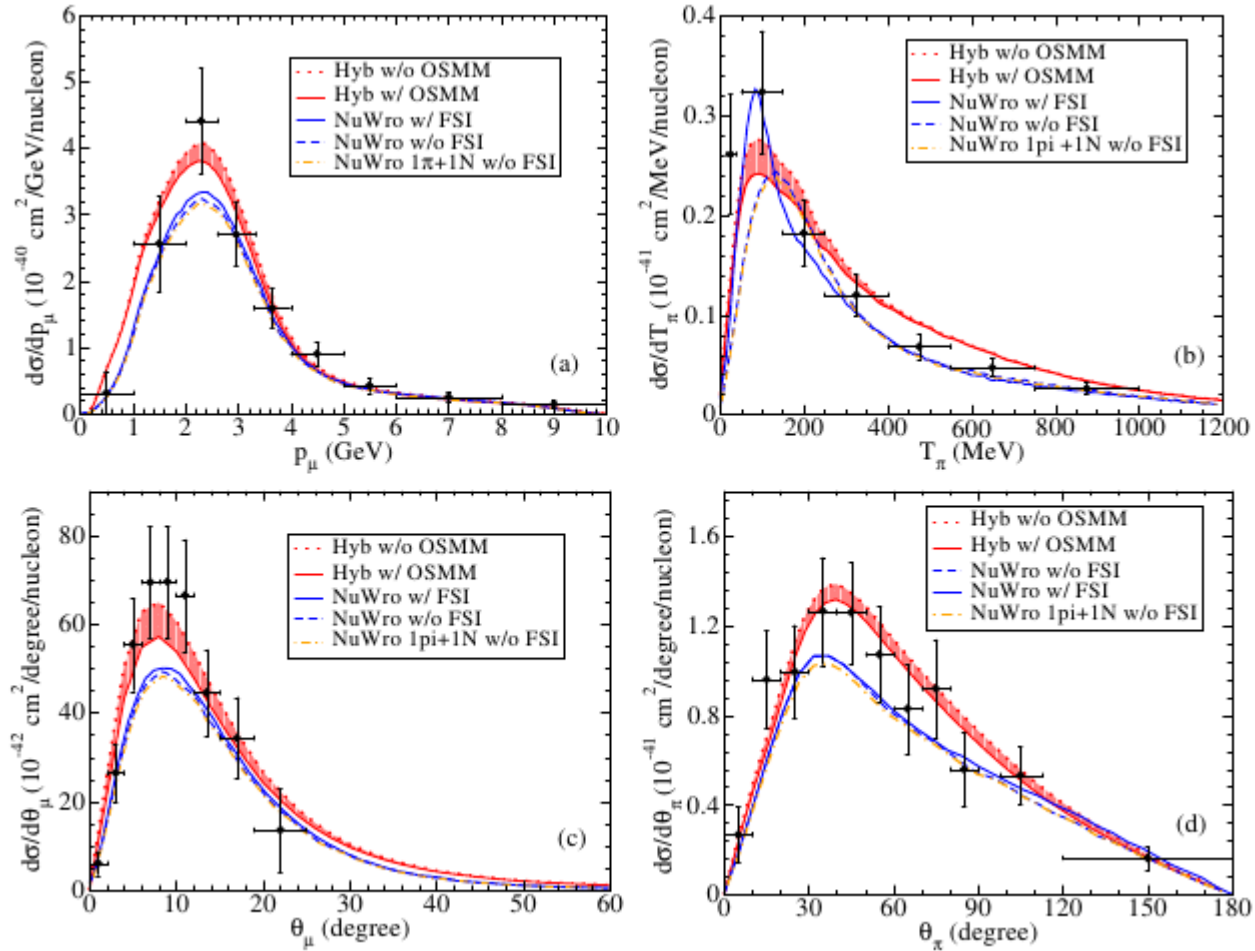
RGJ et al., arXiv:1710.08374 [nucl-th]

## MINERvA neutrino CC 1pion0.



RGJ et al., arXiv:1710.08374 [nucl-th]

## MINERvA antineutrino CC 1pion0.



RGJ et al., arXiv:1710.08374 [nucl-th]

# Conclusions

- ✓ **Neutrino-nucleus cross sections** are important to reduce systematics in neutrino-oscillation analyses. We need to improve our current understanding of the neutrino-nucleus and neutrino-nucleon interaction.
- ✓ New theoretical **developments should be implemented in the MC event generators** that are used in the oscillation analyses.
- ✓ We are working to provide a **microscopic description** of the main reaction mechanisms at intermediate energies: QE scattering, 2-nucleon emission, pion production.

Lot of work to do...



*Dziękuję za  
uwagę!*

# *Backup slides*

# Results in the sub-GeV region ( $E_{lepton} < 1.3 \text{ GeV}$ )

## Kam I and Kam II

Physics Letters B 280 (1992) 146–152  
North-Holland

PHYSICS LETTERS B

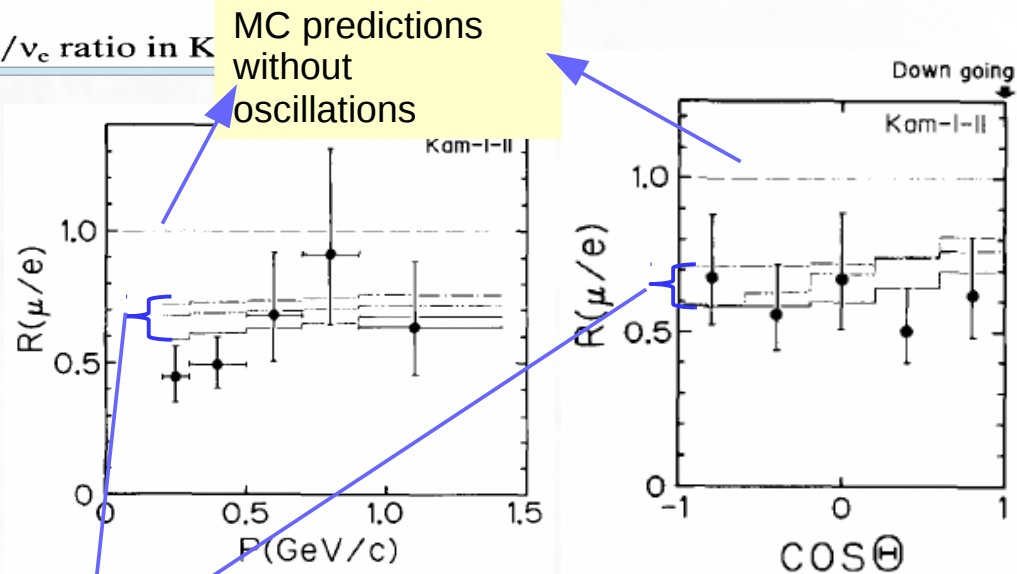
4.92 kton yr sample

Observation of a small atmospheric  $\nu_\mu/\nu_e$  ratio in Kam

The estimation of the expected event rate distribution in the detector requires knowledge of the neutrino flux, cross section and experimental conditions. Theoretical predictions of the fluxes differ by as much as 30%. HOWEVER, the ratio

$$R = (\nu_\mu + \bar{\nu}_\mu) / (\nu_e + \bar{\nu}_e),$$

where  $\nu_{\mu,e}$  represent the event rates distribution, agrees upon by all authors to within 5%.



MC predictions without oscillations

MC predictions within different oscillation scenarios

They found:

$$R(\mu/e) = R_{data} / R_{Theory} = 0.60 \pm 0.07$$

**Far from 1 !!!**

(actually, more than  $4\sigma$  below 1.)

### Conclusion

decays relative to all single ring events. Neutrino oscillations, with the totality of atmospheric neutrino and solar neutrino data favoring the channel  $\nu_\mu \leftrightarrow \nu_\tau$ , might account for the observations.

# Results in the multi-GeV region ( $E_{lepton} > 1.3 \text{ GeV}$ )



ELSEVIER

1 September 1994

PHYSICS LETTERS B

---

Physics Letters B 335 (1994) 237-245

---

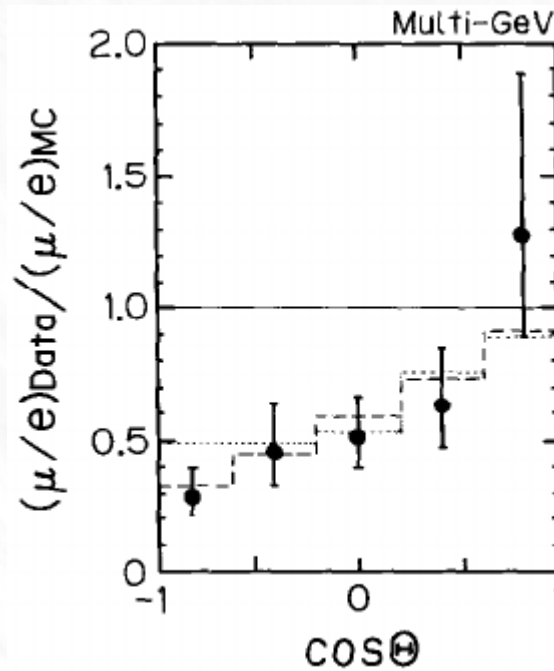
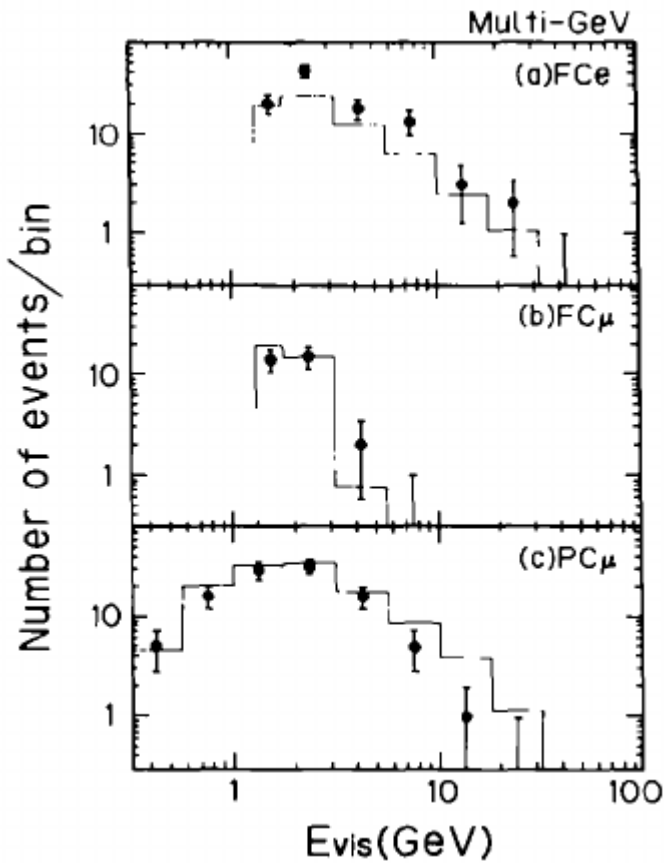
Atmospheric  $\nu_{\mu}/\nu_e$  ratio in the multi-GeV energy range

8.2 kton yr sample

They found:

$$R(\mu/e) = R_{\text{data}} / R_{\text{Theory}} = 0.58 \pm 0.08$$

(in agreement with the sub-GeV result)



**Strong dependence on the zenith angle**

**Strong dependence on the zenith angle that increases with the energy**



## OSCILLATIONS

$$P_{a \rightarrow b} = \sin^2 2\theta \sin^2 \left( \frac{1.27 \Delta m^2 (\text{eV}^2) L (\text{km})}{E_\nu (\text{GeV})} \right),$$

$\sin^2 2\theta = 0.95$   
 $\Delta m^2 = 4 \times 10^{-4} \text{ eV}^2$

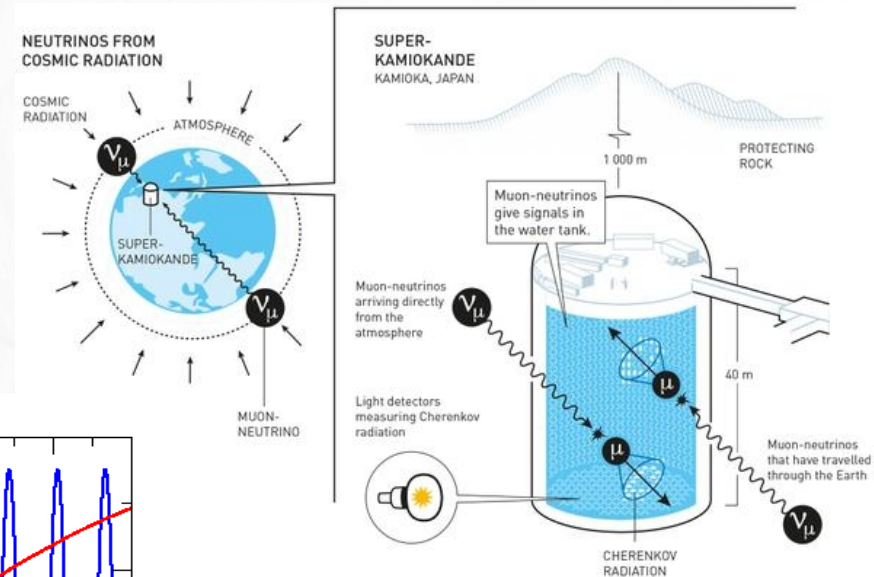
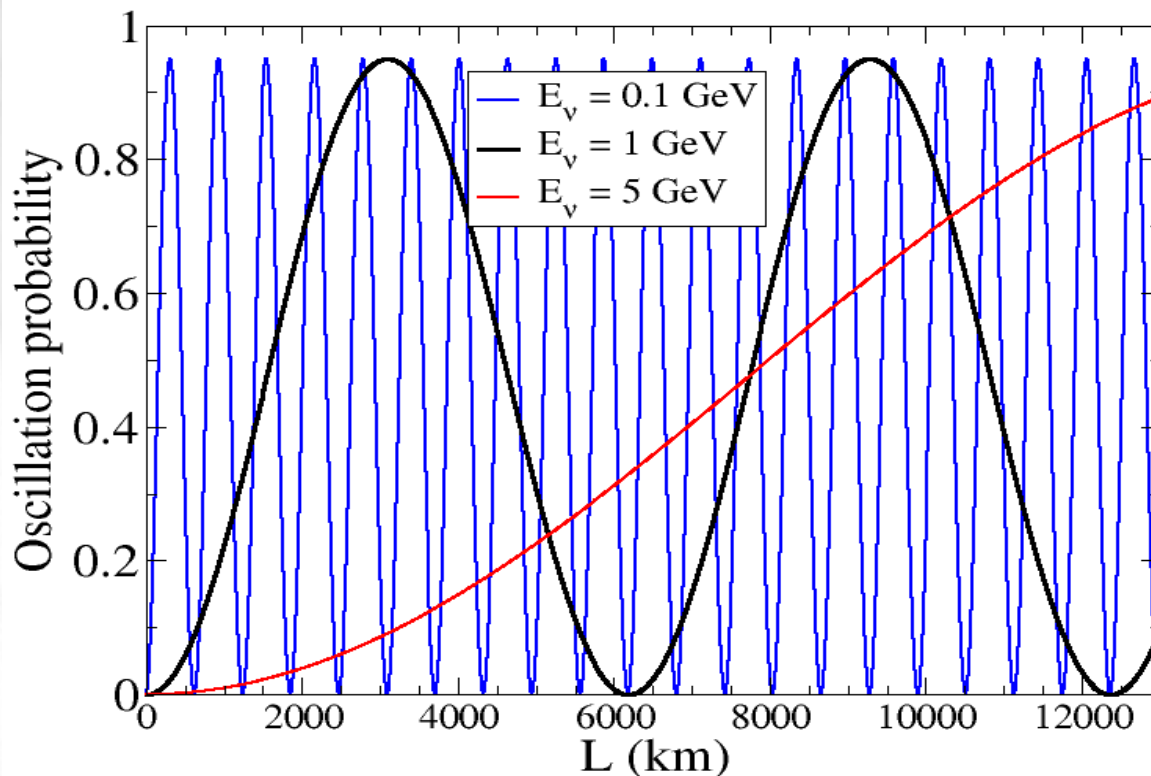
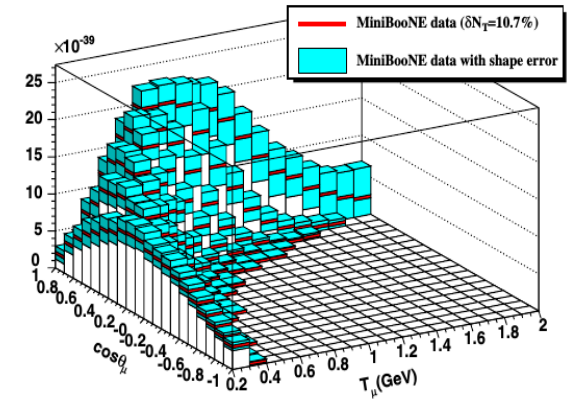


Illustration: © Johan Jarnestad/The Royal Swedish Academy of Sciences

## Example: the reconstruction procedure at the MiniBooNE experiment:

1) In MiniBooNE a **QE-like event** happens when a muon and no pions are detected. The event is characterized by the scattering angle and the energy of the muon.



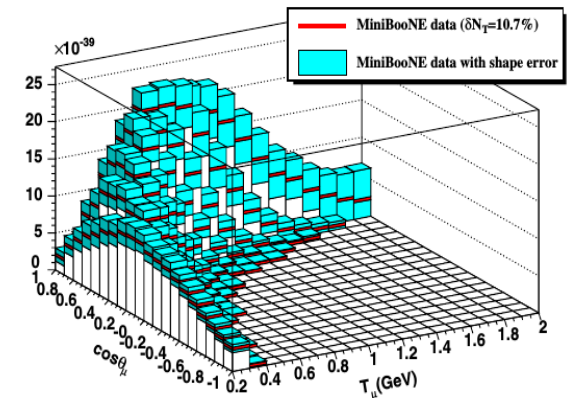
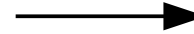
## Example: the reconstruction procedure at the MiniBooNE experiment:

1) In MiniBooNE a **QE-like event** happens when a muon and no pions are detected. The event is characterized by the scattering angle and the energy of the muon.

2) The neutrino energy is reconstructed using the formula:

$$E_{\nu}^{QE} = \frac{m_p^2 - m_n'^2 - m_{\mu}^2 + 2m_n' E_{\mu}}{2(m_n' - E_{\mu} + p_{\mu} \cos \theta_{\mu})}$$

So, we go from **N(E ?)** to **N(E<sup>QE</sup>)**



## Example: the reconstruction procedure at the MiniBooNE experiment:

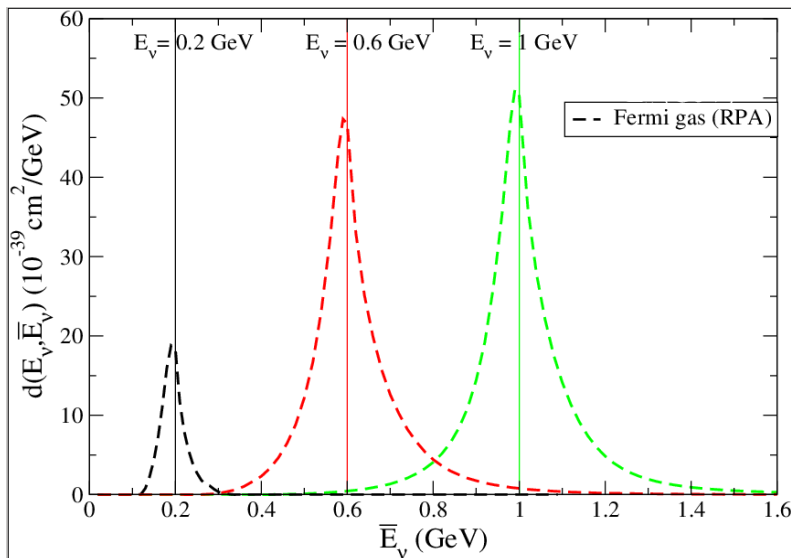
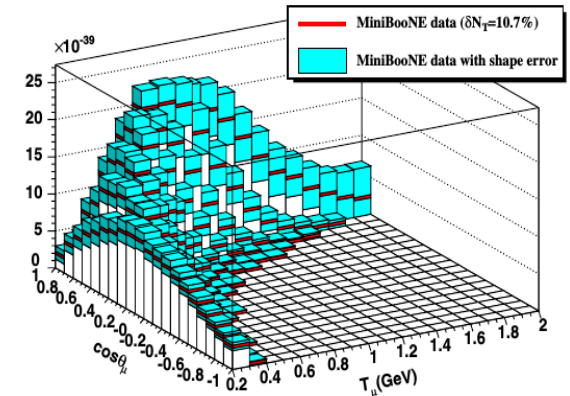
1) In MiniBooNE a **QE-like event** happens when a muon and no pions are detected. The event is characterized by the scattering angle and the energy of the muon.

2) The neutrino energy is reconstructed using the formula:

$$E_{\nu}^{QE} = \frac{m_p^2 - m_n'^2 - m_{\mu}^2 + 2m_n' E_{\mu}}{2(m_n' - E_{\mu} + p_{\mu} \cos \theta_{\mu})}$$

So, we go from **N(E ?)** to **N(E<sup>QE</sup>)**

3) Assuming pure QE interaction one can compute the **probability density of the reconstructed energy E<sup>QE</sup> matching the true energy E: P(E<sup>QE</sup>|E)**  
(MiniBooNE used a Fermi gas model to simulate nuclear system)



## Example: the reconstruction procedure at the MiniBooNE experiment:

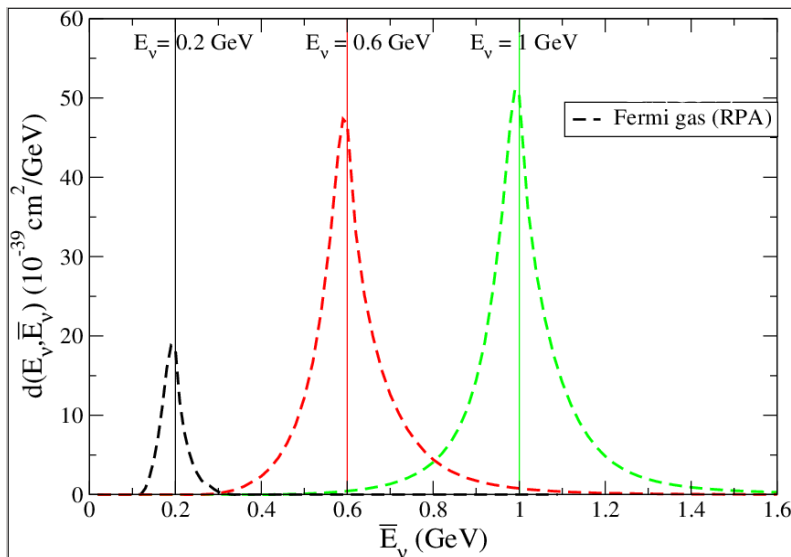
1) In MiniBooNE a **QE-like event** happens when a muon and no pions are detected. The event is characterized by the scattering angle and the energy of the muon.

2) The neutrino energy is reconstructed using the formula:

$$E_{\nu}^{QE} = \frac{m_p^2 - m_n'^2 - m_{\mu}^2 + 2m_n' E_{\mu}}{2(m_n' - E_{\mu} + p_{\mu} \cos \theta_{\mu})}$$

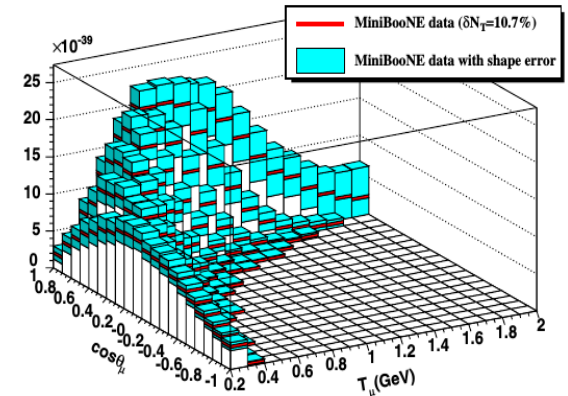
So, we go from **N(E ?)** to **N(E<sup>QE</sup>)**

3) Assuming pure QE interaction one can compute the **probability density of the reconstructed energy E<sup>QE</sup> matching the true energy E: P(E<sup>QE</sup>|E)**  
(MiniBooNE used a Fermi gas model to simulate nuclear system)



4) The **event distribution as a function of the true neutrino energy** results from:

$$N(E) \sim \int N(E^{QE}) P(E^{QE}|E) dE^{QE}$$

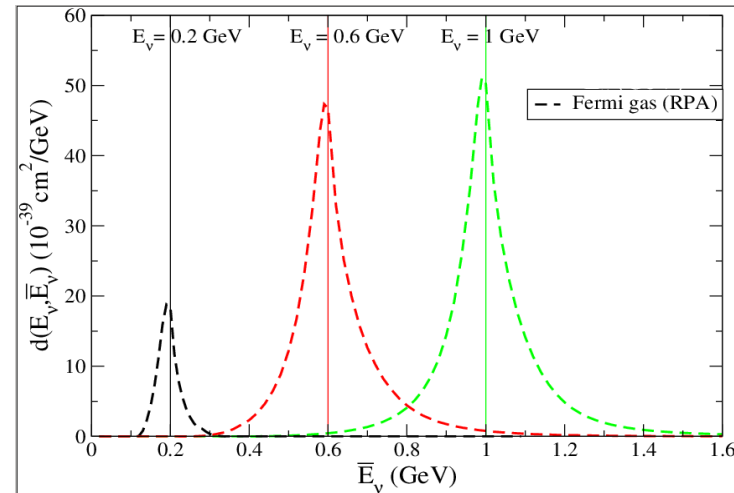
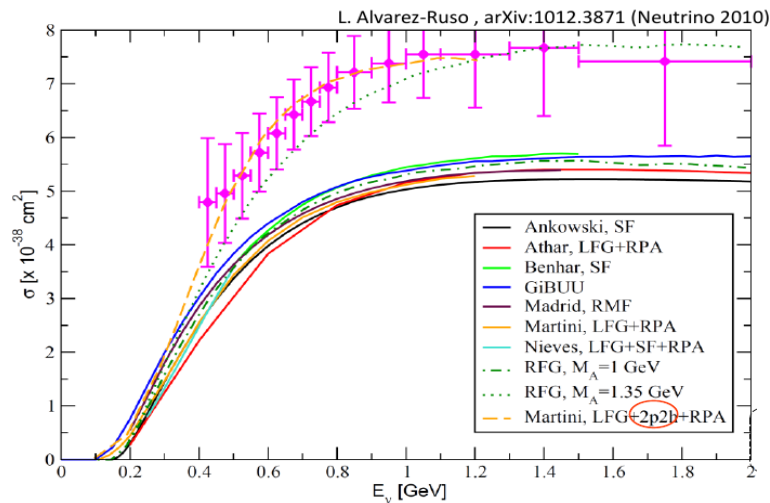


# Sources of **ERRORS**:

- 1) Other processes, like 2-nucleon emission and pionless delta decay, may contribute to the QE-like signal.
- 2) Fermi gas model is not good enough

**Probability distributions (reconstructed energy  $\rightarrow$  true energy)**

**pure QE with Fermi gas  $\neq$  QE+2p2h with better nuclear models**



**Summary: A major source of systematic uncertainties** in neutrino oscillation analyses are the neutrino-nucleus cross sections.

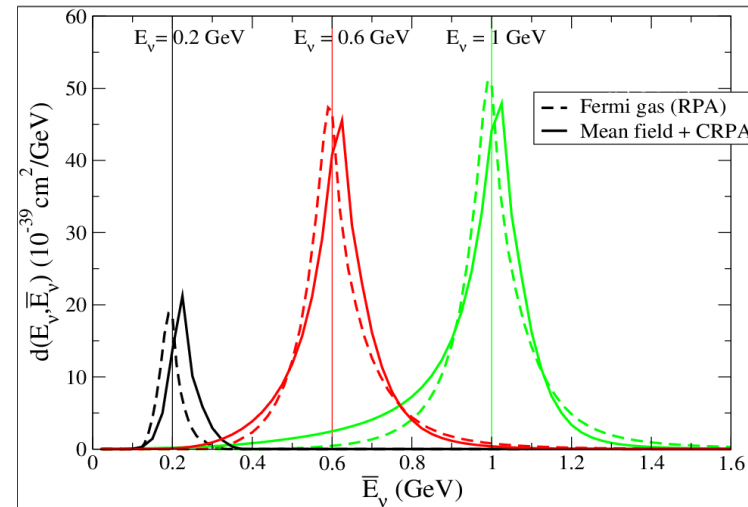
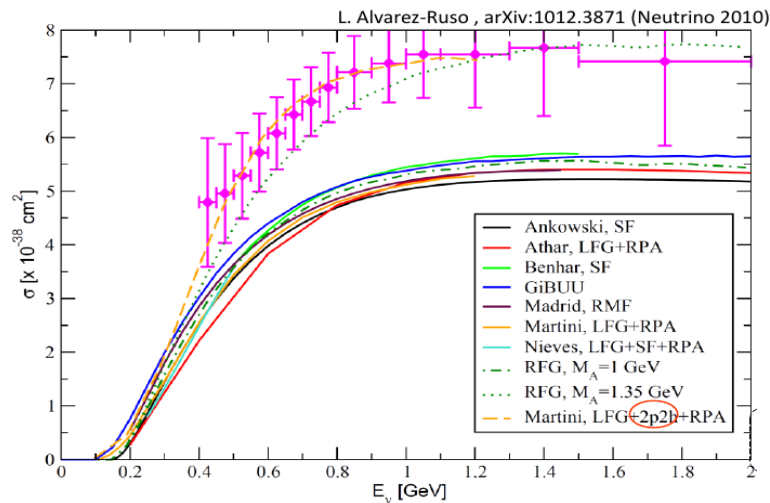
Better description of neutrino-nucleus interaction is needed and has to be implemented in the experimental analyses.

# Sources of **ERRORS**:

- 1) Other processes, like 2-nucleon emission and pionless delta decay, may contribute to the QE-like signal.
- 2) Fermi gas model is not good enough

**Probability distributions (reconstructed energy  $\rightarrow$  true energy)**

**pure QE with Fermi gas  $\neq$  QE+2p2h with better nuclear models**



**Summary: A major source of systematic uncertainties** in neutrino oscillation analyses are the neutrino-nucleus cross sections.

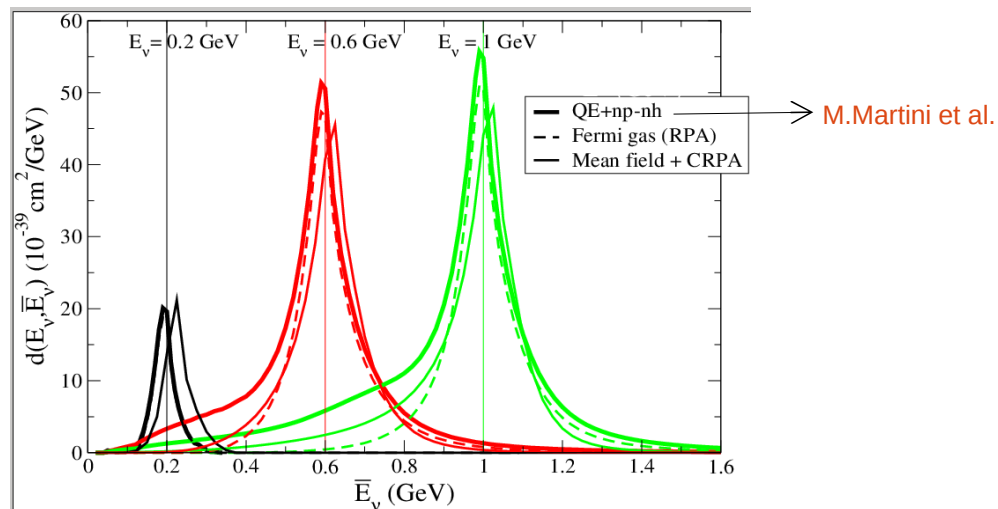
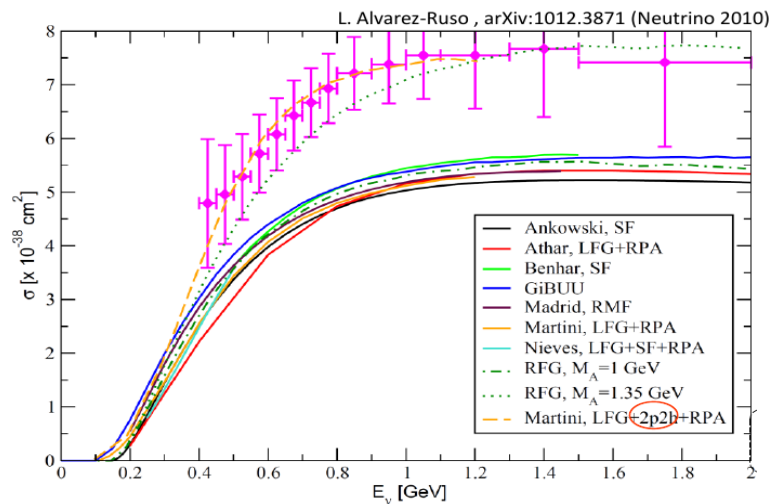
Better description of neutrino-nucleus interaction is needed and has to be implemented in the experimental analyses.

# Sources of **ERRORS**:

- 1) Other processes, like 2-nucleon emission and pionless delta decay, may contribute to the QE-like signal.
- 2) Fermi gas model is not good enough

**Probability distributions (reconstructed energy  $\rightarrow$  true energy)**

pure QE with Fermi gas  $\neq$  QE+2p2h with better nuclear models



**Summary: A major source of systematic uncertainties** in neutrino oscillation analyses are the neutrino-nucleus cross sections.

Better description of neutrino-nucleus interaction is needed and has to be implemented in the experimental analyses.

# Relativistic mean-field model

RMF model provides a microscopic description of the ground state of finite nuclei which is consistent with Quantum Mechanics, Special Relativity and symmetries of strong interaction.

The starting point is a Lorentz covariant Lagrangian density

$$\begin{aligned} \mathcal{L} = & \bar{\Psi} (i\gamma_{\mu}\partial^{\mu} - M) \Psi + \frac{1}{2} (\partial_{\mu}\sigma\partial^{\mu}\sigma - m_{\sigma}^2\sigma^2) - U(\sigma) \\ & - \frac{1}{4}\Omega_{\mu\nu}\Omega^{\mu\nu} + \frac{1}{2}m_{\omega}^2\omega_{\mu}\omega^{\mu} - \frac{1}{4}\mathbf{R}_{\mu\nu}\mathbf{R}^{\mu\nu} + \frac{1}{2}m_{\rho}^2\rho_{\mu}\rho^{\mu} - \frac{1}{4}F_{\mu\nu}F^{\mu\nu} \\ & - g_{\sigma}\bar{\Psi}\sigma\Psi - g_{\omega}\bar{\Psi}\gamma_{\mu}\omega^{\mu}\Psi - g_{\rho}\bar{\Psi}\gamma_{\mu}\boldsymbol{\tau}\rho^{\mu}\Psi - g_e\frac{1+\tau_3}{2}\bar{\Psi}\gamma_{\mu}A^{\mu}\Psi. \end{aligned}$$

Extension of the original  
 $\sigma$ - $\omega$  Walecka model  
(Ann. Phys.83,491 (1974)).

where

$$\begin{aligned} \Omega^{\mu\nu} &= \partial^{\mu}\omega^{\nu} - \partial^{\nu}\omega^{\mu}, \\ \mathbf{R}^{\mu\nu} &= \partial^{\mu}\rho^{\nu} - \partial^{\nu}\rho^{\mu}, \\ F^{\mu\nu} &= \partial^{\mu}A^{\nu} - \partial^{\nu}A^{\mu}. \\ U(\sigma) &= \frac{1}{3}g_2\sigma^3 + \frac{1}{4}g_3\sigma^4 \end{aligned}$$

## Main approximations:

1) Mean-field approximation:

$$\omega_{\mu} \rightarrow \langle \omega_{\mu} \rangle \quad \sigma \rightarrow \langle \sigma \rangle \quad \rho_{\mu} \rightarrow \langle \rho_{\mu} \rangle$$

2) Static limit:

$$\partial^0\omega_0 = \partial^0\rho_0 = \partial^0\sigma = 0 \quad \omega_{\mu} = \delta_{\mu 0}\omega_0, \quad \rho_{\mu} = \delta_{\mu 0}\rho_0$$

3) Spherical symmetry for finite nuclei:

$$\omega_0 = \omega_0(r) \quad \rho_0 = \rho_0(r) \quad \sigma = \sigma(r)$$

# Relativistic mean-field model

Dirac equation for nucleons (eq. of motion for the barionic fields):

$$[-i\boldsymbol{\alpha} \cdot \boldsymbol{\nabla} + V(r) + \beta(M + S(r))]\Psi_i(\mathbf{r}) = E_i\Psi_i(\mathbf{r})$$

where the scalar (S) and vector (V) potential are given by:

$$S(r) = g_\sigma\sigma(r),$$

$$V(r) = g_\omega\omega^0(r) + g_\rho\tau_3\rho_3^0(r) + e\frac{1 + \tau_3}{2}A^0(r)$$

Eqs. of motion for the mesons and the photon:

$$[-\nabla^2 + m_\sigma^2]\sigma(r) = -g_\sigma\rho_s(r) - g_2\sigma^2(r) - g_3\sigma^3(r),$$

$$[-\nabla^2 + m_\omega^2]\omega^0(r) = -g_\omega\rho_B(r),$$

$$[-\nabla^2 + m_\rho^2]\rho_3^0(r) = -g_\rho\rho_\rho(r),$$

$$-\nabla^2 A^0 = e\rho_c,$$

## Current densities

$$\rho_s(r) = \sum_i^A \bar{\Psi}_i(\mathbf{r})\Psi_i(\mathbf{r}),$$

$$\rho_B(r) = \sum_i^A \Psi_i^\dagger(\mathbf{r})\Psi_i(\mathbf{r}),$$

$$\rho_\rho(r) = \sum_i^A \Psi_i^\dagger(\mathbf{r})\tau_3\Psi_i(\mathbf{r})$$

$$\rho_c(r) = \sum_i^A \Psi_i^\dagger(\mathbf{r})\frac{1 + \tau_3}{2}\Psi_i(\mathbf{r})$$

Solution of the couple equations for the fields in a self-consistent way.

# Relativistic mean-field model

In general, the parameters are fit to reproduce some general properties of some closed shell spherical nuclei and nuclear matter.

Parameters for the NLSH model (fitted to the mean charge radius, binding energy and neutron radius of the  $^{16}\text{O}$ ,  $^{40}\text{Ca}$ ,  $^{90}\text{Zr}$ ,  $^{116}\text{Sr}$ ,  $^{124}\text{Sn}$  and  $^{208}\text{Pb}$ ).

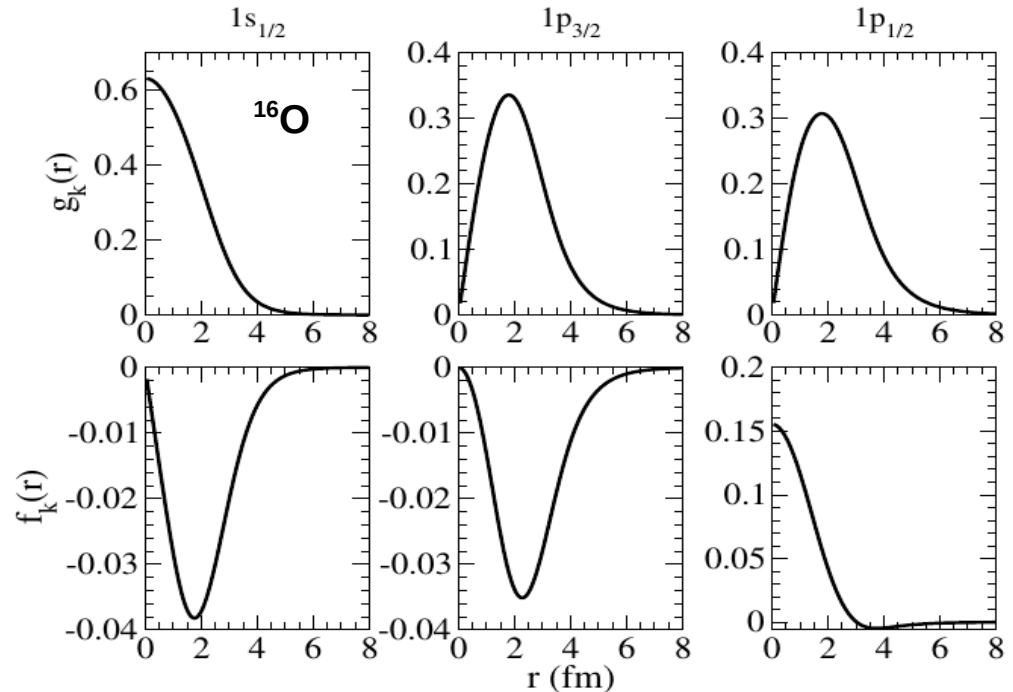
$M_N$	$m_\sigma$	$m_\omega$	$m_\rho$	$g_\sigma$	$g_\omega$	$g_\rho$	$g_2$	$g_3$
939.0	526.059	783.0	763.0	10.444	12.945	4.3830	-6.9099	-15.8337

6 free parameters

$$[-i\boldsymbol{\alpha} \cdot \boldsymbol{\nabla} + V(r) + \beta(M + S(r))]\Psi_i(\mathbf{r}) = E_i\Psi_i(\mathbf{r})$$

$$\Psi_k^{m_j}(\mathbf{r}) = \begin{pmatrix} g_k(r)\varphi_k^{m_j}(\Omega_r) \\ if_k(r)\varphi_{-k}^{m_j}(\Omega_r) \end{pmatrix},$$

$$\varphi_k^{m_j}(\Omega_r) = \sum_{m_\ell s} \langle \ell m_\ell \frac{1}{2} s | j m_j \rangle Y_\ell^{m_\ell}(\Omega_r) \chi^s$$

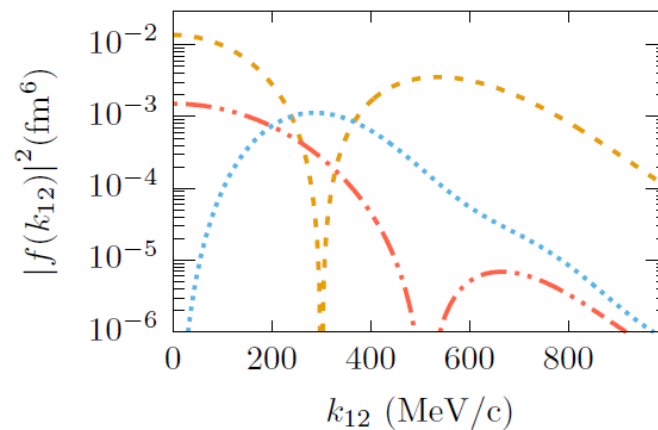
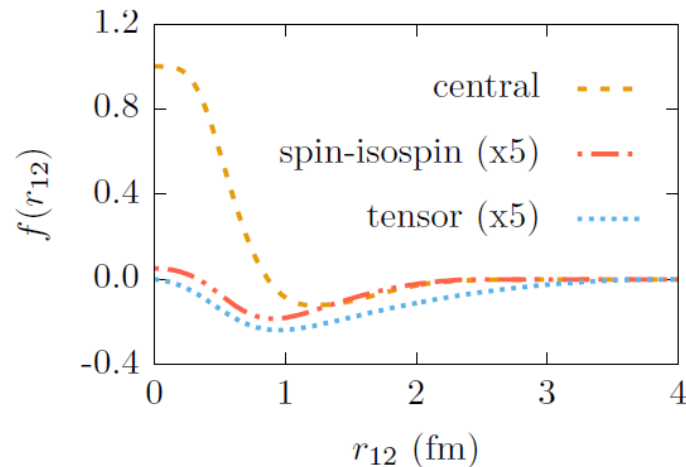


# Short range correlations

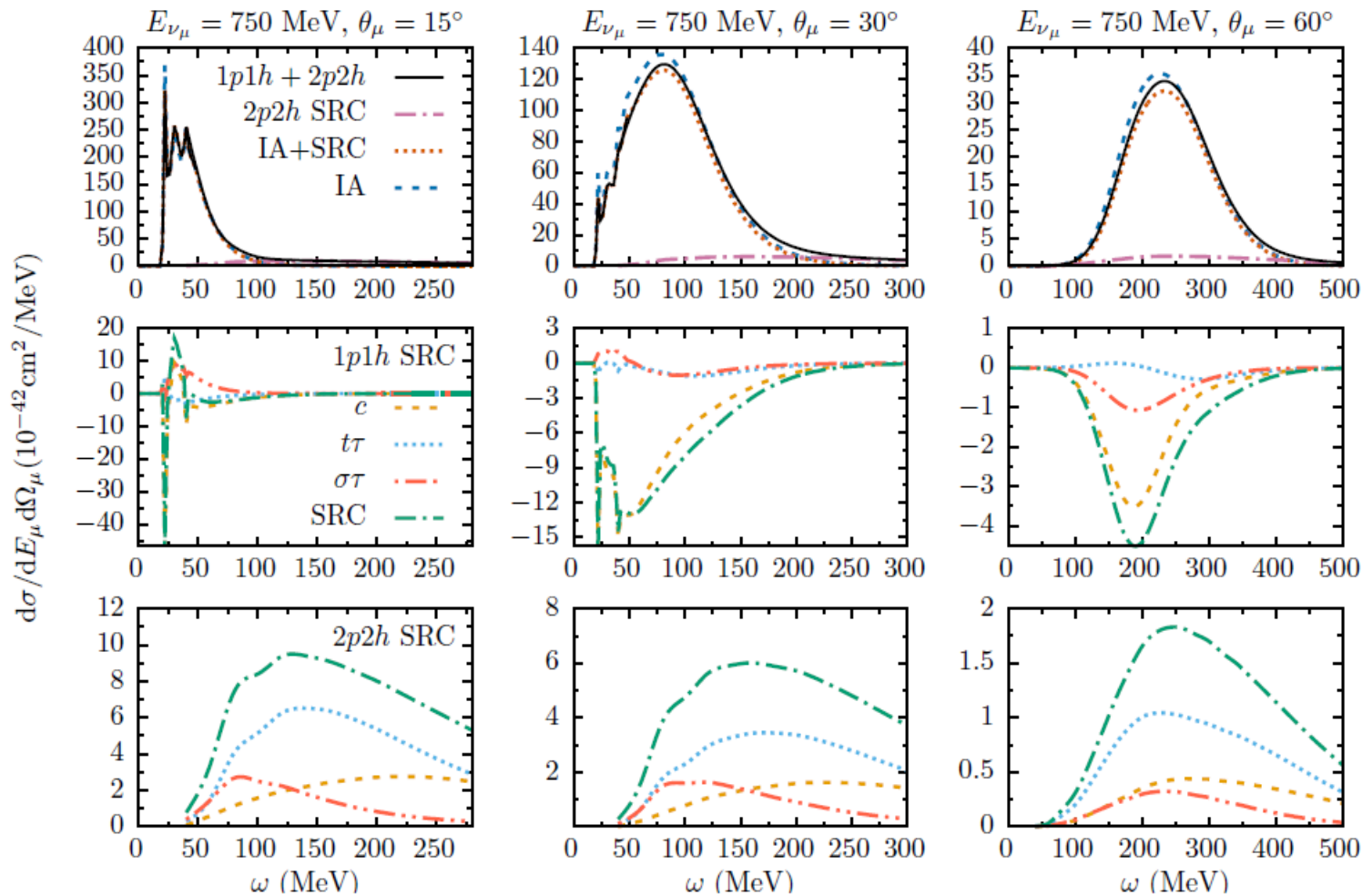
$$|\Psi\rangle = \frac{1}{\sqrt{\mathcal{N}}} \hat{\mathcal{G}} |\Phi\rangle \quad \text{with} \quad \hat{\mathcal{G}} \approx \hat{\mathcal{S}} \left( \prod_{i < j}^A [1 + \hat{l}(i, j)] \right)$$

The complexity induced by correlations is shifted from the wave functions to the operators

$$\hat{l}(i, j) = -g_c(r_{ij}) + f_{\sigma\tau}(r_{ij}) (\vec{\sigma}_i \cdot \vec{\sigma}_j) (\vec{\tau}_i \cdot \vec{\tau}_j) + f_{t\tau}(r_{ij}) \hat{S}_{ij} (\vec{\tau}_i \cdot \vec{\tau}_j),$$



# Short range correlations

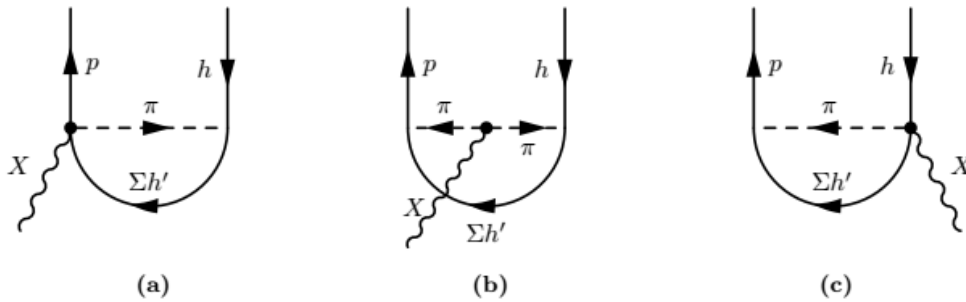


SRC affect the  
1p1h and the  
2p2h responses

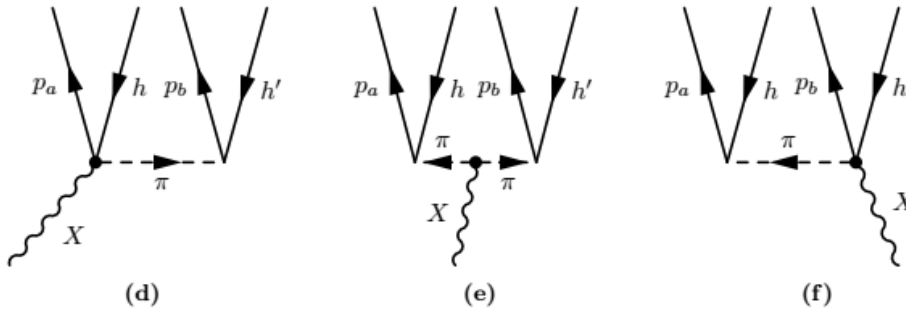
**Van Cuyck et al.,  
Phys. Rev. C 94,  
024611 (2016)**

# Meson-exchange currents

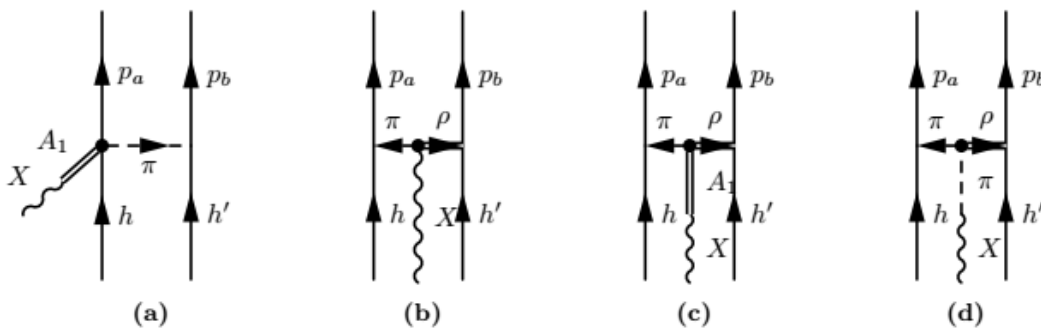
Van Cuyck et al., PRC 95, 054611 (2017)



1p1h contributions (vector current)



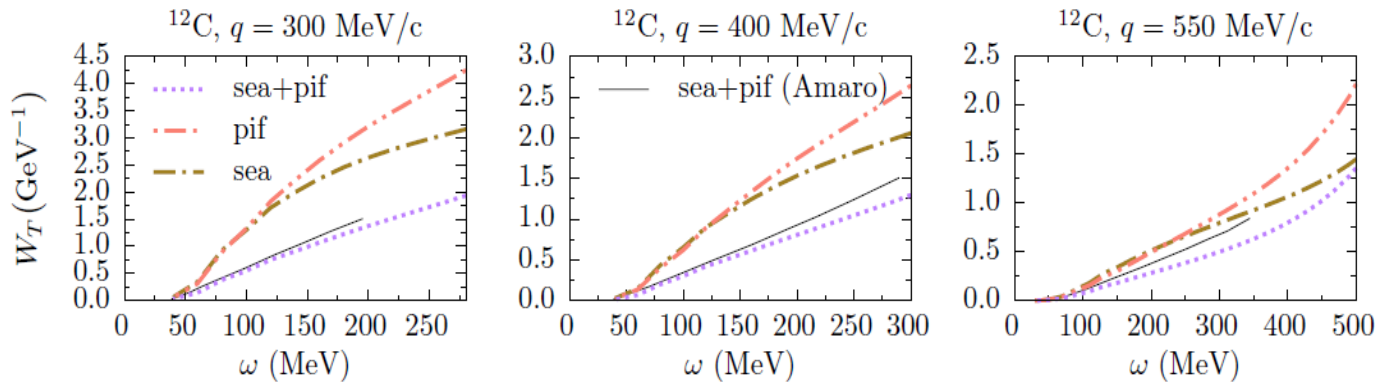
2p2h contributions (vector current)



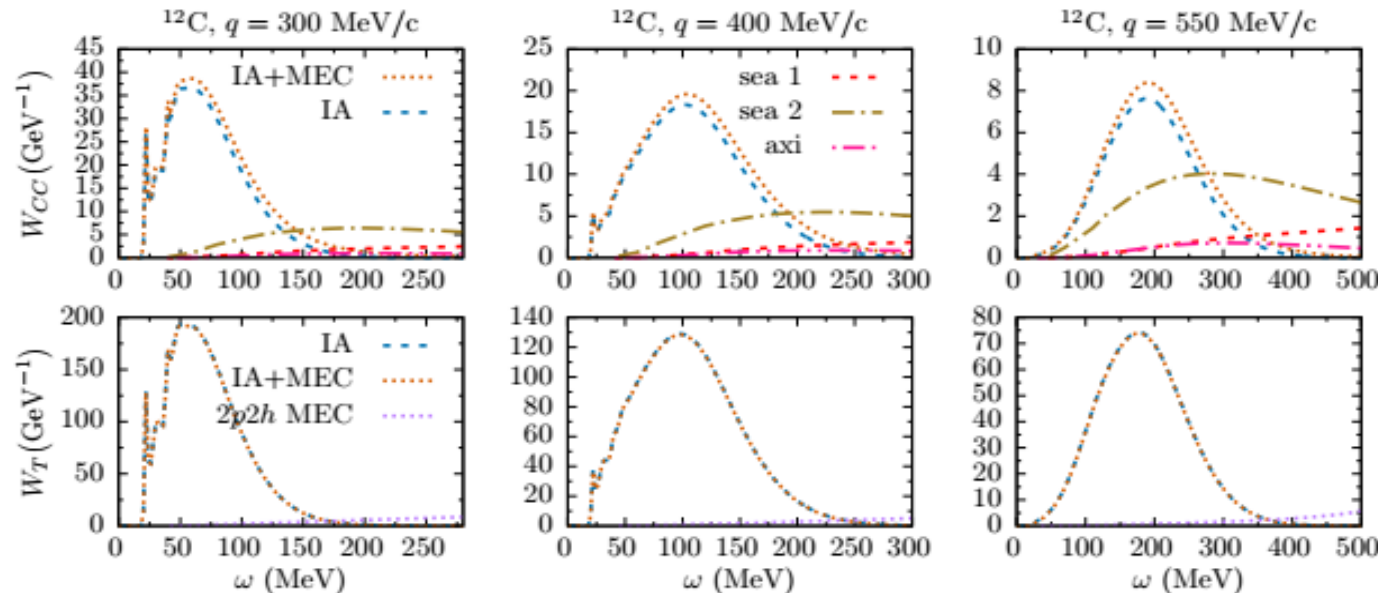
Axial current (1p1h and 2p2h)

# Meson-exchange currents

Good agreement with other predictions [Amaro et al., NPA578, 365 (1994)]:



1p1h and 2p2h contributions to the longitudinal and transverse responses:



# Medium modifications of the Delta

## Delta propagator:

$$S_{\Delta,\alpha\beta} = \frac{-(K_{\Delta} + M_{\Delta})}{K_{\Delta}^2 - M_{\Delta}^2 + iM_{\Delta}\Gamma_{\text{width}}} \left( g_{\alpha\beta} - \frac{1}{3}\gamma_{\alpha}\gamma_{\beta} - \frac{2}{3M_{\Delta}^2}K_{\Delta,\alpha}K_{\Delta,\beta} - \frac{2}{3M_{\Delta}}(\gamma_{\alpha}K_{\Delta,\beta} - K_{\Delta,\alpha}\gamma_{\beta}) \right)$$

with the energy dependent Delta width:

$$\Gamma_{\text{width}}(W) = \frac{1}{12\pi} \frac{(f_{\pi N\Delta})^2}{m_{\pi}^2 W} (\rho_{\pi,cm})^3 (M + E_{N,cm})$$

$$\Gamma_{\text{width}}^{\text{free}} \longrightarrow \Gamma_{\text{width}}^{\text{in-medium}} = \Gamma_{\text{Pauli}} - 2\Im(\Sigma_{\Delta}), \quad M_{\Delta}^{\text{free}} \longrightarrow M_{\Delta}^{\text{in-medium}} = M_{\Delta}^{\text{free}} + \Re(\Sigma_{\Delta}).$$

+  $\Gamma_{\text{Pauli}}$ : some nucleons from  $\Delta$ -decay are Pauli blocked (the  $\Delta$ -decay width decreases).

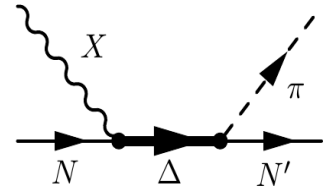
+ The parametrization of  $\Im(\Sigma_{\Delta})$  and  $\Re(\Sigma_{\Delta})$  is given in terms of the nuclear density  $\rho$ :

$$\begin{aligned} -\Im(\Sigma_{\Delta}) &= C_{QE} (\rho/\rho_0)^{\alpha} + C_{A2} (\rho/\rho_0)^{\beta} + C_{A3} (\rho/\rho_0)^{\gamma}, \\ \Re(\Sigma_{\Delta}) &= 40 \text{ MeV} (\rho/\rho_0). \end{aligned}$$

We modify the free  $\Delta\pi N$ -decay constant ( $f_{\Delta\pi N}$ ) to take into account the  $E$ -dependent medium modification of the  $\Delta$  width:

$$f_{\Delta\pi N}^{\text{in-medium}}(W) = f_{\Delta\pi N} \sqrt{\frac{\Gamma_{\text{Pauli}} + 2C_{QE} (\rho/\rho_0)^{\alpha}}{\Gamma_{\text{width}}^{\text{free}}}}$$

# Medium modifications of the Delta



$$-\Im(\Sigma_{\Delta}) = C_{QE} (\rho/\rho_0)^{\alpha} + C_{A2} (\rho/\rho_0)^{\beta} + C_{A3} (\rho/\rho_0)^{\gamma}$$

Each contribution corresponds to a different process:

- QE  $\implies \Delta N \rightarrow \pi NN$  (still one pion in the final state)
- A2  $\implies \Delta N \rightarrow NN$  (no pions in the final state)
- A3  $\implies \Delta NN \rightarrow NNN$  (no pions in the final state)

We modify the free Delta decay constant to take into account the E-dependent medium modification of the Delta-width

$$\Gamma_{\Delta\pi N}^{\alpha} = \frac{f_{\pi N\Delta} P_{\pi}^{\alpha}}{m_{\pi}}$$

$$f_{\Delta\pi N}^{\text{in-medium}}(W) = f_{\Delta\pi N} \sqrt{\frac{\Gamma_{\text{Pauli}} + 2C_{QE} (\rho/\rho_0)^{\alpha}}{\Gamma_{\text{width}}^{\text{free}}}}$$

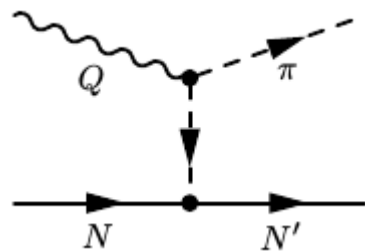
**References:** [\*] E. Oset and L. L. Salcedo, Nucl. Phys. A 468, 631 (1987).

# High-energy model

## Regge approach for the vector amplitudes.

We use the approach of **Guidal, Laget, and Vanderhaeghen** [NPA627, 645 (1997)], originally developed for pion photoproduction ( $Q^2 = 0$ ):

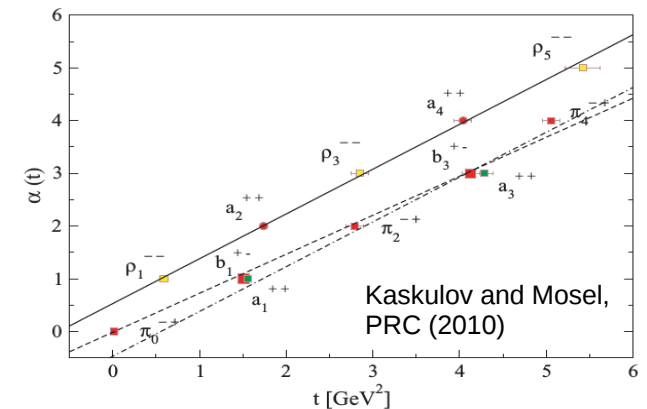
1) Feynman **meson-exchange diagrams** are reggeized.



$$\frac{1}{t - m_\pi^2}$$

The pion propagator is replaced by the Regge trajectory of the pion family

$$\mathcal{P}_\pi(t, s) = -\alpha'_\pi \varphi_\pi(t) \Gamma[-\alpha_\pi(t)] (\alpha'_\pi s)^{\alpha_\pi(t)}$$



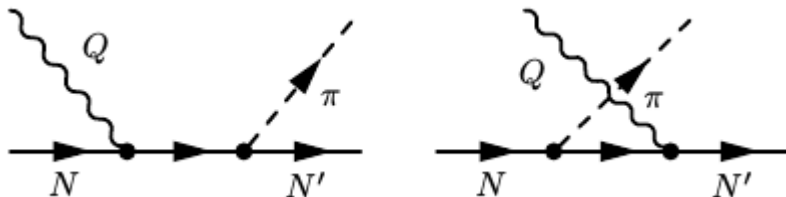
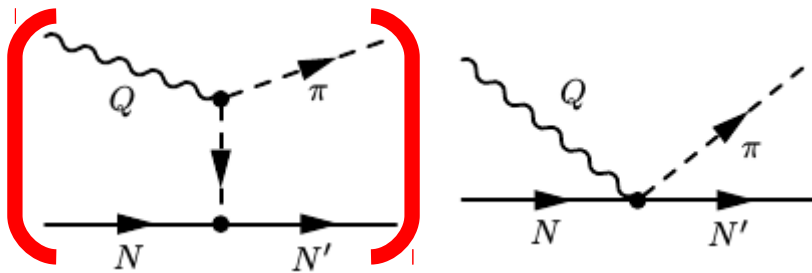
# High-energy model

## Regge approach for the vector amplitudes.

We use the approach of **Guidal, Laget, and Vanderhaeghen** [NPA627, 645 (1997)], originally developed for pion photoproduction ( $Q^2 = 0$ ):

1) Feynman **meson-exchange diagrams** are reggeized.

2) s-channel and u-channel diagrams are included to keep **Conservation of Vector Current**.



$$\frac{1}{t - m_\pi^2}$$

The pion propagator is replaced by the Regge trajectory of the pion family

$$\mathcal{P}_\pi(t, s) = -\alpha'_\pi \varphi_\pi(t) \Gamma[-\alpha_\pi(t)] (\alpha'_\pi s)^{\alpha_\pi(t)}$$

# High-energy model: results (EM current)

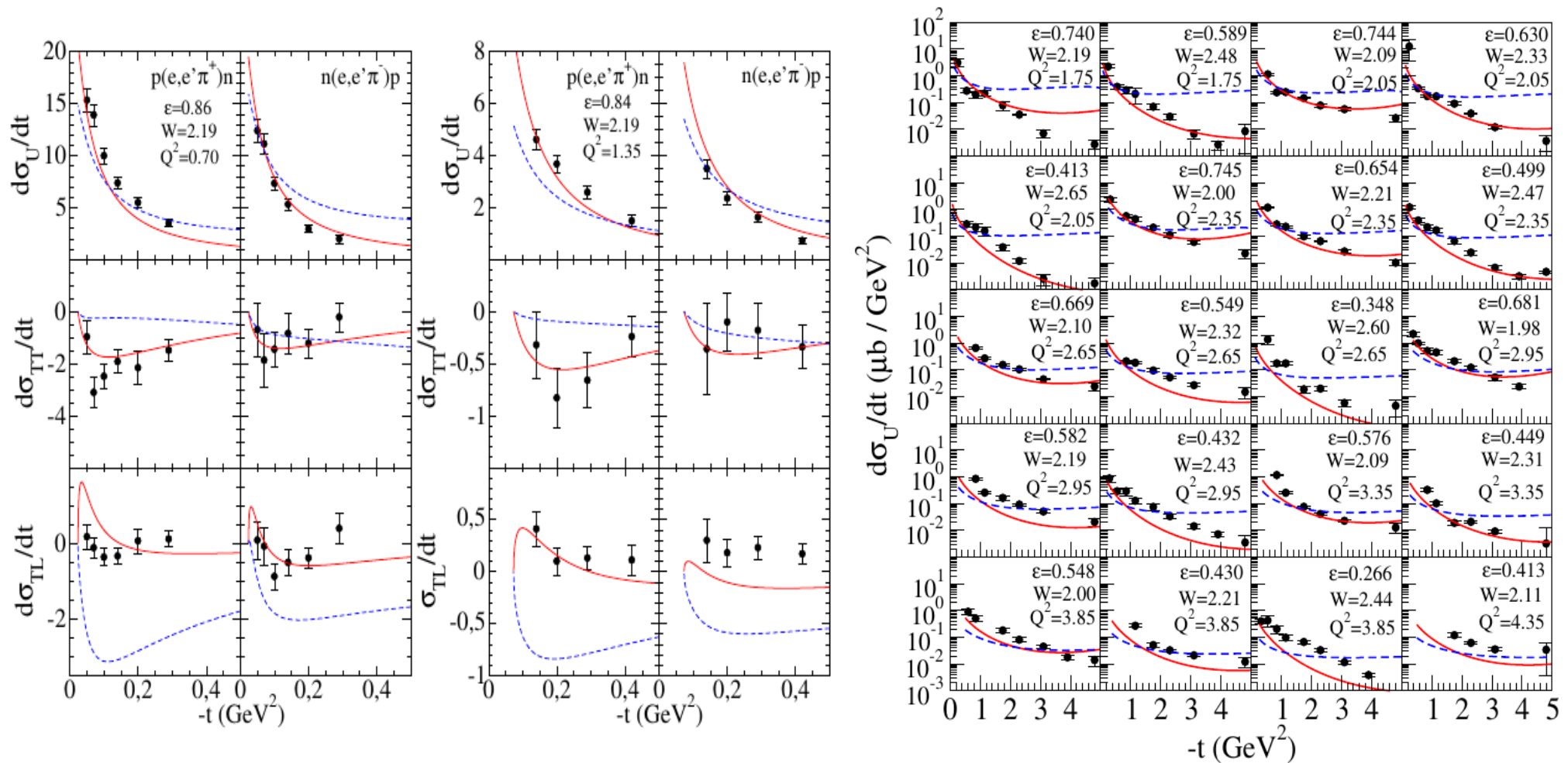


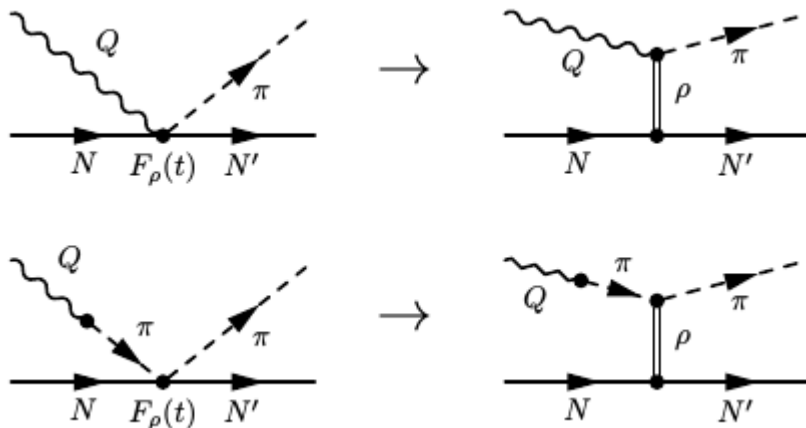
**Figure:** High-energy model (red lines), low-energy model (blue lines) and electron-induced single-pion production data.

# High-energy model

## Regge approach for the axial amplitudes.

We need meson exchange diagrams to apply the reggeization procedure of the current.

**Effective rho-exchange diagrams.** This allows us to consider the rho-exchange as the main Regge trajectory in the axial current.



$$O_{CT\rho}^{\mu} = i\mathcal{I} \frac{m_{\rho}^2}{m_{\rho}^2 - t} F_{A\rho\pi}(Q^2) \frac{1}{\sqrt{2}f_{\pi}} \times \left( \gamma^{\mu} + i \frac{\kappa_{\rho}}{2M} \sigma^{\mu\nu} K_{t,\nu} \right).$$

We consider  $\kappa_{\rho} = 0$  so that the low-energy model amplitude is recovered.

The propagator of the rho is replaced by the Regge trajectory of the **rho family**:

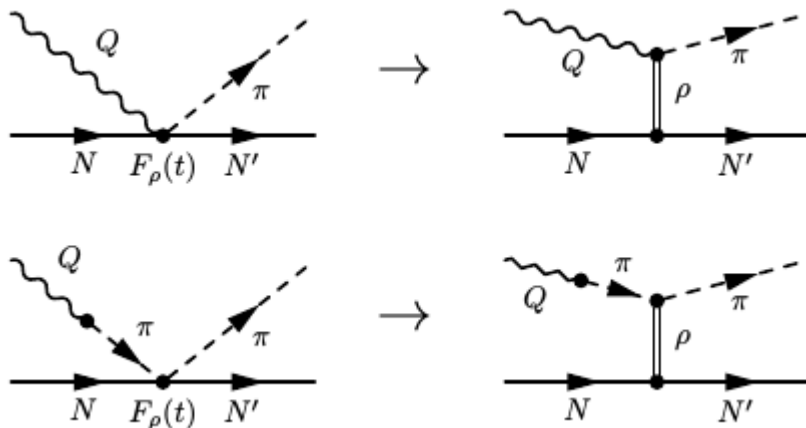
$$\mathcal{P}_{\rho}(t, s) = -\alpha'_{\rho} \varphi_{\rho}(t) \Gamma[1 - \alpha_{\rho}(t)] (\alpha'_{\rho} s)^{\alpha_{\rho}(t) - 1}$$

# High-energy model

## Regge approach for the axial amplitudes.

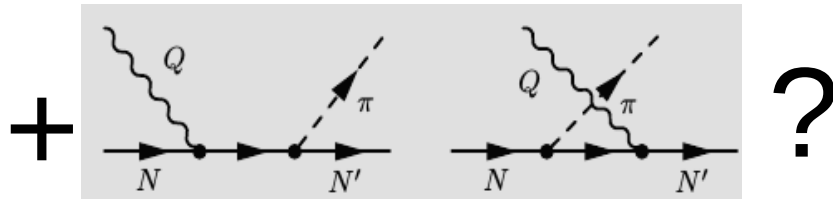
We need meson exchange diagrams to apply the reggeization procedure of the current.

**Effective rho-exchange diagrams.** This allows us to consider the rho-exchange as the main Regge trajectory in the axial current.



$$O_{CT\rho}^\mu = i\mathcal{I} \frac{m_\rho^2}{m_\rho^2 - t} F_{A\rho\pi}(Q^2) \frac{1}{\sqrt{2}f_\pi} \times \left( \gamma^\mu + i \frac{\kappa_\rho}{2M} \sigma^{\mu\nu} K_{t,\nu} \right).$$

We consider  $\kappa_\rho = 0$  so that the low-energy model amplitude is recovered.



# High-energy model

“Reggeizing” the ChPT background:

$$\mathcal{O}_{ReChi,V}^\mu = \mathcal{O}_{ChPT,V}^\mu \mathcal{P}_\pi(t, s)(t - m_\pi^2)$$

high-energy model:  
ReChi (from Reggeized  
ChPT background)

low-energy model (only  
the ChPT background)

The pion propagator is replaced  
by the **Regge propagator** of the  
pion trajectory

$$\mathcal{O}_{ReChi,A}^\mu = \mathcal{O}_{ChPT,A}^\mu \mathcal{P}_\rho(t, s)(t - m_\rho^2)$$

# High-energy model: results

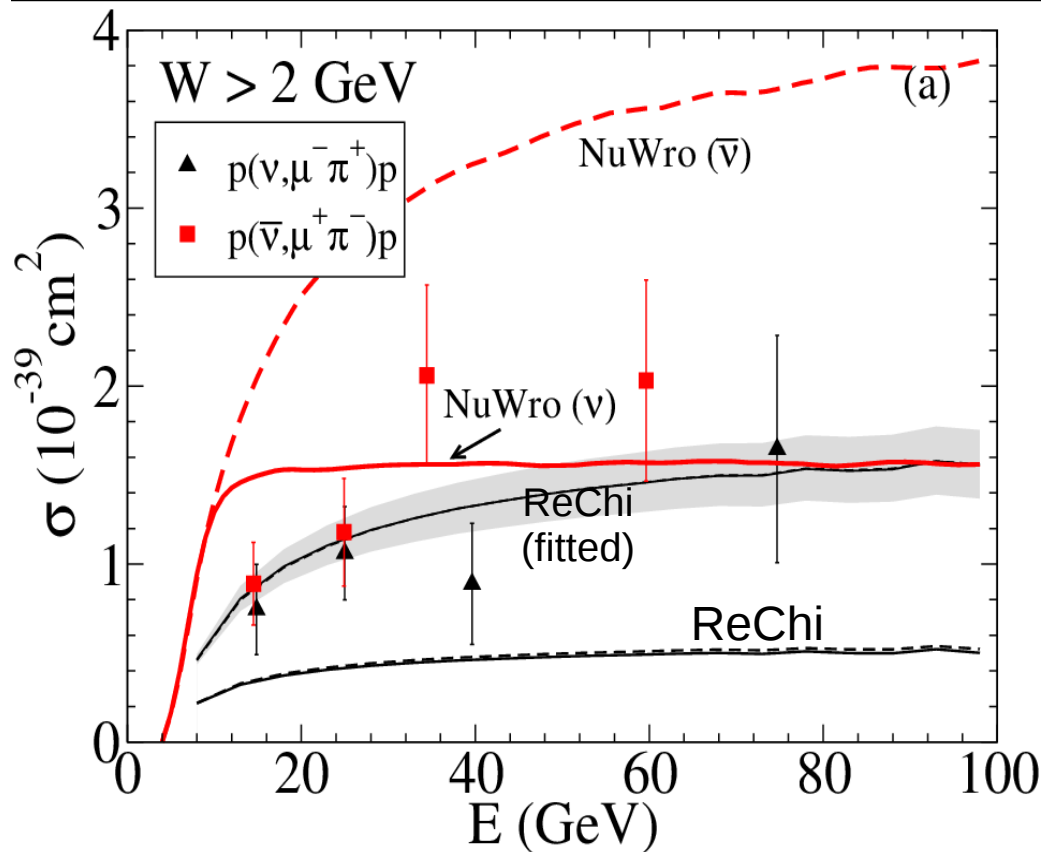
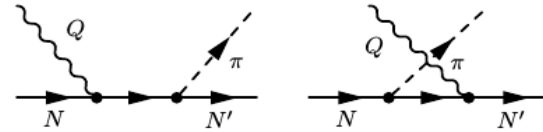


**Figure:** ReChi model and NuWro predictions are compared with high energy cross section data for neutrino and antineutrino reactions (Note the high energy cut  $W > 2 \text{ GeV}$  !!). Data from Allen et al. NPB264, 221 (1986).

**ReChi model:** One free parameter in the boson-nucleon-nucleon vertex



$$G_A[Q^2, s(u)] = g_A \left( 1 + \frac{Q^2}{\Lambda_{Apn^*} [s(u)]^2} \right)^{-2}$$

$$\Lambda_{Anp^*}(s) = \Lambda_{Apn} + (\Lambda_{\infty}^A - \Lambda_{Apn}) \left( 1 - \frac{M^2}{s} \right)$$

$$\Lambda_{\infty}^A = (7.20 \pm 2.09 / 1.32) \text{ GeV} !!!$$

**NuWro:** Based on DIS formalism and PYTHIA for hadronization.

Antineutrino cross section is  $\sim 2$  the neutrino one:

$$\bar{\nu} + \overbrace{uud}^p \rightarrow \mu^+ + \overbrace{\bar{u}d}^{\pi^-} + uud,$$

$$\nu + uud \rightarrow \mu^- + \underbrace{u\bar{d}}_{\pi^+} + uud.$$

# Hybrid model

1) Regularizing the behavior of resonances (u- and s-channel contributions): we multiply the resonance amplitude by a dipole-Gaussian form factor

$$F(s, u) = F(s) + F(u) - F(s)F(u)$$

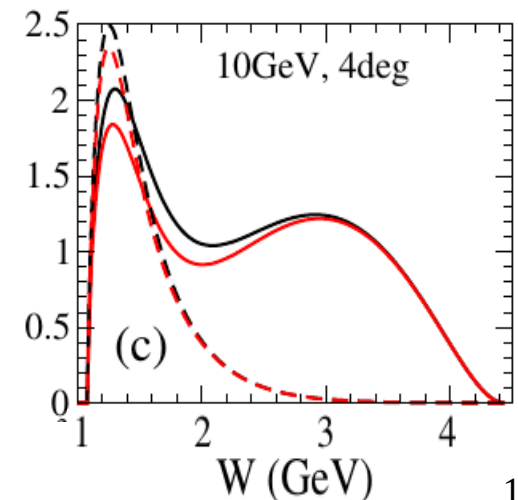
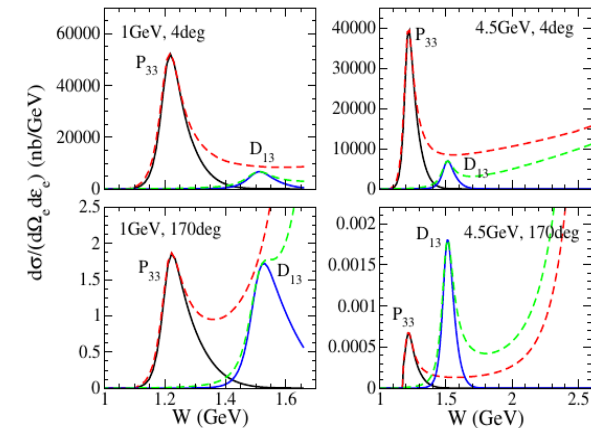
$$F(s) = \exp\left(\frac{-(s - M_R^2)^2}{\lambda_R^4}\right) \frac{\lambda_R^4}{(s - M_R^2)^2 + \lambda_R^4}$$

2) Gradually replacing the ChPT background by the High-energy (ReChi) model: we use a phenomenological transition function

$$\tilde{\mathcal{O}} = \cos^2 \phi(W) \mathcal{O}_{ChPT} + \sin^2 \phi(W) \mathcal{O}_{ReChi}$$

$$\phi(W) = \frac{\pi}{2} \left( 1 - \frac{1}{1 + \exp\left[\frac{W - W_0}{L}\right]} \right), \quad W_0 = 1.7 \text{ GeV}$$

$$L = 100 \text{ MeV}$$



103

# Hybrid model: results

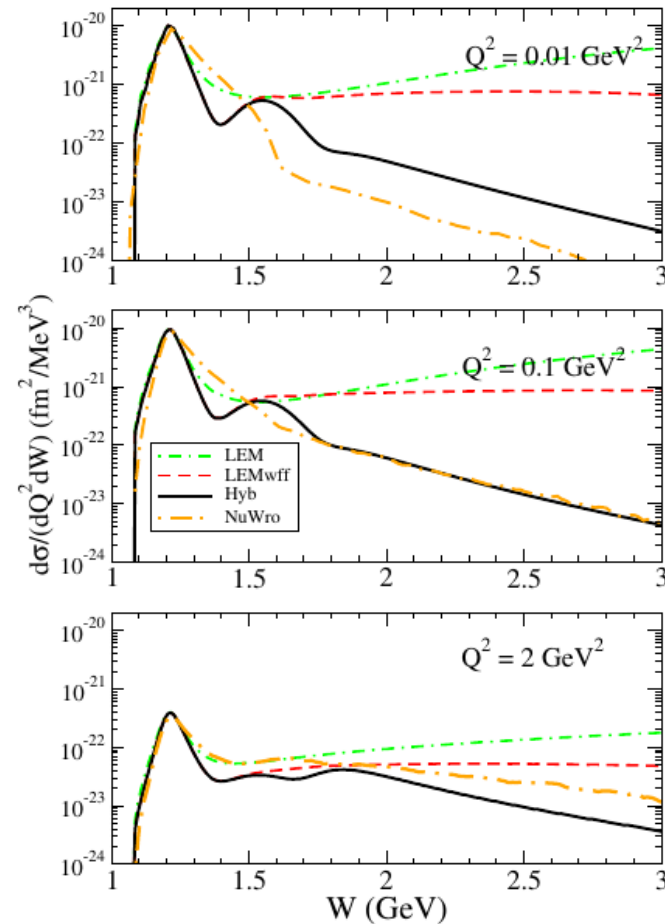
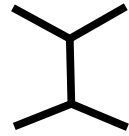


FIG. 21. (Color online) Different model predictions for the differential cross section  $d\sigma/(dQ^2 dW)$ , for the channel  $p(\nu_\mu, \mu^- \pi^+)p$ . The incoming neutrino energy is fixed to  $E_\nu = 10$   $\text{GeV}$ .

# Why does this happen?

Cross channels:



$$\mathcal{A}(t, s) = \sum_{\ell} (2\ell + 1) A_{\ell}(t) P_{\ell}(z_t)$$

$$P_{\ell}(z_t) \xrightarrow{s \rightarrow \infty} (2s)^{\ell}$$

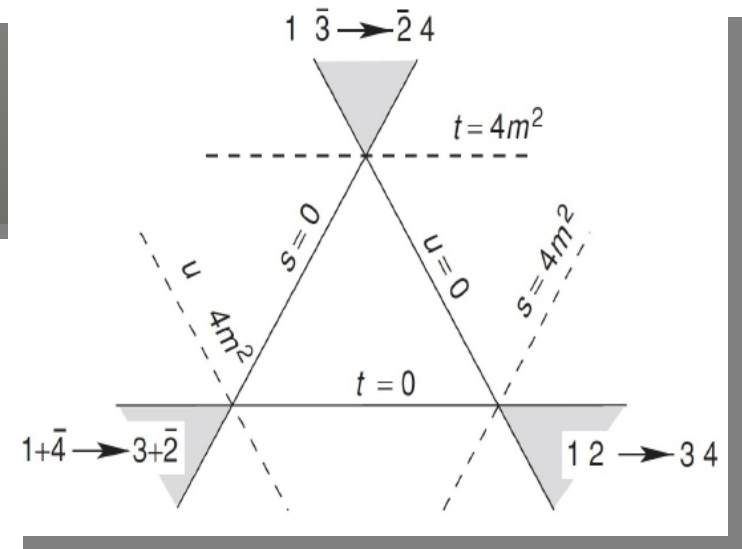
Direct channels:



$$\mathcal{A}(s, t) = \sum_{\ell} (2\ell + 1) A_{\ell}(s) P_{\ell}(z_s)$$

$$A_{\ell}(s) \sim \left( \frac{s - 4m^2}{2} \right)^{\ell}$$

**Behavior at threshold (barrier factor).**  
Feynman diagrams provide the right behavior at threshold but not at high s



$$z_t \equiv \cos \theta_t = 1 + \frac{2s}{t - 4m^2}$$

$$z_s \equiv \cos \theta_s = 1 + \frac{2t}{s - 4m^2}$$

# Regge Theory

Based on unitarity, causality and crossing symmetry, Regge Theory predicts the following **high energy ( $s \rightarrow \infty$ ) behavior** for the invariant amplitude:

$$A(s,t) \sim \beta(t) s^{\alpha(t)}$$

Regge theory does not predict the **t-dependence** of the amplitude.

For that, one needs a model.

$\alpha(t)$ : Families or Regge trajectories

